Development of Practical Methodologies for Co(II) Catalyzed Hydrofunctionalizations

Undergraduate Research Thesis

Presented in Partial Fulfillment of the Requirements for graduation *with research distinction* in Chemistry in the undergraduate colleges of The Ohio State University

By

Milauni Mehta

The Ohio State University

10 April 2018

Project Advisor: Dr. T.V. RajanBabu

Abstract

Catalytic transition metal mediated hydrofunctionalization of readily accessible 1,3-dienes provides synthetic utility for pharmaceutical products and fine chemical synthesis. Historical works have focused on using rare and expensive transition metals that are not as cheap or as earthly abundant at cobalt. Hydrovinylation of olefins is an extensively studied field of hydrofunctionalization. The cobalt-mediated hydrovinylation conditions were adapted to other hydrofunctionalizations such as hydroboration and the heterodimerization of alkyl acrylates and 1,3-dienes. Hydroboration, a more common type of hydrofunctionalization, affords allylic and homoallylic boronate esters. These boronate esters are excellent intermediates for conversion into a variety of functional groups such as amines, alcohols, carbonyls, as well as other boronate species. This research focuses on the reduction of Co(II) to the highly active cationic Co-(I) catalyst to effect high regio- and chemo-selective hydroboration. Using this system, the ligand effects, solvent effects, counter-ion effects, temperature, and the presence or absence of an additive were studied to optimize the efficacy of Co(I). The heterodimerization of alkyl acrylates and 1,3-dienes, a less common type of hydrofunctionalization, affords selective regio-, chemo- and enantioselective adducts. This research focuses on more practical, cost-effective and green conditions for the established heterodimerization reaction. These heterodimerized products can further be transformed via Michael Addition reactions for further molecular complexity. The products from both hydrofunctionalization reactions can potentially be useful for the synthesis of intermediates for large scale production of commercially relevant chemicals.

Acknowledgements

Of all the directions I thought my life would take, I really did not expect to be in this field and going to graduate school when I first started college. I would foremost like to thank Dr. Chris Callam for introducing me to organic chemistry and to Dr. RajanBabu's lab group. I am certain that I would still be lost if it were not for him making me realize that I can transform the passion I had for organic chemistry in the classroom to a lab setting and eventually into a career. Dr. Callam's faith in my abilities and intellect, and his tolerance of me constantly asking his advice for graduate school and life in general, over the past three years have been a constant source of support through all of the endeavors I have attempted.

Through Dr. Callam's recommendation I joined the RajanBabu group, a decision that quite literally changed my life. I can easily say that I have 'grown up' in this lab group and I am sincerely appreciative of the guidance and support that Dr. RajanBabu has given me over the two years. Not only have I learned about chemistry from him, I have also learned about how important humility and dedication is to the work that is being done. I have cherished my time learning from him and hope that I can make him proud in the future.

I would also like to thank the rest of the RajanBabu group: Montgomery Gray, Mahesh Parsutkar, Dr. Stanley Jing, Krishnaja Duvvuri, Dr. Kendra Dewese, Dr. Vinayak Pagar, Jon Gordon, and Dr. Srinivas Tenetti. These people made coming into lab so much fun; I've thoroughly enjoyed the conversations we've had and the tradition of having lunch at Joy's Village.

I would also like to acknowledge Sydney Sillart. She has been the best homie to survive the upper level chemistry classes with and the most fun human to go to Germany, Nebraska, and

New Orleans with. I've experienced successes and failures with her and she has supported me through it all; I will miss seeing her every single day for multiple hours a day going forward.

Lastly, I would like to thank my two families – my actual family and my OSU family. I would like to thank the '3 Gen of Norwich' crew for being my home away from home, for being there for me during my most stressful time, for providing my life with joy and love and laughter, and for the endless support over these past few years. This group of 11 women are the most phenomenal people I have met at OSU and I consider myself so lucky to be able to call them my family. As for my actual family, I would be nothing without them. I am perpetually grateful to them for their love and encouragement.

Table of Contents

List of Tables

List of Figures

List of Schemes

List of Abbreviations

α	alpha
acac	acetylacetonate
β	beta
BARF	*tetrakis*[bis-(3,5-trifluoromethyl) phenyl] borate
BDPP	2,4-bis(diphenylphosphino)pentane
°C	degrees centigrade/Celsius
COE	cyclooctenyl
conv.	conversion
CSP-GC	chiral stationary phase gas chromatography
δ	chemical shift in parts per million
d	doublet (NMR)
DCM	dichloromethane
dd	doublet of doublets (NMR)
DIOP	[2,2-dimethyl-1,3-dioxalane-4,5-diylbismethylene] bisdiphenylphosphine
dppb	1,4-bis(diphenylphosphino)butane
dppe	1,2-bis(diphenylphosphino)ethane
dppm	1,1-bis(diphenylphosphino)methane
dppp	1,3-bis(diphenylphosphino)propane
dpppent	1,5-bis(diphenylphosphino)pentane
dppf	1, 1'-bis(diphenylphosphino)ferrocene

dt	doublet of triplets (NMR)
ee	enantiomeric excess
E	entgegen (*trans*)
equiv/eq	equivalent
Et	ethyl
g	gram
GC	gas chromatography
h	hour
m	meter (SI)/ milli- (SI)/ multiplet (NMR)
Me	methyl
MAO	methylaluminoxane
min	minute
mol	moles
NMR	nuclear magnetic resonance
Ph	phenyl
q	quartet (NMR)
rt	room temperature
R_t	retention time (GC)
s	singlet (NMR)
t	triplet (NMR)
temp	temperature
THF	tetrahydrofuran

TMA	trimethylaluminium
TMS	trimethylsilyl
Z	zusammen (cis)

Chapter 1: Introduction and Background

Hydroboration is one of the most well-known and frequently used hydrofunctionalization reactions. Uncatalyzed hydroboration reactions follow classical chemistry rules where the boron group is added to the less substituted carbon, leading to, after oxidative work-up, anti-Markovnikov addition of water to a double bond.[1] Recent works have explored metal catalyzed hydroboration which provides control over the chemo-, regio-, and stereoselectivity of boron group addition.

Scheme 1.1: Catalyzed vs. uncatalyzed oxidation of hydroboration reactions[1]

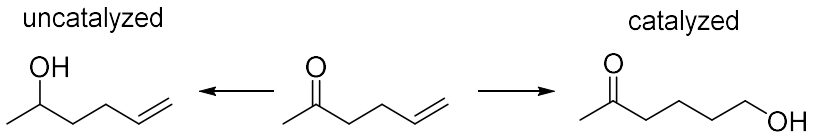

Männig and Nöth first introduced hydroboration of an alkene in the presence of a ketone using Wilkinson's catalyst and catecholborane in 1985[2]. Without the metal catalyst, the catecholborane adds across the carbonyl group, but with the rhodium catalyst, the catechol borane adds selectively to the terminal alkene (Scheme 1.1). This discovery shows the importance of control established by metal catalysts and resulted in the development of metal catalyzed hydroboration of alkenes over the next few years.[1] Many transitions metals similar to rhodium were explored including iridium[3,4] and samarium[5] but the high cost of these metals severely limited the utility of the reaction on a large scale. Pereira and Srebnik reported that pinacol borane is more stable than catecholborane and the pinacol boronic ester product can be easily isolated via column chromatography unlike its catechol counterpart.[6] Catecholborane undergoes decomposition in the presence of triphenylphosphine – a common reagent in hydroboration conditions thus limiting its success in hydroboration.

With the success of hydroboration on alkenes, the natural direction this field was directed to was hydroboration of dienes. Some conjugated dienes such as butadiene, pentadiene, isoprene, etc. are commercially available but more complex conjugated dienes are commonly accessible via Wittig reaction from the cheap and abundant aldehyde starting material. Diene synthesis is also quite tolerant to many functional groups thus allowing for the formation of dienes with many different functional groups. Suzuki *et al* reported the first palladium catalyzed 1,4-addition of catecholborane to isoprene, a simple 1,3-diene.[7] In 1997, Zaidlewicz and Meller reported success of hydroboration using Ni(II) and Co(II) catalysts – metals that are significantly cheaper and earthly abundant when compared to previous metals used in hydroboration[8]. They reported more reactivity with Ni(II) than with Co(II) showing that the nickel catalyzed reaction reached completion in 6 hours and yielded 87% selective for the desired 1,2-addition product whereas the cobalt catalyzed reaction reached completion in 24 hours and yielded 66% but was still highly selective for the 1,2-addition product.

Scheme 1.2: Zaidlewicz and Meller's Metal Catalyzed Hydroboration

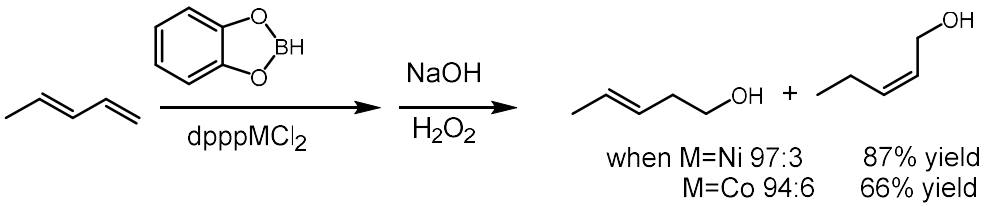

Boronate esters provide excellent synthetic utility as they are an extremely versatile intermediate (Figure 1.1). The carbon-boron bond can easily be transformed into carbon-carbon bonds, carbon-nitrogen bonds as well alcohols and other boron groups which can be further oxidized. Use of acyclic 1,3-dienes as substrates in hydroboration has limited references in literature due to the incompatibility of the catalyst conditions with the conjugated diene.

Figure 1.1: Transformation of boronate ester to various functional groups[9]

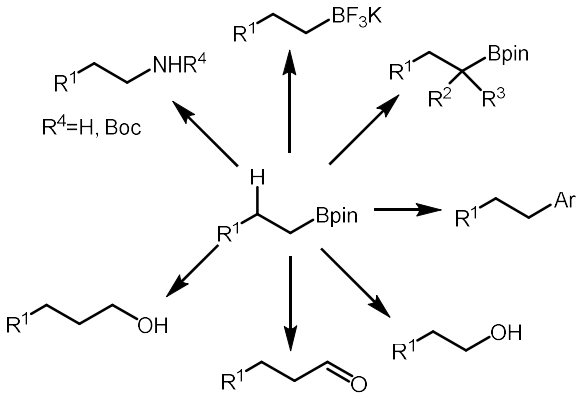

Dr. Kendra Dewese explored hydroboration of 1,3-(*E*)-dienes with a cobalt catalyst for her doctoral dissertation: her established conditions served as inspiration for this project. Dr. Dewese developed an unprecedented system for selective 1,2 addition hydroboration with dpppCoCl$_2$ as the catalyst and methylaluminoxane (MAO) as the activator. Limitations for this reaction and inspiration for this project are further discussed in Chapter 2.

Alongside the development of the hydroboration catalytic system, the heterodimerization of alkyl acrylates and 1,3-(E)-dienes was also being explored by Dr. Stanley Jing using similar metal complexes and activators.[11] Alkyl acrylates are a cheap feedstock source of carbon and have found wide industrial application in the creation of polymeric materials such as plastics, fibers, cosmetics, and more.[12] The first reported reaction between butadiene and alkyl acrylates was in 1964 by Wittenberg[13] with a Co catalyst. In 1966, Misono *et al.* reported a successful heterodimerization reaction with butadiene and alkyl acrylates using an active catalyst derived from Co(acac)$_3$ and Et$_3$Al[14] (Scheme 1.3). The highest isolated yield for this reaction was 20-30% and for many years there were few scattered reports improving yields and selectivity of this reaction. In 1983, Tkatchenko *et al* reported a high yield and high selectivity of the heterodimerized product using cationic allyl-palladium catalyst in the presence of tributylphosphine with the Diels-Alder adduct as the minor product.[15]

Scheme 1.3: Co(III) Catalyzed Heterodimerization Reaction by Misono *et al.*

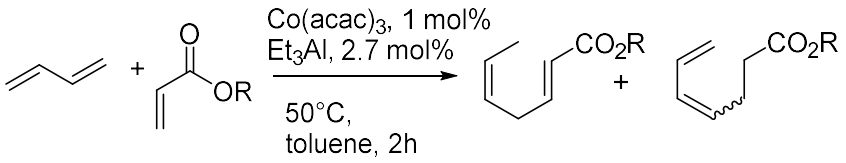

Scheme 1.4: First Report of Pd-catalyzed Heterodimerization by Tkatchenko *et al*

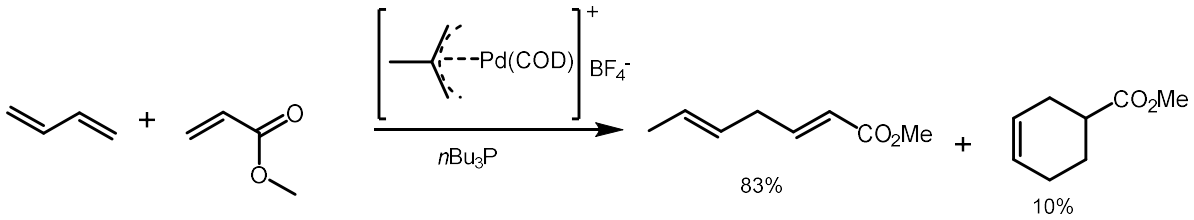

In 1990, Feldman and Grega reported successful Co-mediated coupling of butadiene and methyl acrylate with moderate yield using the well-known species (COD)Co(COE$^-$) but required heating the reaction mixture to 50°C and afforded 53% as the highest yield of the desired heterodimerized adduct[16]. After a decade, Hilt *et al* reported the heterodimerized product in 92% yield even though their method was developed to target the Diels Alder product (Scheme 1.4). [17] The heterodimerization adducts were not further explored by Hilt and co-workers and there was a period of little activity in this field until 2012 when Hirano and co-workers reported the use of Ru(0) complexes for the codimerization of butadiene and methyl acrylate (Figure 1.5).[18]

Scheme 1.5: Early Heterodimerization Reactions by Hilt *et al.*

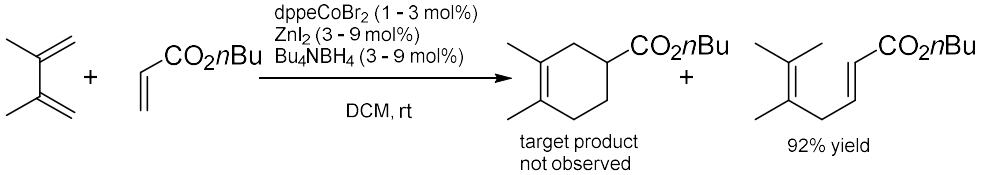

Using a Ru(0) catalyst, Hirano and co-workers reported enantioselective heterodimerization of dienes and alkyl acrylates to afford chiral products. However, the supposed chiral products were

isolated with a considerably low 58% enantiomeric excess[19] and any modification to the conditions of the experiment did not improve the enantioselectivity of the compound.

Scheme 1.6: Expansion of the heterodimerization reaction with Ru(0) by Hirano *et al.*

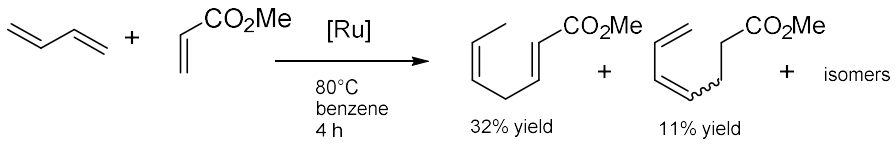

Scheme 1.7: Hydrovinylation of 1,3-(*E*)-dienes reaction conditions by the RajanBabu Group

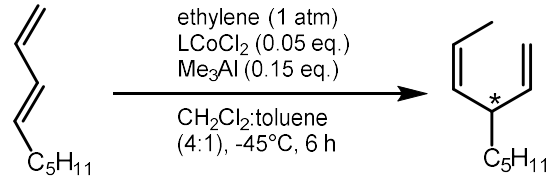

Inspired by the success of the Co catalyzed conditions reported by the RajanBabu group for asymmetric hydrovinylation of 1,3-*(E)*-dienes,[21,22] Dr. Stanley Jing applied the reaction conditions of the hydrovinylation reaction to heterodimerization of 1,3-(*E*)-diene and methyl acrylate. Though the reaction conditions worked for heterodimerization of ethylene and dienes, they did not work well with alkyl acrylates and dienes, thus calling for a new methodology to be developed which is further introduced in Chapter 3. The established method[24] for this reaction provide inspiration for more practical and cost-effective methods to be developed for the synthesis of enantiopure skipped 1,4-diene esters.

Chapter 2: Cobalt (I) Mediated Hydroboration of 1,3-(*E*)-dienes

2.1 - Initial scouting experiments for 1,3-(*E*)-dodecadiene

Thus far, the seemingly best conditions for Co-catalyzed hydroboration were established as the isolated (P~P)CoX_2 (0.05 eq.), methylaluminoxane (2.0 eq.), pinacol borane (1.1 eq.) in dichloromethane (DCM) at room temperature with reactions times as short as 5 mins.[10] Although these reaction conditions provided excellent regioselectivity at a ratio of 9:1 favoring the 1,2-addition product (homoallylic), the synthesis of the reagent methylaluminoxane (MAO) proved time-consuming and costly. Other alkylaluminium additives were tested but trimethylaluminium (TMA) and MAO were the only two additives that allowed the reaction to progress.

Scheme 2.1: Established conditions for hydroboration of 1,3-dienes

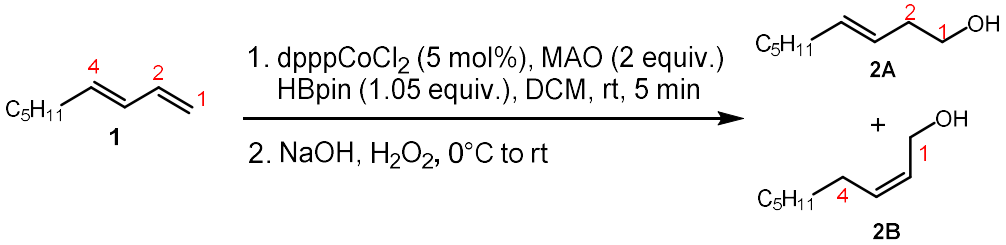

Table 2.1: Activator scan completed by Dr. Kendra Dewese[10]

[a]Entry	Cat. Loading	Activator	Temp.	Time	[b]Conv.
1	5 mol%	2 eq. MAO	rt	5 min	100%
2	5 mol%	2 eq. MAO	0°C	10 min	100%
3	10 mol%	30% TMA	-10°C	15 min	100%
4	5 mol%	15% TMA	-20°C	15 h	90%
5	5 mol%	1.1 eq. $La(OTf)_3$	rt	30 min	0%
6	5 mol%	1.1 eq. $AlCl_3$	rt	15 min	0%
7	5 mol%	1.1 eq. Et_3Al	rt	30 min	0%
8	5 mol%	1.1 eq. $EtAlCl_2$	rt	15 min	0%
9	5 mol%	1.1 eq. Et_2AlCl	rt	15 min	0%
10	5 mol%	1.1 eq. Me_2AlCl	rt	30 min	0%
11	5 mol%	40% EtMgBr	rt	30 min	0%
12	5 mol%	20% $NaBHEt_3$	rt	48 h	0%

[a]Scheme 2.1 for reaction conditions. [b]Remaining material was starting material

We hypothesized that TMA and MAO were dual acting – first reducing the Co(II) into Co(I) and then the resulting aluminum chloride acting as a Lewis acid to abstract the methyl

group or a proton to form the active cationic Co(I) species during catalysis. The Co(II) complex was reduced externally with Zn to Co(I) to ensure that it was a Lewis acid was necessary to activate the Co(I) and this reduced species was tested to be a precursor to the active cationic catalyst. To test the Co(I) intermediate hypothesis, initial scouting experiments were conducted with various Lewis acids and isolated Co(I) complexes (Table 2.2).

Scheme 2.2: Conditions for initial scouting experiments

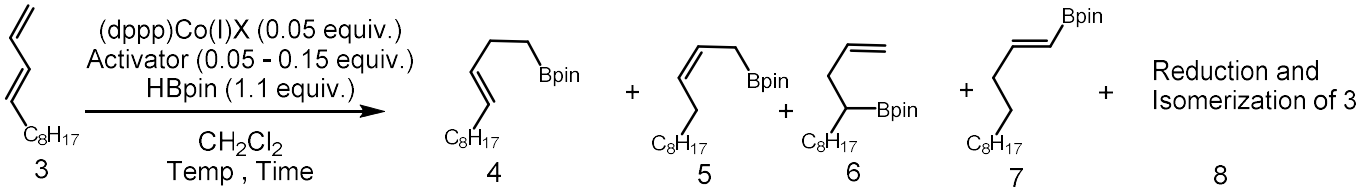

Table 2.2: Initial Scouting experiments completed by Dr. Stanley Jing**

Entry	(P~P)CoX (5 mol%)	Additive, (mol%)	Temp (°C), Time (h)	[a]Conv (%)	[b]GC-analysis of reaction mixture (%)				
					4	5	6	7	8
1	dpppCoBr	NaBARF, 10	-10 – 23, 1	100	80	13.5	1.4	3	1
2	dppbCoEt	$B(C_6F_5)_3$, 15	0 – 23, 1	100	82	13.4	1.2	1.7	1.6
3	(*S,S*)-DIOPCoEt	$B(C_6F_5)_3$, 15	0, 1	100	79	<1	16.3	1	-
4	(*S,S*)-BDPPCoCOE$^-$	$H(Et_2O)_2$BARF, 5	-10 – 23, 1	100	69	4	27	-	-
5	BINAPCoCOE$^-$	$H(Et_2O)_2$BARF, 5	0 – 23, 1	100	42.8	33.3	-	-	24
6	**L1**CoBr	NaBARF, 10	0 – 23, 1	100	12.5	72	-	-	1
7	**L2**CoCl	NaBARF, 10	0 – 23, 1	100	65	12	8	-	8
8	**L3**CoBr	NaBARF, 10	0 – 23, 1	56*	46	-	-	-	9

[a]All (P~P)Co(I)X (X = Cl, Br) derived from reduction of the corresponding (P~P)Co(I)X_2 (X = Cl, Br); dppbCoEt derived from treatment of dppbCoCl_2 with EtMgCl (3.0 equiv.) respectively. [b]Conversions based on GC integration of volatile components of reaction mixture. *44% is **3** (starting material diene) **Unpublished results from Dr. Stanley Jing and Milauni Mehta

Almost all of these initial experiments are conducted in the presence of an activator to eliminate the possibility that should the reaction not work, it is not because of the absence of the activator. We hypothesized that pinacol borane can act as an activator as well as the catalyst which is why the hydroboration reaction goes to completion in the absence of an activator (Table 2.3, entries 1 and 2). However, for non-halide counter-ions such as ethyl (Table 2.2, entries 2 and 4) or eta-3-cyclooctadienyl (Table 2.2, entries 5 and 6) there was a strong hypothesis that pinacol

borane did not possess enough Lewis acidity to promote the reaction without an additive. To avoid confusion associated with the activity of the catalyst, the subsequent reactions were conducted in the presence of an additive, the activator. In this connection, employing the conditions for hydroboration with dpppCoBr and $B(C_6F_5)_3$ works well (Table 2.4, entries 1 and 2). These preliminary results present an opportunity to further explore various effects of the reactions conditions on the regioselectivity of the hydroboration addition to the 1,3-diene.

2.2 - Counter Ion Effect

The product distribution of this reaction generally favors the 1,2-addition product **4** over the 1,4-addition product **5** apart from one experiment where **L1**CoBr is used as the catalyst (Table 2.2, entry 7), which will be discussed in the next section (see Figure 2.1 for structures of the ligand). The reversal of favored product indicates that either the counter ion or the ligand determines regioselectivity. First, a counter-ion scan was done using the precursor from a cobalt complex containing halides, eta-3-cyclooctadienyl and ethyl groups to see how this would affect the regioselectivity (Table 2.3).

Scheme 2.3: Counter-Ion scan conditions

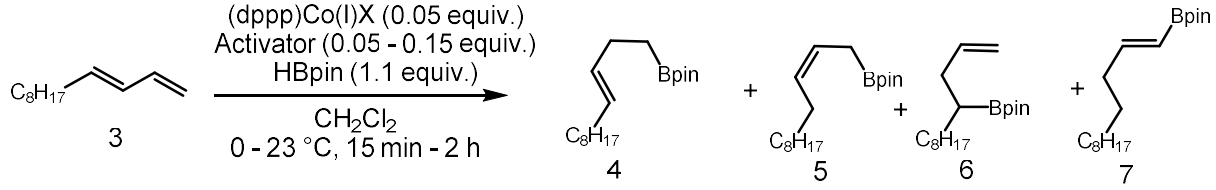

We determined that the group on Co(I) is not affecting the regioselectivity of the reaction as for each of the experiments the product distribution still favored the 1,2-addition product **4** over the 1,4-addition product **5** in the established ~80:15 ratio. Although in the initial scan experiments the conditions with dpppCoX reached full conversion in 1 hour (Table 2.2, entry 1), the reactions were all tracked at 30 mins to compare the percent conversion of starting material

to products with the different conditions. With the combination of dpppCoX and no activator, the reaction does not reach full conversion at 30 mins, thus indicating that in the absence of the additive the reaction requires longer run times to reach full completion. When compared to other combinations of catalysts and activators, the system of dpppCoX/no activator is not as efficient as the combination of dpppCo(COE$^-$)/ $H(Et_2O)_2BARF$ – an acid activator as known as Brookhart's acid.

Table 2.3: Results on Survey of Counter-ions

Entry	[ab](P~P)CoX (mol%)	Additive, (mol%)	Temp (°C), Time (h)	[c]Conv (%)	GC analysis of reaction mixture (%)				
					3	4	5	6	7
1	(dppp)CoCl, 5	none	0 – 23, 0.5	68	32	50	9	1	2
2	(dppp)CoBr, 5	none	0 – 23, 0.5	56	44	37	7	<1	1
3	(dppp)Co(COE$^-$), 5	$H(Et_2O)_2BARF$, 5	0 – 23, 0.5	>98	0	74	15	-	-
4	(dppp)Co(COE$^-$), 5	$H(Et_2O)_2BARF$, 5	-20, 0.5	>99	0	79	14	1.5	-
5	(dppp)Co(COE$^-$), 5	$H(Et_2O)_2BARF$, 5	-45, 0.5	>99	0	77	14	1.5	2
6	(dppp)Co(COE$^-$), 1	$H(Et_2O)_2BARF$, 1	0 – 23, 0.5	>98	0	78	13	2	2
7	(dppp)Co(COE), 0.1	$H(Et_2O)_2BARF$, 0.1	0 – 23, 0.5	44	56	31	7	<1	2
8	(dppp)Co(COE), 0.1	$H(Et_2O)_2BARF$, 0.1	23, 15	83	17	59	12	1.5	4
9	(dppp)CoEt, 5	$B(C_6F_5)$, 15	0 – 23, 15	50	50	22	-	-	-

[a](dppp)CoCl derived from Zn reduction of $(dppp)CoCl_2$. [b](dppp)CoBr derived from Zn reduction of $(dppp)CoBr_2$.
[c]Conversions based on GC integration of volatile components of reaction mixture

Furthermore, with this combination of the eta-3-cycooctadienyl counter ion and Brookhart's acid, both the catalyst and activator loading can be as low as 1 mol% or 0.01 equivalents with respect to the starting material and still fully convert the diene to the hydroboration product in 0.5 hours. This demonstrates that the most robust system for this reaction is the combination of dpppCo(COE$^-$)/ $H(Et_2O)_2BARF$, both at 0.01 equivalents with respect to starting material, ran from 0-23°C allows for almost full conversion of starting material to desired product in 30 mins. With this reaction, some of the starting material dimerizes

or reduces to an alkane thus reducing the conversion to desired product from 100% to about 98%.

2.3 - Effect of Ligand on Regioselectivity

Once it was determined that the source of Co(I) is not a factor that is affecting the regioselectivity, it was hypothesized that the ligand could be determining how the catalyst was interacting with the substrate thus controlling the regioselectivity of the addition. Since the source of Co(I) was not affecting the regioselectivity, interchanging between halide counter-ions and alkyl counter-ions would not affect the ligand scan results in this section.

Scheme 2.4: Conditions for ligand scan

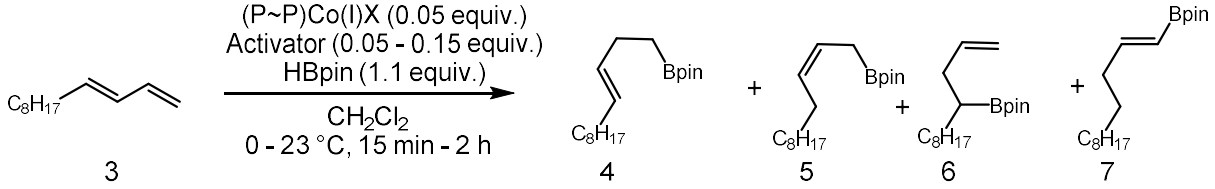

Table 2.4: Ligand Effect of Co(I) hydroboration of 1,3-(*E*)-dodecadiene

Entry	[a](P~P)CoX (5 mol%)	Additive, (mol%)	Temp (°C), Time (h)	[b]Conv. (%)	GC analysis of reaction mixture (%)			
					4	5	6	7
1	(dppm)CoCl	$B(C_6F_5)$, 15	0 – 23, 2	88	51	19	51	1
2	(dppe)CoCl	$B(C_6F_5)$, 15	0 – 23, 2	77	55	25	<1	<1
3	(dppp)CoCl	none	0 – 23, 0.5	68	50	9	1	2
4	(dppb)Co(COE^-)	$H(Et_2O)_2BARF$, 5	0 – 23, 0.5	100	84	-	-	8
5	(dpppent)CoBr	$B(C_6F_5)$, 10	0 – 23, 2	13	-	8	-	-
6	(dppf)CoEt	$B(C_6F_5)$, 15	0 – 23, 2	64	45	10	1	2
7	(+)DIOPCo(COE^-)	$H(Et_2O)_2BARF$, 5	0 – 23, 0.5	100	83	1	7.6	-
8	(*S,S*)-BDPPCo(COE^-)	$B(C_6F_5)$, 15	0 – 23, 0.5	>98	66	5	25	<1
9	(*S,S*)-BDPPCoBr	NaBARF	0 – 23, 2	68	51	3.8	9	<1
10	**L1**CoBr	none	0 – 23, 2	90	<1	82	<1	-
11	**L1**CoBr	NaBARF, 15	0 – 23, 0.5	100	15	63	2	-
12	**L2**CoCl	none	0 – 23, 2	50	12	<1	-	38
13	**L3**CoCl	none	0 – 23, 2	68	61	<1	<1	7

[a]All (P~P)Co(I)X (X = Cl, Br) derived from reduction of the corresponding (P~P)Co(I)X_2 (X = Cl, Br).; dppbCoEt and dppfCoEt derived from treatment of $dpppCoCl_2$ and $dppfCoCl_2$ with EtMgCl (3.0 equiv.) respectively.
[b]Conversions based on GC integration of volatile components of reaction mixture.

This reaction tolerates varying bite angles of α,ω-diphenylphosphino-alkyl ligands as evidenced by percent conversions greater than 60% and short reaction times, ranging from 30 mins to 2 hours (Table 2.4, entries 1-4). After testing the tolerability of this reaction of ligands with alkyl backbones, the tolerability of larger ligands as well as chiral ligands were tested. All of the ligands except the phenyl version of phosphine-oxazoline ligand **L1**,[22] gave the 1,2-addition product **4**. With or without the activator, [**L1**]CoBr gives the 1,4 addition product **5** as the major product. The activator increases the rate of reaction evidenced by the reaction reaching

Figure 2.1: Structures of ligands employed in ligand scan

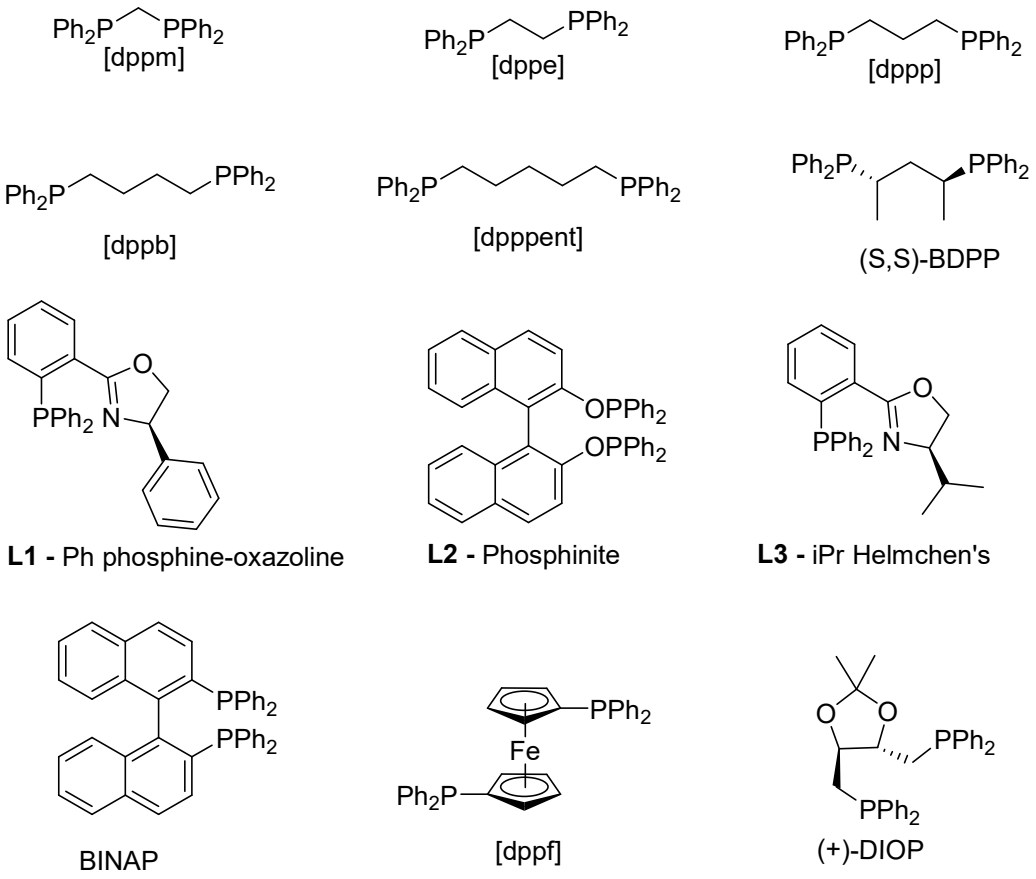

full completion in 30 mins (Table 2.4, entry 10 vs entry 11), but did not give as selective of a product distribution as the experiment done without any activator present (Table 2.4, entry 11),

which took 2 hours to almost reach full completion, but gave almost exclusively the 1,4-addition product. Further studies need to be done to fully confirm these theories, however these initial results show promising potential for the ability to control the regioselectivity and product distribution of the Co-catalyzed hydroboration reaction.

Ligands with different bite angles, rings, electronic properties, chirality and bulk were tested (Figure 2.1). This reaction is tolerant of most of these variables with the exception of (dpppent)CoBr; perhaps the bite angle of 1,3-bis(diphenylphosphino)-pentane was too large to effect the reaction (Table 2.4, entry 5). Notable poor reaction conditions were with the isopropyl version of the phox Ligand **L3** (Table 2.4, entry 13), 1,1'-bis(diphenylphosphino)ferrocene (Table 2.4, entry 16), and the phosphinite ligand **L2** (Table 2.4, entry 12).

2.4 - *in situ* Generation of Active Catalyst

As mentioned before, the hypothesized original role of MAO was to first reduce the Co(II) species to Co(I) and then further to $Co(I)^+$ as the active species. Both the counter-ion and ligand scans were conducted with isolated Co(I) complex since the proposed mechanism indicated that Co(I) was the pre-catalyst that became the active cationic Co(I) species.[23] The Co(II) complexes were reduced externally by activated Zn dust, thus it was hypothesized that the external reducing agent and the newly discovered Lewis acid activators could generate the active catalyst *in situ* instead of using MAO to reduce and activate the pre-catalyst. This methodology proposes significant advantages as it eliminates the need for storing the activator at -8°C; NaBARF can be stored at room temperature as a stable white crystalline solid.

Scheme 2.5: Optimized conditions for *in situ* generation of active Co-catalyst

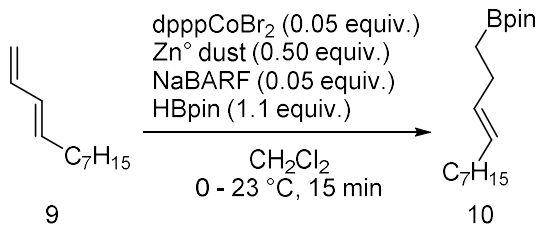

To test this hypothesis, isolated dpppCoBr$_2$, slight excess of the reducing agent Zn dust and activator NaBARF were combined in DCM and allowed to stir for a few minutes. The solution was then cooled to 0°C, the starting material diene was added followed by the pinacol borane, and the reaction was allowed to warm to room temperature. The reaction was tracked at 15 minutes and indicated full consumption of the starting material with an isolated yield of 81% of the 1,2-addition product, thus confirming the hypothesis that the active catalyst could be generated in situ using more readily available materials such as Zn and NaBARF. The full procedure for this reaction can be found in the Experimental Section 2.6.

2.5 - Summary and Conclusions

Although the established conditions for the hydroboration of 1,3-(*E*)-dienes afforded the 1,2-hydroborated product in good yield, a more facile system was developed through further analysis of this reaction. From the first initial experiments, it was determined that alternative Lewis acids other than MAO activated the catalyst just as well as MAO did and provided the same selectivity for the 1,2-addition product with one exception (Table 2.2, entry 6), which provided the 1,4-addition product. To further explore the cause of this difference in addition, a counter- ion scan and ligand scan were conducted. Changing the counter ion from a halide to different alkyl groups did not affect the regioselectivity of the reaction, but provided insight into the limitations of the reaction.

The ligand scan determined that it was the identity of the ligand that affected the selectivity of the addition. The excellent ratio of regioselectivity indicates that the addition can be fully controlled. Based on this discovery controlling the regioselectivity with the identity of the ligand, the original conditions with MAO were reviewed again. As it was hypothesized that MAO served a dual purpose of reducing the catalyst from Co(II) to Co(I) to $Co(I)^+$, the new conditions of using NaBARF as a Lewis acid to activate the catalyst were applied to this hypothesis. This discovery reduced the number of steps required to prepare the catalyst from two steps to one; instead of forming the Co(II) complex and then reducing that externally to Co(I), the new system allows for *in situ* generation of the Co(I) catalyst. The generation of *in situ* active catalyst eliminates the need for forming, isolating and storing the Co(I) complex thus allowing one to reach the highly versatile boronate ester from a readily available 1,3-diene in one step.

2.6 – Experimental Procedures

General Methods: Air-sensitive reactions were run under an atmosphere of argon using a Schlenk line or a Vacuum Atmospheres glovebox. Dichloromethane (DCM) was dried over calcium hydride (CaH_2) and was freshly distilled before transferring into the dry-box. TLCs were run on pre-coated (0.25 mm) silica gel 60 F254 plates from Silicyle. Flash column chromatography was performed over silica gel 40 acquired from Sorbtech Chemicals. Gas chromatograms were obtained on an Agilent HP-5 with a methyl silicone column (30 m x 0.32 mm, 0.25 μm thickness) using hydrogen for the carrier gas. The GC was equipped with FID detectors and integrators.

Typical Procedure for Catalytic Co(I) Hydroboration: In the dry-box, a 25-mL oven dried Schlenk flask was charged with a magnetic stirrer bar, Co(I)-complex (0.05 eq), and activator (0 to 0.15 eq) and a septum. The flask was taken out of the dry-box and connected to an argon Schlenk line and subjected to three vacuum-then-refill cycles with Ar. Freshly distilled methylene chloride was added via septum. The reaction mixture was cooled to the desired temperature and then (*E*)-1,3-dodecadiene (1.0 eq) was added neat via micro-liter syringe followed by pinacol borane (HBpin) (2.0 eq) and the resulting green solution stirred and warmed to the desired temperature and monitored via G.C-FID by taking an aliquot and adding *n*-pentane or hexanes, filtered through a short pad of silica in a glass pipette and eluting with ether. Upon completion of the reaction, the mixture is diluted with *n*-pentane/ether (1: 1) and filtered over a short pad of silica using a fritted glass funnel (I.D = 1 inch, height of silica pad ~1.5 inch) and concentrated to afford crude product.

Procedure for Table 2.4, entry 4: Prepared according to the typical procedure using (*E*)-1,3-dodecadiene (55 mg, 0.335 mmol), pinacolborane (47 mg, 0.369 mmol), dppbCo(COE$^-$) (10 mg, 0.0168 mmol), H(Et$_2$O)$_2$BARF (13.4 mg, 0.0168 mmol), and DCM (2 mL). Upon completion of the reaction (0.5 h), the reaction was exposed to air and diluted with hexanes and filtered through a short pad of silica using a fritted glass funnel (I.D = 1 inch, height of silica pad ~1.5 inch), and concentrated to afford the tittle compound as a colorless oil (72 mg, 91% yield).

^{1}H NMR (400 MHz, $CDCl_3$, δ): 5.47 – 5.34 (m, 2 H), 2.11 – 2.06 (m, 2 H), 1.96 – 1.91 (m, 2 H), 1.25- 1.23 (br, m, 23 H), 0.87 (t, *J* = 6.4 Hz, 3 H), ^{13}C NMR ($CDCl_3$, δ): 132.2, 129.7, 83.2, 32.9, 32.6, 29.9, 29.8, 29.6, 29.5, 27.2, 25.2, 25.1, 23.0, 14.4.

GC (*methyl silicone*, 120°C for 5 mins then ramp to 250°C at 20°C/min): R_t 10.99 min

Procedure for Table 2.4, entry 11: Prepared according to the typical procedure using (*E*)-1,3-dodecadiene (41 mg, 0.245 mmol**),** pinacolborane (35 mg, 0.269 mmol), **L1**CoBr (10 mg, 0.0184 mmol), NaBARF (9.4 mg, 0.0184 mmol), DCM (2 mL). Upon completion of the reaction (0.5 h), the reaction was exposed to air and diluted with hexanes and filtered through a short pad of silica using a fritted glass funnel (I.D = 1 inch, height of silica pad ~1.5 inch), and concentrated to afford the tittle compound as a colorless oil (55 mg, 76% yield).

^{1}H NMR (400 MHz, $CDCl_3$, δ): 5.51 – 5.38 (m, 1 H), 5.38 – 5.33(m, 1 H), 2.02 – 1.97 (m, 2 H), 1.66 (br, d, *J* = 7.7Hz, 2 H), 1.25- 1.23 (br, m, 23 H), 0.87 (t, *J* = 6.4 Hz, 3 H), ^{13}C NMR ($CDCl_3$, δ): 130.3, 124.2, 83.4, 32.2, 29.9, 29.8, 29.6, 27.3, 25.1, 24.9, 22.9, 14.3

GC (*methyl silicone*, 120°C for 5 mins then ramp to 250°C at 20°C/min): R_t 10.95 min

Procedure for *in situ* generation of active catalyst (Scheme 2.5): Prepared according to the typical procedure using dpppCoBr_2 (10 mg, 0.0159 mmol, 0.05 eq), Zn dust (10 mg, 0.1589 mmol, 0.5 eq.), NaBARF (10 mg, 0.0159 mmol, 0.05 eq), DCM (2 mL), 1,3-(*E*)-dodecadiene (48 mg, 0.3174 mmol, 1.0 eq), HBpin (50 µL, 0.3492 mmol, 1.1 eq.) Upon completion of the reaction (0.25 h) the mixture is diluted with *n*-pentane/ether (1: 1) and filtered over a short pad of silica using a fritted glass funnel (I.D = 1 inch, height of silica pad ~1.5 inch) and concentrated to afford the title compound as a colorless oil (72 mg, 81% yield).

^{1}H NMR (400 MHz, $CDCl_3$ δ): 5.47 – 5.34 (m, 2 H), 2.11 – 2.06 (m, 2 H), 1.96 – 1.91 (m 2 H), 1.25- 1.23 (br, m, 23 H), 0.87 (t, *J* = 6.4 Hz, 3 H), ^{13}C NMR ($CDCl_3$, δ): 132.2, 129.7, 83.2, 32.9, 32.6, 29.9, 29.8, 29.6, 29.5, 27.2, 25.2, 25.1, 23.0, 14.4.

GC (*methyl silicone*, 120°C for 5 mins then ramp to 250°C at 20°C/min): R_t 10.99 min

Chapter 3: Cobalt (II) Mediated Heterodimerization of 1,3-(*E*)-dienes and Methyl Acrylates

3.1 – Established Conditions for Heterodimerization

Heterodimerization reactions between dienes and acrylates have the potential for broad synthetic utility. The starting materials for this reaction are readily available: 1,3-dienes can be synthesized via the Wittig reaction and acrylates are produced in a multi-ton scale for industrial application. The established conditions for this reaction by Jing and co-workers[23] include combining the isolated metal complex (0.05 eq.), sodium tetrakis[3,5-bis(trifluoromethyl)-phenyl] borate, hereafter mentioned as NaBARF, as the activator (0.075 eq.), activated Zn dust as the reducing agent (1.00 eq.), the diene (1.00 eq.) and the acrylate (1.10 eq.) in DCM at room temperature to yield nearly enantio-pure skipped 1,4-diene esters (Scheme 3.1).

Scheme 3.1 Established conditions for heterodimerization Reaction[23]

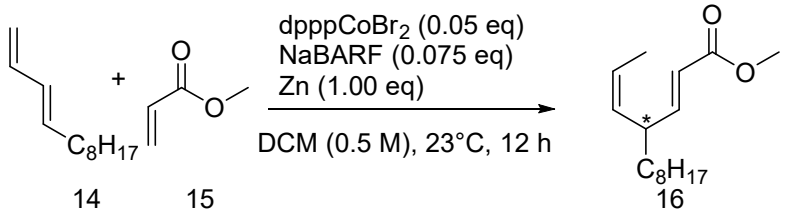

All of the optimization reactions were done using Co(I) and reported in Dr. Stanley Jing's doctoral dissertation.[11] Limitations for these reaction conditions include cost-prohibitive methods of synthesizing NaBARF. Although NaBARF is commercially available, the high cost of purchasing this activator, $146.50 for 250 mg from the seller Sigma-Aldrich, was slightly offset by manually synthesizing it. Synthesizing NaBARF is a time-consuming process. In the scan for activators, Dr. Jing had noticed that $ZnCl_2$ was the only other activator that gave full conversion however the slow reaction time discouraged further study of the Lewis Acid. Leitner *et. al* had explored the activation of Ni-catalyzed hydrovinylation with Lewis acids in 2009.[25] Inspired by

Leitner's success of using cost-effective activators, new reaction conditions for the heterodimerization reaction were explored using other Lewis Acids activators as a replacement for NaBARF. This chapter deals with the explorations of these activators that led to the discovery of practical processes for the heterodimerization reaction.

3.2 – Optimization of New Reaction Conditions

In Leitner's activator scan, the only Lewis Acid that gave greater than 90% conversion to the hydrovinylated product was InX_3 (X = Cl, Br) with -40°C as the activation temperature.

Scheme 3.2: Hydrovinylation scheme from Leitner *et al*

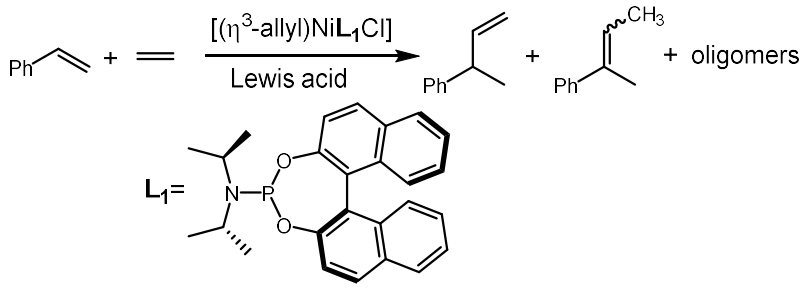

Thus, for the first experiment to test if the Lewis Acid could generate the active catalyst, $InBr_3$ was added in excess as a substitute for NaBARF but the reaction temperature, catalyst loading, and Zn as the reducing agent, were kept constant. Surprisingly, activation of the catalyst with $InBr_3$ gave full conversion of starting material to products with the same GC distribution of the heterodimerized adduct as the established conditions (Figure 3.1 vs Figure 3.3).

Inspired by this, the necessity of using Zn as the reducing agent was examined. At least half equivalent of Zn with respect to the starting material was needed as the reducing agent. Additionally, using Zn as a reducing agent in this reaction yields a side product of ZnX_2 which in

Figure 3.1: Achiral Stationary Phase Gas Chromatogram of established experiments with Zn/NaBARF[23]

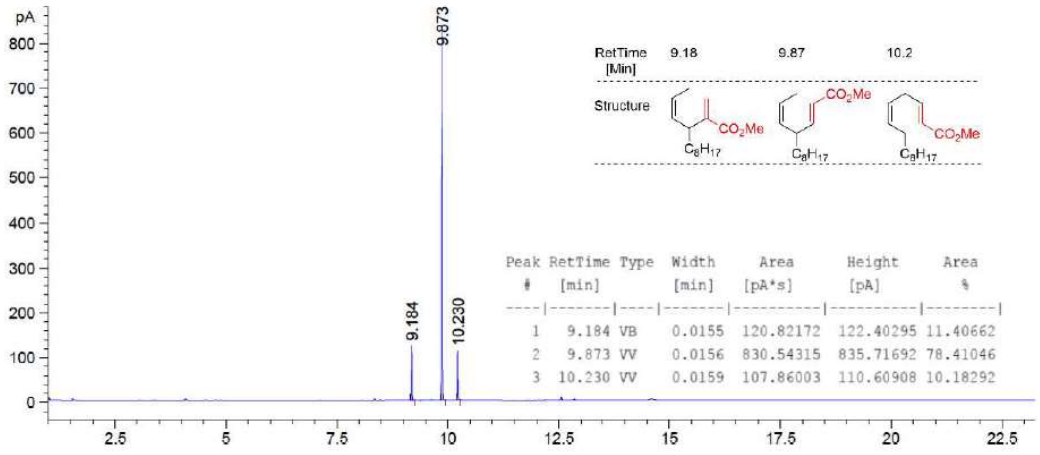

itself is a Lewis acid. This limits the reaction as acid sensitive functional groups would not survive under the reaction conditions. To find alternatives to Zn, different transition-metal free reducing agents were scanned.

Scheme 3.3: Conditions for reducing agent and activator scan

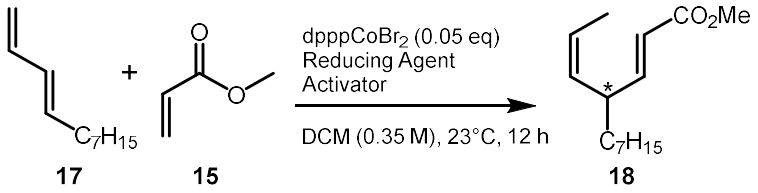

The reducing agents scanned were lithium nitride, 1,4-*bis*-(trimethylsilane)-1,4-dihydropyrazine and 2,3,5,6-tetramethyl-1,4-*bis*-(trimethylsilane)-1,4-dihydropyrazine. Of the three reducing agents, lithium nitride most consistently gave full conversion from starting material to products. The other two heterocyclic organic reducing agents, 1,4-*bis*-(trimethylsilyl)-1,4-dihydropyrazine and 2,3,5,6-tetramethyl-1,4-*bis*-(trimethylsilyl)-1,4-dihydropyrazine (Figure 3.1), gave poor or no conversion using either $InBr_3$ or NaBARF as the activator. The poor reactivity with the catalyst system when the pyrazine derived reducing agents

could potentially be attributed to side polymerization reactions with the acrylate induced by the non-metallic reducing agent or to inhibition by the heterocyclic byproduct which could serve as a ligand thus causing inhibition.

Table 3.1: Results on Survey of Reducing agents and activators

Entry	Catalyst	Reducing agent (0.25 eq.)	Activator (0.10 eq.)	[a]Conv. (%)	Time (h)	Isolated Yield (%)
1	dpppCoBr$_2$	Li$_3$N	InBr$_3$	100	7	65
2	dpppCoBr$_2$	Li$_3$N (0.10 eq.)	InBr$_3$	100	2	79
3	dpppCoBr$_2$	Li$_3$N (0.10 eq.)	NaBARF	100	2	52
4[b]	dpppCoBr$_2$	Li$_3$N	InCl$_3$	100	2	83
5	dpppCoBr$_2$	TMS-DHPy	InBr$_3$	46	12	20
6	dpppCoBr$_2$	TMS-DHPy	NaBARF	7	24	-
7	dpppCoBr$_2$	TMS-DHPy	InCl$_3$	0	24	-
8	dpppCoBr$_2$	Tetra-Me-TMS-py	InBr$_3$	1	24	-
9	dpppCoBr$_2$	Tetra-Me-TMS-py	NaBARF	28	24	-
10	dpppCoBr$_2$	Tetra-Me-TMS-py	InCl$_3$	18	24	-
11	dpppCoCl$_2$	Li$_3$N (0.10 eq.)	InBr$_3$	98	0.25	91
12	dpppCoCl$_2$	Li$_3$N (0.10 eq.)	NaBARF	100	24	70
13	dpppCoCl$_2$	Li$_3$N	InCl$_3$	80	24	-
14	dpppCoCl$_2$	TMS-DHPy	InBr$_3$	9	24	-
15	dpppCoCl$_2$	TMS-DHPy	NaBARF	0	24	-
16	dpppCoCl$_2$	TMS-DHPy	InCl$_3$	0	24	-
17	dpppCoCl$_2$	Tetra-Me-TMS-py	InBr$_3$	10	24	-
18	dpppCoCl$_2$	Tetra-Me-TMS-py	NaBARF	49	24	-
19	dpppCoCl$_2$	Tetra-Me-TMS-py	InCl$_3$	11	24	-

[a]Conversion based on disappearance of starting material on GC; [b]InCl$_3$ loading was 0.30 eq. with respect to catalyst

Leitner *et. al*[25] reports that both InBr$_3$ and InI$_3$ provide excellent conversion to product for the hydrovinylation reaction (Scheme 3.2). The heterodimerization reaction was tested with InCl$_3$ as an activator as well, and these conditions provide the same results as does InBr$_3$. There is no significant difference observed when using the Li$_3$N/InX$_3$ (X = Cl, Br) combination with dpppCoX$_2$ (X = Cl, Br) (Table 3.1, entries 2 and 11). Although these reactions all indicated 100% conversion from starting materials to products, some product was lost during the isolation of product. NaBARF is not as easy to separate from the reaction mixture as the metal halides are.

Figure 3.2: Achiral Stationary Phase Gas Chromatogram of starting material

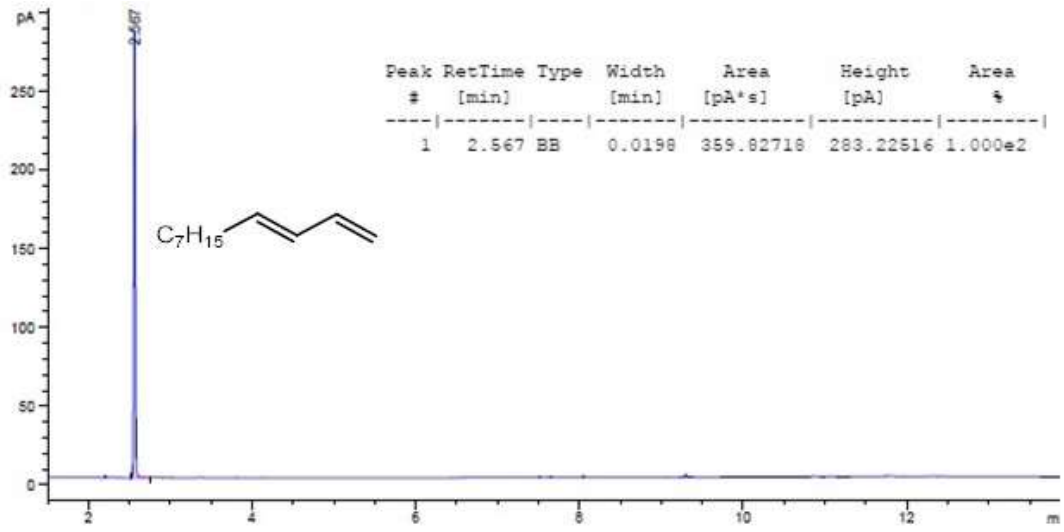

Figure 3.3: Achiral Stationary Phase Gas Chromatogram of Table 3.1, Entry 11 ($Li_3N/InBr_3$)

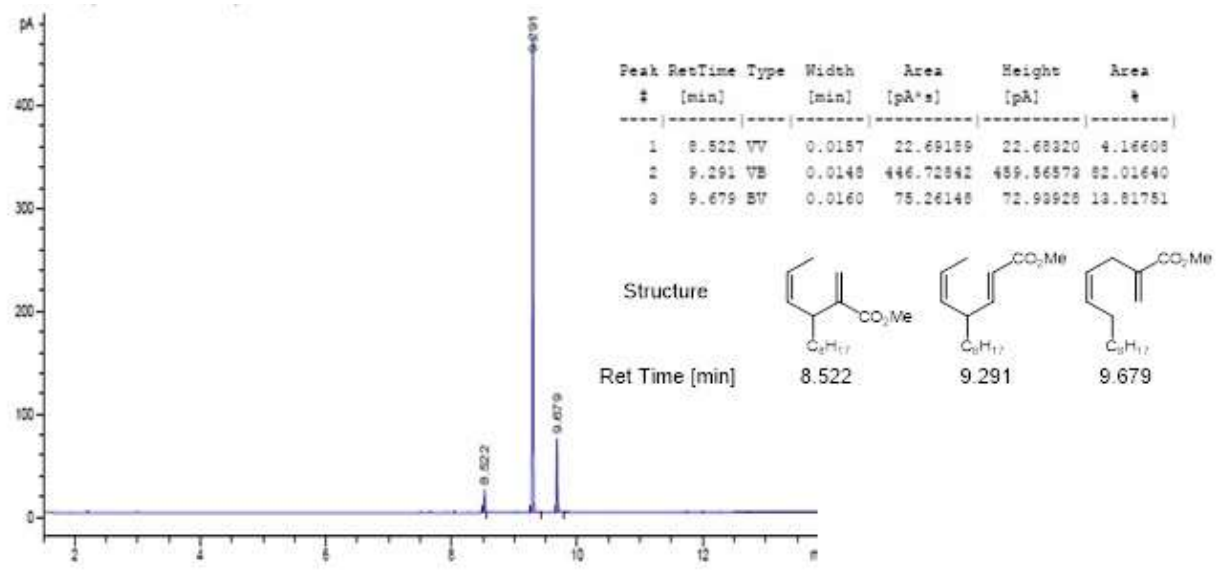

The metal halide reactions only require filtering through a short pad of silica, provided the reaction has undergone full conversion, whereas separation from NaBARF requires a longer pad of silica. Since residues from NaBARF is not as polar as the metal halides, there is a chance that if the silica pad is too short, the activator residues will end up in the isolated product which can be determined by a pink tint in the supposed isolated compound vial. When this happens, the

solvent is evaporated and the product is ran through another short pad of silica, however these multiple runs through silica to isolate the product all result in the loss of some product in the silica itself or in transfer from glassware. These scans were done on a 40 mg scale thus any transferal or secondary filtration step saw some loss of yield, which explains the lower isolated yields with NaBARF as the activator.

Figure 3.4: Structures of reducing agents

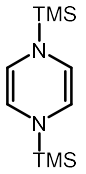

1,4-bis(trimethylsilyl)-1,4-dihydropyrazine
[TMS-DHPy]

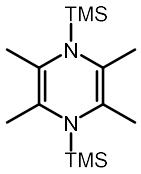

2,3,5,6-tetramethyl-1,4-bis(trimethylsilyl)-1,4-dihydropyrazine
[Tetra-Me-TMS-py]

Although 1,4-*bis*-(TMS)-1,4-dihydropyrazine and 2,3,5,6-tetramethyl-1,4-*bis*-(TMS)-1,4-dihydropyrazine indicate some conversion of the starting material to the target product, the rate of conversion is too slow. After twenty-four hours, even if the reaction is being run in the glovebox, the catalyst is considered dead so there would be no further conversion to product (Table 3.2, entries 14-19). Though these reducing agents show promise of entirely transition metal free reaction conditions, further optimization is necessary with an activator that is more suited to the heterodimerization conditions in order to reach full conversion to desired products.

To ensure continuity throughout the scans in Table 3.1, all experiments were tracked after the first two hours, then based on percent conversion the reactions were either allowed to continue stirring or quenched to be worked up. When testing the new activators, each was added at 0.25 equivalents with respect to substrate. The activator InX_3 (X = Cl, Br) was then optimized to 0.10 equivalent loading with respect to substrate. The activator NaBARF has been reported to work with loading as low as 0.07 equivalents[23], but NaBARF was used at a 0.10 equivalent loading to

stay consistent with the equivalence of the indium-based activators. The reducing agents were also loaded at 0.25 equivalents with respect to substrate when first testing their reactivity with these starting materials.

Lithium nitride was optimized to 0.10 equivalents due to its reactivity whereas the other two pyrazine-based reducing agents were kept at 0.25 equivalent loading since they did not give quantitative conversion. The pyrazine based reducing agents still gave poor conversion even though they were used in excess with respect to the catalyst which further indicated that these conditions were not compatible with this specific reaction (Table 3.2, entries 5-10 and 14-19). However, the experiment with the $Li_3N/InBr_3$ conditions was tracked at fifteen minutes and showed full conversion (Table 3.1, entry 11) as compared to no conversion to the desired product with the 1,4-*bis*-(TMS)-1,4-dihydropyrazine/$InBr_3$ combination (Table 3.1, entry 14) or 2,3,5,6-tetramethyl-1,4-*bis*-(TMS)-1,4-dihydropyrazine/$InBr_3$ combination (Table 3.1, entry 17). This indicates that this combination of reducing agent and activator converts the starting material to product at a rate comparable to the established conditions by Jing *et al.* The reducing agent and activator scan indicate that Li_3N and InX_3 are excellent substitutes for the original reagents NaBARF and Zn dust.

3.3 – *in situ* Generation of Active Metal Complex

Discovering the ability to reduce the Co(II) metal complex to Co(I) *in situ* reduces the number of steps of the reaction. Both the catalyst and diene need to be previously prepared and stored which compounds time for the heterodimerization reaction. To further simplify the preparation of the reaction, the metal complex needs to be generated *in situ* as well – this would make this reaction truly a ‘dump and stir’ reaction. Using the newly discovered reaction

conditions of $Li_3N/InBr_3$, commercially available ligands such as 1,3-*bis*(diphenylphosphino)-propane, abbreviated as dppp, and cobalt salt were combined with the activator and Lewis Acid in DCM, and then the starting materials were added. This procedure also affords greater than 97% conversion to the desired heterodimerized adduct as shown by the gas chromatogram below (Figure 3.5). These are truly optimized conditions for the heterodimerization reaction as none of the materials, aside from the diene which is prepared from an aldehyde via a simple Wittig reaction, need to be prepared prior to executing the experiment. This experiment reaches full completion in fifteen minutes under inert atmosphere at room temperature (Scheme 3.4).

Scheme 3.4: Optimized *in situ* generation of catalyst conditions

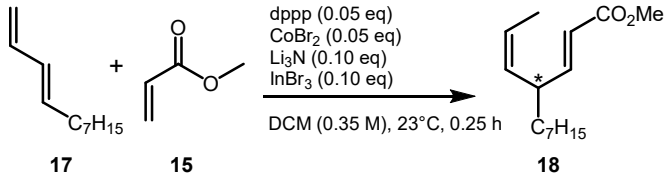

Figure 3.5: Achiral Stationary Phase Gas Chromatogram of *in situ* generation of catalyst

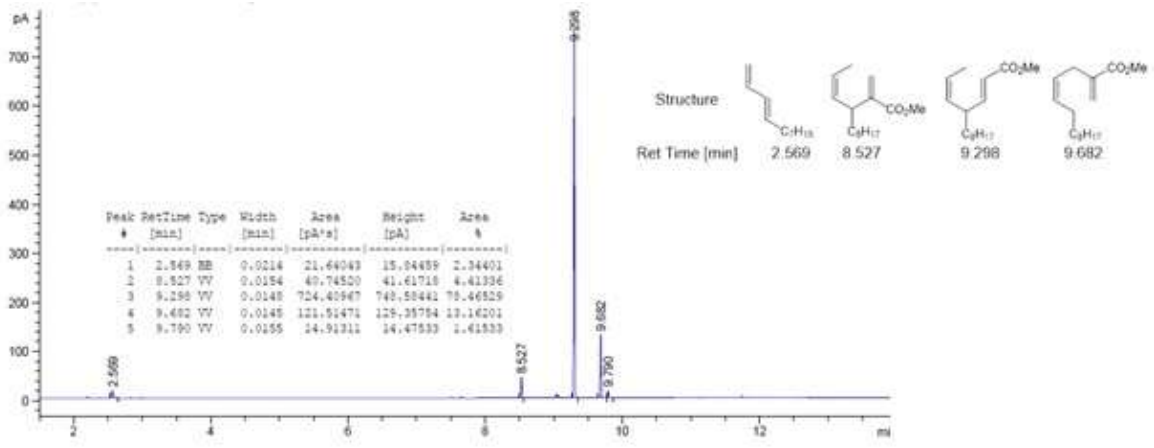

The heterodimerization reaction yields a chiral center but when conducted with achiral ligands such as dppp the product is racemic. To test whether these new conditions would provide the same enantioselectivity as previously established[22] the chiral version of dppp, (*S,S*)-BDPP was used in these reaction conditions as shown in Scheme 3.5 below. The resulting product

provided the *R* enantiomer in excellent enantiomeric excess, 99% ee (Figure 3.6), although the yield was low as the reaction did not go to full completion even after four hours (Figure 3.7).

Scheme 3.5: Enantioselectivity with New Conditions

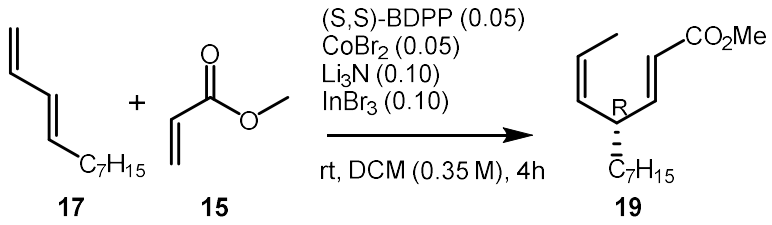

Figure 3.6: Chiral Stationary Phase Gas Chromatogram showing Enantioselectivity of Reaction Shown in Scheme 3.5

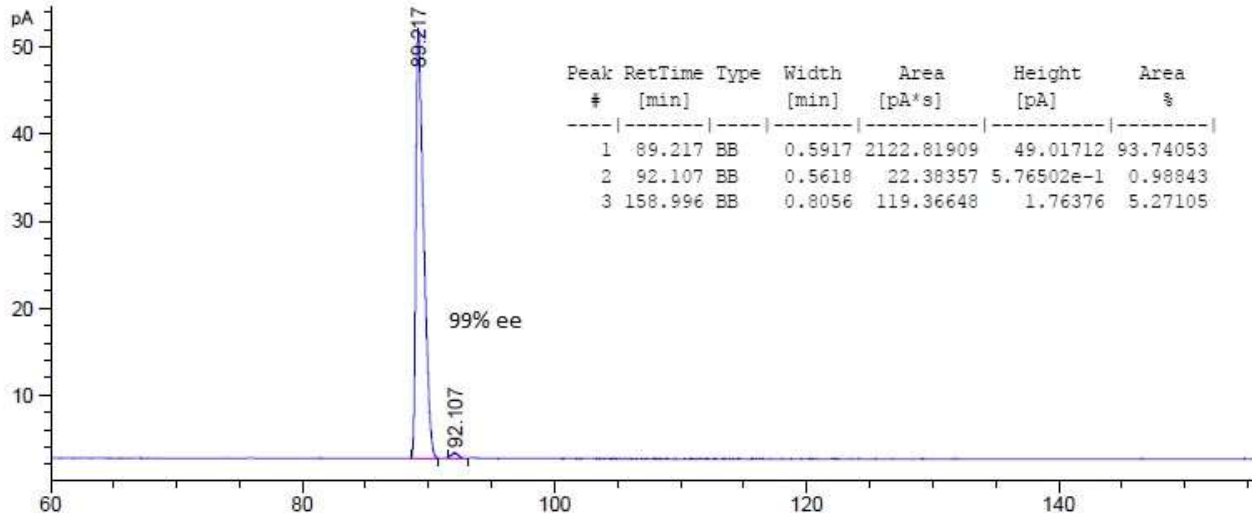

The slower rate of reaction can be attributed to the increased steric demand and orientation of the methyl groups on (*S,S*)-BDPP. The chiral version of the heterodimerization reaction requires reaction times as long as four hours when compared to relatively short reaction times its racemic counterpart dppp requires to afford full conversion of starting materials to products. The heterodimerized adduct is afforded in 99% *ee* with (*S,S)*-BDPP which inspires further studies to be conducted with different chiral ligands to fully explore the scope of this reaction.

Figure 3.7: Achiral Gas Chromatogram showing Incomplete Conversion of Reaction Shown in Scheme 3.5

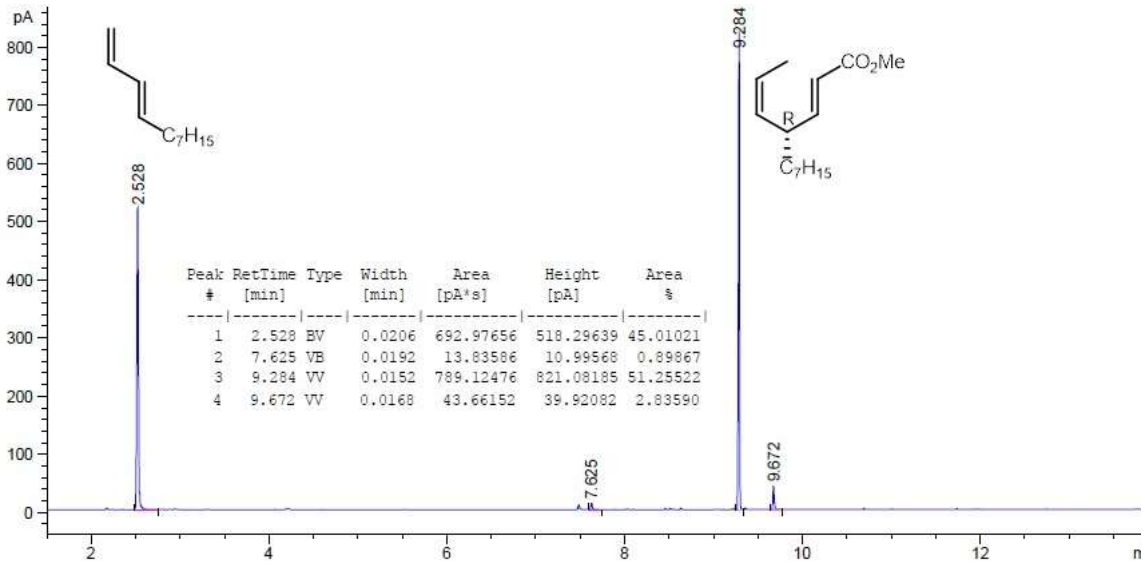

Peak #	RetTime [min]	Type	Width [min]	Area [pA*s]	Height [pA]	Area %
1	2.528	BV	0.0206	692.97656	518.29639	45.01021
2	7.625	VB	0.0192	13.83586	10.99568	0.89867
3	9.284	VV	0.0152	789.12476	821.08185	51.25522
4	9.672	VV	0.0168	43.66152	39.92082	2.83590

3.4 – Further Functionalization of skipped 1,4-diene esters

The heterodimerization reaction yields an α,β-unsaturated carboxylic ester moiety which allows for further functionalization of the product via the Michael Addition reaction. This addition reaction increases the complexity of the compound by introducing a second chiral center adjacent to the chiral center set by the heterodimerization reaction. The experimental conditions and yields for the three Michael addition products that were prepared are summarized in Figure 3.8 with the full procedures and NMR data detailed in the Experimental Section.

Although these reactions afford a poor yield, these products were purified, isolated and analyzed. The 1,4-addition reaction was attempted with an organocopper reagent, however excess MeLi in the reaction mixture yielded a reduced tertiary alcohol. Through ^{1}H NMR and ^{13}C NMR analysis, the product was determined to be diastereomeric alcohols, however the fact that there is a methyl substitution at the C4 position of **22** proves that alkyl addition is possible at that position. The ^{1}H NMR and ^{13}C NMR data for compound **21** indicate clean separation from

Figure 3.8: Further functionalization of heterodimerized adduct

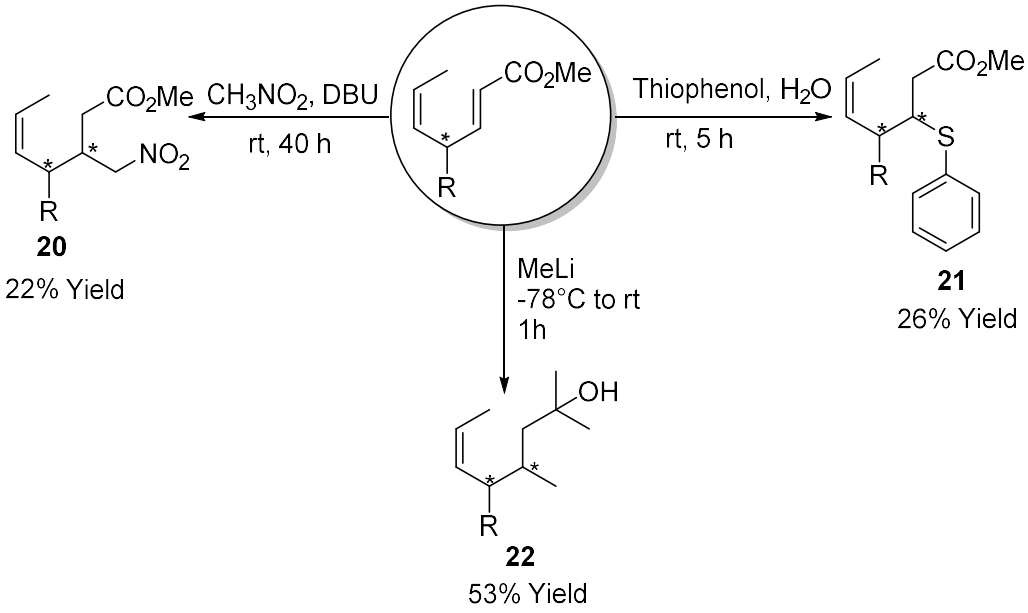

any other impurities in the reaction mixture thus providing high potential for utilizing this reaction to make a more complex molecule. Compound **20** was not able to be as cleanly separated from impurities in the reaction mixture. Upon analysis of ^{1}H NMR peaks and splitting patterns specific to the **20**, it was determined that the desired compound was formed albeit in low yields.

3.5 – Summary and Conclusion

The novel heterodimerization reaction provides an excellent way to yield highly enantiopure skipped 1,4-diene esters. The established conditions for these reactions afford high yields and high enantioselectivity but are cost prohibitive due to the use of NaBARF. The established conditions are also limiting in terms of acid-sensitive functional groups due to the Lewis acid byproduct formed when using Zn as the reducing agent. To circumvent these limitations, different reducing agents and activators were scanned to see if they can substitute the established reagents. The Li_3N/InX_3 combination of reducing agent and activator afford the desired product

in the highest yield and in the shortest reaction times with dpppCoX_2 as the catalyst. The electron rich pyrazine reducing agents probably do not work as they trap the electron deficient methyl acrylate which would eliminate the possibility of the heterodimerization reaction in the reaction mixture.

To further simplify this reaction, the conditions were optimized to simply adding the ligand, Co salt, reducing agent, activator and starting materials – a 'dump and stir' reaction – to yield the same distribution of products as the reaction with the isolated metal complex did. These new conditions were then tested with the chiral version of dppp, (*S,S*)-BDPP and resulted in 99% enantioselective excess though the reaction did not reach full conversion in four hours. Further optimization is needed before the scheme can be fully implemented. The α,β-unsaturated carboxylic ester moiety of the heterodimerized product can also be utilized to increase the complexity of the compound (Figure 3.8).

For future work, the electron rich alkene connected to an electron deficient α,β-unsaturated carboxylic ester by a chiral center provides opportunities for further functionalization other than those discussed in this thesis. The one-step approach to synthesizing this skipped 1,4-diene ester with commercial reagents greatly increases the time and cost effectiveness of the reaction thus providing significant benefits to large-scale synthesis of advanced intermediates containing the 1,4-diene ester moiety. Further studies will involve expanding these reagent conditions to other hydrofunctionalization reaction such as hydroboration, hydrosilylation and hydrovinylation as well as expanding the functional group scope at the C-4 position.

3.6 – Experimental Section

General Details:

Glass vials used for reactions were purchased from VWR (8 mL, screw-thread sample vials, PTFE-faced silicone septa) and the caps were dried in a desiccator over night while the vials were dried in an oven at 160 °C for 24 h before transferring into the dry-box. Dichloromethane (DCM) was dried over calcium hydride (CaH_2) and was freshly distilled before transferring into the dry-box. Flash column chromatography was carried out on silica gel 40 (Scientific Adsorbents Incorporated, Microns Flash). Gas chromatographic analysis of reaction mixtures was done on an Agilent HP 5890 GC equipped with HP- 5MS column (30 m, 0.32 mm I.D, 0.25μm) and hydrogen as carrier gas with FID detector at 250 °C. GC-MSD analysis was performed on a 6850GC-5975MSD equipped with an EI impact ionization. Enantiomeric excesses of chiral compounds were determined by chiral gas chromatrographic analyses which were performed on an Agilent 7850 A equipped with a cyclosil-B or cyclodex-B column, hydrogen carrier gas, and an FID detector at 250°C.

Procedure for 1,3-(*E*)-undecadiene Synthesis:

1,3-(*E*)-undecadiene was prepared following typical C-1 Wittig procedure using methyltriphenylphosphonium bromide (28 g, 78.383 mmol, 1.1 eq.), *n*-butyllithium (34 mL, 2.5 M in hexane, 1.2 eq.), and 2-(*E*)-decenal (10 g, 71.428 mmol, 1.0 eq.) in THF (315 mL, 0.25 M). Upon completion of the reaction (1 h), the product was quenched with NH_4Cl, extracted with Et_2O (100 mL x 3, purified via flash chromatography in pentane, and concentrated to afford the title compound as a colorless oil (7.00 g, 71% yield).

^{1}H NMR (400 MHz, $CDCl_3$, δ): 6.31 (dt, *J* = 17 Hz 1H), 6.05 (dd, *J* = 15 Hz 1H), 5.70 (quin., *J* = 15 Hz, 1 H), 5.10 (d, *J* = 17 Hz, 1H), 4.96 (d, *J* = 10 Hz, 1H), 1.31-1.24 (m, 12H), 0.88 (t, *J* = 7 Hz, 3H)

GC (*methyl silicone*, 100°C for 5 mins then ramp to 250°C at 20°C/min): R_t 2.52 min

Typical Procedure for Table 3.1 Experiments (all reactions done in drybox):

In the dry box, an 8-mL oven dried vial with a septum cap was charged with magnetic stirrer bar, isolated metal complex (0.05 eq.), reducing agent (0.25 eq.), activator (0.10 eq.) and DCM (0.35 M). The vial was capped and while stirring the mixture, neat (*E*)-1,3-undecadiene (1.00 eq.) followed by distilled methyl acrylate (1.10 eq.) was added via micro-liter syringe. The resulting green solution was allowed to stir at room temperature and monitored via GC-FID by taking an aliquot with a glass pipette, removing from dry box atmosphere, adding 1:1 ether/hexanes, filtering through a short pad of silica in a glass pipette, and eluting with ether. Upon completion of the reaction, the mixture is diluted with 1:1 ether/hexane, filtered over a short pad of silica using a fritted glass funnel (I.D = 1 inch, height of silica pad ~1.5 inch), and concentrated.

Procedure for Table 3.1, Entry 2:

Prepared according to typical procedure using dpppCoX_2 (0.05 eq.), Li_3N (1.14 mg, 0.0329 mmol), $InBr_3$ (13 mg, 0.0329 mmol) DCM (0.94 mL), (E)-1,3-undecadiene (50 mg, 0.3289 mmol), and distilled methyl acrylate (31 mg, 0.3618 mmol). Upon completion of the reaction (2 h), the mixture is exposed to air and diluted with 1:1 ether/hexane, filtered over a

short pad of silica using a fritted glass funnel, and concentrated to afford the title compound (61 mg, 79% yield) as a colorless oil.

^{1}H NMR (400 MHz, $CDCl_3$,δ): 6.84 (q, *J* = 15 Hz, 1H), 5.80 (dd, *J* = 15 Hz, 1H), 5.57-5.53 (m, 1H), 5.22-5.17 (m, 1H), 3.72 (s, 3H), 3.20-3.13 (m, 1H), 1.60 (dd, *J* = 7 Hz, 3H), 1.50-1.45 (m, 1H), 1.40-1.33 (m, 1H), 1.26 (s, 12H), 0.86-0.89 (t, 3H),; ^{13}C NMR ($CDCl_3$, δ): 167.7, 152.2, 133.4, 126.0, 119.8, 51.7, 40.3, 34.9, 32.2, 29.8, 29.5, 29.3 27.4, 22.9, 14.4, 13.5.

GC (*methyl silicone*, 100°C for 5 mins then ramp to 250°C at 20°C/min): R_t 9.28 min

*The above procedure was employed with $X_2 = Cl_2$ (8.8 mg, 0.0164 mmol), Br_2 (10 mg, 0.0164 mmol); as well as with activators NaBARF (29 mg, 0.0329 mmol), $InCl_3$ (7.3 mg, 0.0329 mmol) and reducing agents 1,4-*bis*-(TMS)-1,4-dihydropyrazine (18 mg, 0.0822 mmol) and 2,3,5,6-tetramethyl-1,4-*bis*-(TMS)-1,4-dihydropyrazine (23 mg, 0.0822 mmol).

General Procedure for *in situ* generation of metal complex:

An 8 mL oven dried vial equipped with a septum cap was charged with a magnetic stirrer bar, ligand (0.05 eq.), cobalt (II) salt (0.05 eq.) and DCM (0.35 M) and allowed to stir for 15 min. Reducing agent (0.10 eq.) was then added and the solution was allowed to stir for another 15 minutes. Activator (0.10 eq.), 1,3-(E)-undecadiene (50 mg, 0.3289 mmol, 1.00 eq.), and distilled methyl acrylate (31 mg, 0.3618 mmol, 1.10 eq.) were then added via micro-liter syringe. The mixture was stirred at room temperature and monitored by taking an aliquot using a glass pipette, diluting with mixture of ether/hexane (1:1) and filtered through a short pad of silica in a glass pipette eluting with ether and analyzed via GC. Upon completion of the reaction (0.25 h), the mixture is exposed to air and diluted with 1:1 ether/hexane, filtered over a short pad of silica

using a fritted glass funnel (I.D = 1 inch, height of silica pad ~1.5 inch), and concentrated to afford the title compound as a colorless oil.

Scheme 3.4: Optimized *in situ* Generation of Catalyst Conditions (Racemic):

Prepared according to the typical procedure using dppp (9 mg, 0.0222 mmol), cobalt dibromide salt (4.0, 0.0181 mmol, mg), DCM (0.94 mL, 0.35 M), Li_3N (1.14 mg, 0.0329 mmol), $InBr_3$ (11 mg, 0.0329 mmol), 1,3-(E)-undecadiene (50 mg, 0.3289 mmol), and distilled methyl acrylate (31 mg, 0.3618 mmol). Upon completion of the reaction (0.25 h), the mixture is exposed to air and diluted with 1:1 ether/hexane, filtered over a short pad of silica using a fritted glass funnel, and concentrated to afford the title compound (71 mg, 91% yield) as a colorless oil.
^{1}H NMR (400 MHz, $CDCl_3$,δ): 6.84 (q, *J* = 15 Hz, 1H), 5.80 (dd, *J* = 15 Hz, 1H), 5.57-5.53 (m, 1H), 5.22-5.17 (m, 1H), 3.72 (s, 3H), 3.20-3.13 (m, 1H), 1.60 (dd, *J* = 7 Hz, 3H), 1.50-1.45 (m, 1H), 1.40-1.33 (m, 1H), 1.26 (s, 12H), 0.86-0.89 (t, 3H),; ^{13}C NMR ($CDCl_3$, δ): 167.7, 152.2, 133.4, 126.0, 119.8, 51.7, 40.3, 34.9, 32.2, 29.8, 29.5, 29.3 27.4, 22.9, 14.4, 13.5.
GC (*methyl silicone*, 100°C for 5 mins then ramp to 250°C at 20°C/min): R_t 9.28 min

Scheme 3.5: Enantioselectivity with New Conditions (Chiral):

Prepared according to the typical procedure using (S,S)-BDPP (9.7 mg, 0.0222 mmol), cobalt dibromide salt (4.0, 0.0181 mmol, mg), DCM (0.94 mL, 0.35 M), Li_3N (1.14 mg, 0.0329 mmol), $InBr_3$ (11 mg, 0.0329 mmol), 1,3-(E)-undecadiene (50 mg, 0.3289 mmol), and distilled methyl acrylate (31 mg, 0.3618 mmol). Upon completion of the reaction (0.25 h), the mixture is exposed to air and diluted with 1:1 ether/hexane, filtered over a short pad of silica using a fritted

glass funnel, and concentrated to afford the title compound (40 mg, 50% yield, 99% ee) as a colorless oil.

^{1}H NMR (400 MHz, $CDCl_3$,δ): 6.84 (q, *J* = 15 Hz, 1H), 5.80 (dd, *J* = 15 Hz, 1H), 5.57-5.53 (m, 1H), 5.22-5.17 (m, 1H), 3.72 (s, 3H), 3.20-3.13 (m, 1H), 1.60 (dd, *J* = 7 Hz, 3H), 1.50-1.45 (m, 1H), 1.40-1.33 (m, 1H), 1.26 (s, 12H), 0.86-0.89 (t, 3H),; ^{13}C NMR ($CDCl_3$, δ): 167.7, 152.2, 133.4, 126.0, 119.8, 51.7, 40.3, 34.9, 32.2, 29.8, 29.5, 29.3 27.4, 22.9, 14.4, 13.5.

GC (*methyl silicone*, 100°C for 5 mins then ramp to 250°C at 20°C/min): R_t 9.28 min

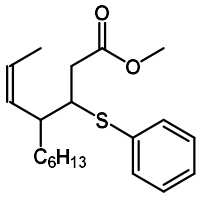

Thiol Addition to Heterodimerized Product (21):

Methyl-(*E*)-4-((*Z*)-prop-1-en-1-yl)dec-2-enoate (50 mg, 0.2224 mmol, 1.0 eq.) in water (0.50 mL) was treated with thiophenol (21 mg, 0.2450 mmol, 1.1 eq.)) under magnetic stirring at room temperature until complete consumption of the starting material (30 mins: TLC). The reaction mixture was extracted with EtOAC (3 x 5 mL). The combined EtOAc extracts were dried (Na_2SO_4) and concentrated under reduced pressure to afford an oil which on passing through a column of silica gel and elution with EtOAc:hexane (1:1) afforded the β-substituted product: methyl-(*Z*)-2-(phenylthio)-4-prop-1-en-yl)decanoate as a colorless oil (20 mg, 26% yield).

^{1}H NMR ($CDCl_3$, 400 MHz) δ: 7.50-6.83 (m, 5H), 5.77-5.79 (dd, 1H), 5.59-5.54 (m, 1H), 5.21-5.18 (m, 1H), 3.72 (s,3H), 3.19-3.14 (m 1H), 1.60 (dd, *J* = 6.8 Hz, 1.7 Hz 3H), 1.25 (s,12H), 0.86-0.89 (t, *J* = 7.05 Hz, 3H). ^{13}C NMR ($CDCl_3$, 75 MHz) δ: 167.3, 152.4, 130.9, 129.1, 127.5, 127.2, 125.7, 119.5, 51.4, 39.9, 34.6, 31.7, 29.5, 29.4, 27.1, 22.7, 14.1, 13.1.

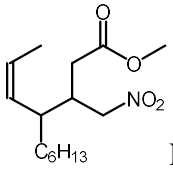

Nitromethane Addition to Heterodimerized Product (20):

Methyl-(*E*)-4-((*Z*)-prop-1-en-1-yl)dec-2-enoate (50 mg, 0.2224 mmol, 1.0 eq.) in CH_3NO_2 (60 µL, 1.11 mmol, 5.0 eq.) was treated with DBU (6.6 µL, 0.0446 mmol, 0.2 eq.) under magnetic stirring at room temperature (25°C). The reaction mixture was tracked by GC and extracted with Et_2O (3 x 5 mL) upon complete consumption of the starting material (40 h). The combined Et_2O phases were combined, washed with 1N HCl/H_2O (2 x 5 mL), dried (Na_2SO_4) and concentrated under reduced pressure to afford an oil. The residue was purified by silica get column chromatography (hexane/EtOAc, 6:1) to afford the β-substituted product: methyl (*Z*)-3-(nitromethyl)-4-(prop-1-en-1-yl)decanoate as a colorless oil (14 mg, 22% yield). ^{1}H NMR ($CDCl_3$, 400 MHz) δ: 5.56-5.54 (m, 4H), 4.51-4.47 (m, 1H), 4.42-4.39 (m, 1H), 3.68 (m, 5H), 3.66 (br s, 1H), 3.15 (d, *J* = 7.3 Hz, 1H), 2.98 (d, *J* = 7.0 Hz, 1H), 2.07 (q, *J* = 7.7 Hz, 4H), 1.77-1.76 (dd, *J* = 7.0 Hz, 1.7 Hz 2H), 1.58 (dd, *J* = 6.8 Hz, 1.7 Hz, 3H), 1.55 (dd, *J* = 6.8 Hz, 1.7 Hz, 2H), 1.25 (s, 35H), 0.88-0.86 (t, *J* = 6.9 Hz, 8H),; ^{13}C NMR ($CDCl_3$, 75 MHz) δ: 140.2, 132.2, 130.7, 130.2, 128.3, 126.0, 120.1, 117.9, 52.1, 38.9, 38.1, 37.9, 37.6, 34.8,343, 33.7, 32.2, 29.8, 22.9, 14.4.

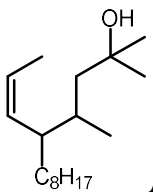

Alkyl Addition to Heterodimerized Product (22):

In the dry-box, a 25-mL oven dried Schlenk flask was charged with a magnetic stirrer bar and CuI (42 mg, 0.2183 mmol). The flask was taken out of the dry box and connected to an argon Schlenk line and flushed once with argon. The salt was then dissolved in freshly distilled THF (1.5 mL, 0.15M) and cooled to -78°C. Methyllithium (0.70 mL, 0.4365 mmol) was slowly added at -78°C, then the solution was allowed to warm to 0°C and stir for 30 mins. The solution was then cooled back down to -78°C, the substrate, methyl-(*E*)-4-((*Z*)-prop-1-en-1-yl)dodec-2-enoate (50 mg, 0.1981 mg), was added via micro-liter syringe, and the solution was allowed to warm to room temperature. The product was extracted with Et_2O (5 mL x 3), dried over Na_2SO_4, concentrated, and purified via column chromatography eluting with 5% Et_2O/Hexane to afford a diastereomeric mixture of (Z)-2,4-dimethyl-5-(prop-1-en-1-yl)tridecan-2-ol as a colorless oil (28 mg, 53% yield).

^{1}H NMR ($CDCl_3$, 400 MHz) δ: 7.36 (s, 1H), 7.26 (s, 1H), 5.51-5.546 (m, 2H), 5.19 (t, J = 6.8 Hz, 1H), 2.98 (quint, J = 15 Hz, 1H), 1.61-1.60 (dd, J = 6.8 Hz, 1.7 Hz, 3H), 1.27 (d, J = 7 Hz, 25H), 0.87 (t, J = 0.87 Hz, 5H);^{13}C NMR ($CDCl_3$, 75 MHz) δ: 136.9, 133.7, 130.4, 123.7, 70.8, 65.9, 39.7, 35.7, 32.0, 30.9, 30.0, 29.9, 29.4, 27.2, 22.7, 15.4, 14.2, 13.2.

References

(1) Crudden, Cathleen M. and Edwards, D. *Eur. J. Org. Chem*., **2003**: 4695–4712.

(2) Männig, D.; Nöth, H. *Angew. Chem. Int. Ed. Engl*. **1985**, 24 (10), 878–879.

(3) M. G. L. Mirabelli, L. G. Sneddon, *J. Am. Chem. Soc*. **1988**, 110, 449.

(4) J. R. Knorr, J. S. Merola, *Organometallics* **1990,** 9, 3008**.**

(5) K. N. Harrison, T. J. Marks, *J. Am. Chem. Soc*. **1992,** 114, 9220.

(6) S. Pereira, M. Srebnik, *J. Am. Chem. Soc*. **1996**, 118, 909.

(7) Satoh, M.; Nomoto, Y.; Miyaura, N.; Suzuki, A. *Tetrahedron Lett*. **1989**, 30 (29), 3789–3792.

(8) Zaidlewicz, M.; Meller, *J. Tetrahedron Lett*. **1997**, 38 (41), 7279–7282.

(9) Thomas, Stephen P; Greenhalgh, Mark, D. *Chem. Commun.,* **2013**, 49, 11230.

(10) Dewese, Kendra, R. Cobalt-Catalyzed Hydrofunctionalization of 1,3-Dienes. Ph.D. Dissertation. The Ohio State University, Columbus OH, **2016.**

(11) Jing, Stanley, M. Cationic Cobalt (I) Mediated Heterodimerizations: From Mechanistic Insights to Reaction Discovery. Ph.D. Dissertation. The Ohio State University, Columbus OH, **2017.**

(12) Slone, R. V., *In Encyclopedia of Polymer Science and Technology*, John Wiley & Sons, Inc.: **2002.**

(13) Wittenberg, D., *Angew. Chem. Int. Ed*. **1964**, 3 (2), 153-153.

(14) Akira, M.; Yasuzo, U.; Taro, S.; Keiichi, U., *Bull. Chem. Soc. Jpn*. **1967**, 40 (8), 1889-1893.

(15) Grenouillet, P.; Neibecker, D.; Tkatchenko, I., *J. Chem. Soc., Chem. Comm*. **1983**, (9), 542-543.

(16) Feldman, K. S.; Grega, K. C., *J. Organomet. Chem*. **1990**, 381 (2), 251-260.

(17) Hilt, G.; du Mesnil, F. X.; Luers, S., *Angew. Chem. Int. Ed*. **2001**, 40 (2), 387-389.

(18) Hirano, M.; Arai, Y.; Hamamura, Y.; Komine, N.; Komiya, S., *Organomet*. **2012**, 31 (10), 4006-4019.

(19) Hiroi, Y.; Komine, N.; Komiya, S.; Hirano, M., *Organomet*. **2014**, 33 (22), 6604-6613.

(20) Sharma, R. K.; RajanBabu, T. V., *J. Am. Chem. Soc.* **2010,** *132* (10), 3295 – 3297

(21) Timsina, Y. N.; Sharma, R. K.; RajanBabu, T. V., *Chemical Science.* **2015**, 6 (7), 3994-4008.

(22) Helmchen, G.; Pfaltz, A. *Acc. Chem. Res*., **2000**, *33*, 336-345.

(23) Jing, S. M., Balasanthiran, V., Pagar, V., Gallucci, J. C., and RajanBabu, T.V. *J. Am. Chem. Soc.* **2017** *139* (49), 18034-18043

(24) Sarpong, R., Fischer, D. F. *J. Am. Chem. Soc.*, **2010**, *132* (17), pp 5926–5927

(25) Lassauque, N.; Francio, G.; Leitner, W. *Eur. J. Org. Chem* **2009** 3199-3902.

(26) Andruszkiewicz, R.; Silverman, R. *Synthesis* **1989**, *19*, 953-955.

(27) Chakraborti, A.; Kumar, R.; Khatik, G. *Organic Letters* **2006**, *8*, 2433-2436.

(28) Fischer, D.M.; Sarpong, R. *J. Am. Chem. Soc.* 132, **2010**, *17,* 5926-5927

Data Appendix

Appendix A1: Achiral Gas Chromatograms for Table 2.2

Table 2.2, Entry 1

GC conditions: HP-5MS, 120 °C, 5 min, 20 °C/min to 250 °C

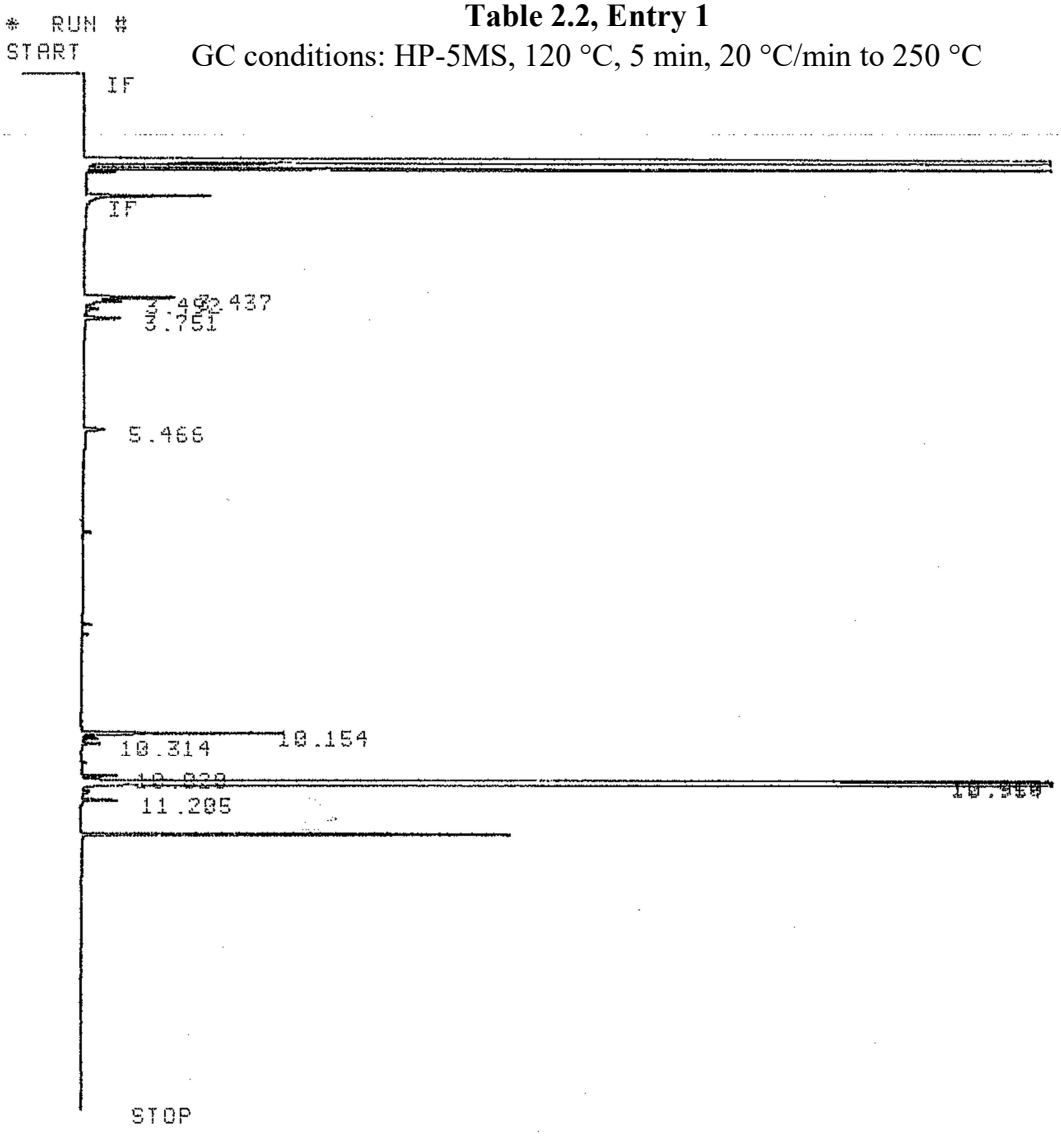

Closing signal file M:SIGNAL .BNC

RUN# 1202 JUN 16, 1901 21:01:38

SIGNAL FILE: M:SIGNAL.BNC
AREA%

RT	AREA	TYPE	WIDTH	AREA%
3.437	3068	BV	.034	1.05531
3.492	1517	VV	.041	.52181
3.751	1148	PB	.031	.39488
10.154	4187	VV	.021	1.44022
10.910	39384	PV	.021	13.54706 ✓
10.954	232586	VB	.022	80.00346 ✓
11.730	8830	PB	.020	3.03729

TOTAL AREA- 290720
MUL FACTOR-1.0000E+00

Table 2.2, Entry 2

GC conditions: HP-5MS, 120 °C, 5 min, 20 °C/min to 250 °C

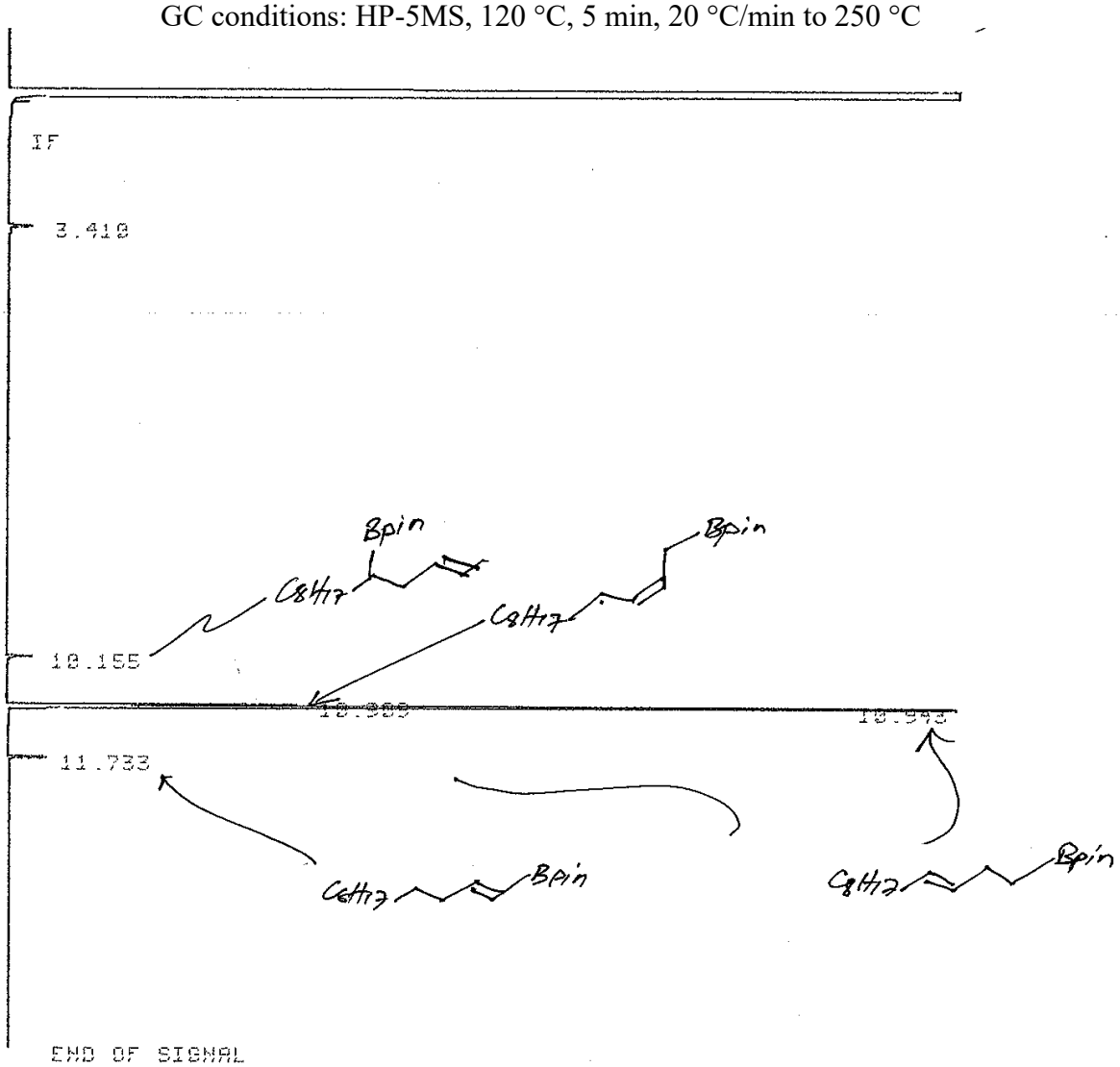


```
Closing signal file M:SIGNAL   .BNA

RUN#  1324           JUL   5, 1901   23:57:45

SIGNAL FILE: M:SIGNAL.BNA
AREA%
       RT       AREA TYPE  WIDTH       AREA%
    3.410        686   BB    .020     1.63715
   10.155        509   PU    .019     1.21474
   10.909       5622   BU    .019    13.41702
   10.943      34377   UB    .019    82.04144
   11.733        708   PB    .019     1.68966

TOTAL AREA-  41902
MUL FACTOR-1.0000E+00
```

Table 2.2, Entry 3

GC conditions: HP-5MS, 120 °C, 5 min, 20 °C/min to 250 °C

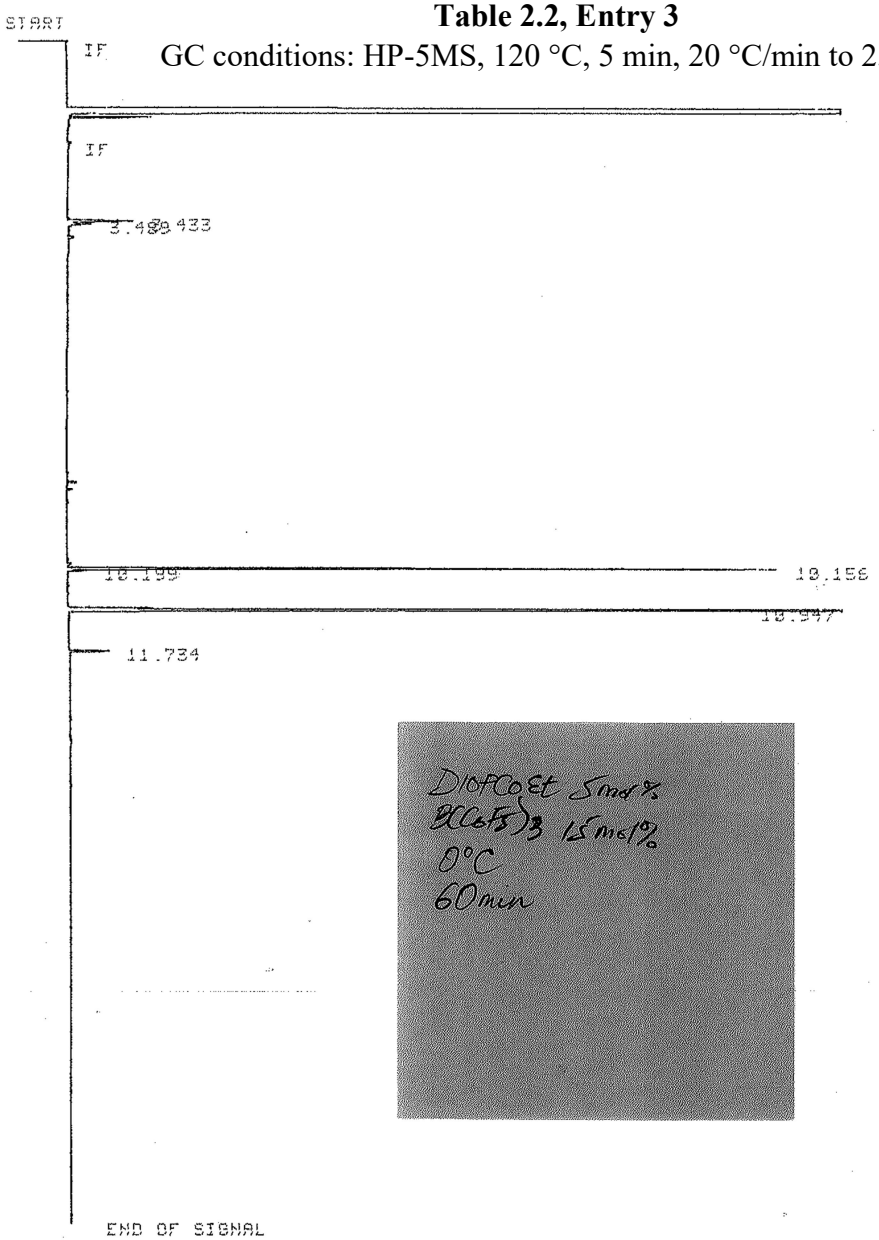

Diff Co Et 5 mol%
B(C6F5)3 15 mol%
0°C
60 min

Closing signal file M:SIGNAL .BNA

RUN# 1325 JUL 6, 1901 00:29:20

SIGNAL FILE: M:SIGNAL.BNA
AREA%

RT	AREA	TYPE	WIDTH	AREA%
3.433	2371	BV	.029	2.19039
3.489	933	VB	.031	.85799
10.156	17683	BV	.020	16.26143
10.199	464	VV	.019	.42670
10.947	86170	BB	.020	79.24262
11.734	1121	PB	.022	1.03088

TOTAL AREA- 108742
MUL FACTOR-1.0000E+00

Table 2.2, Entry 4

GC conditions: HP-5MS, 120 °C, 5 min, 20 °C/min to 250 °C

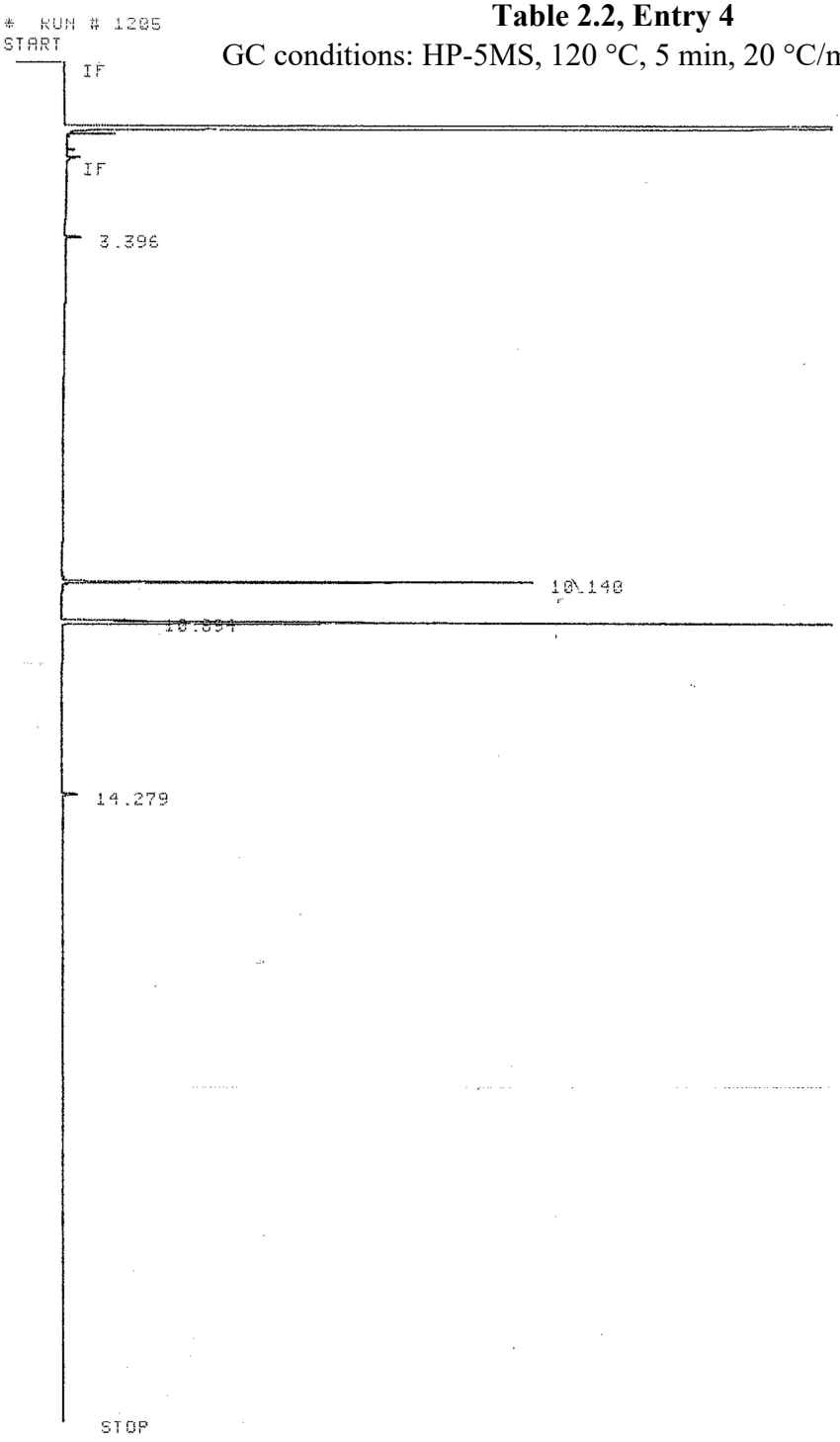

Closing signal file M:SIGNAL .BNC

RUN# 1205 JUN 16, 1901 22:44:25

SIGNAL FILE: M:SIGNAL.BNC
AREA%

RT	AREA	TYPE	WIDTH	AREA%	
10.140	11803	VV	.020	26.84148	← internal
10.894	1947	PV	.019	4.42772	← 1,4
10.928	30223	VB	.020	68.73082	← 1,2

Table 2.2, Entry 5

GC conditions: HP-5MS, 120 °C, 5 min, 20 °C/min to 250 °C

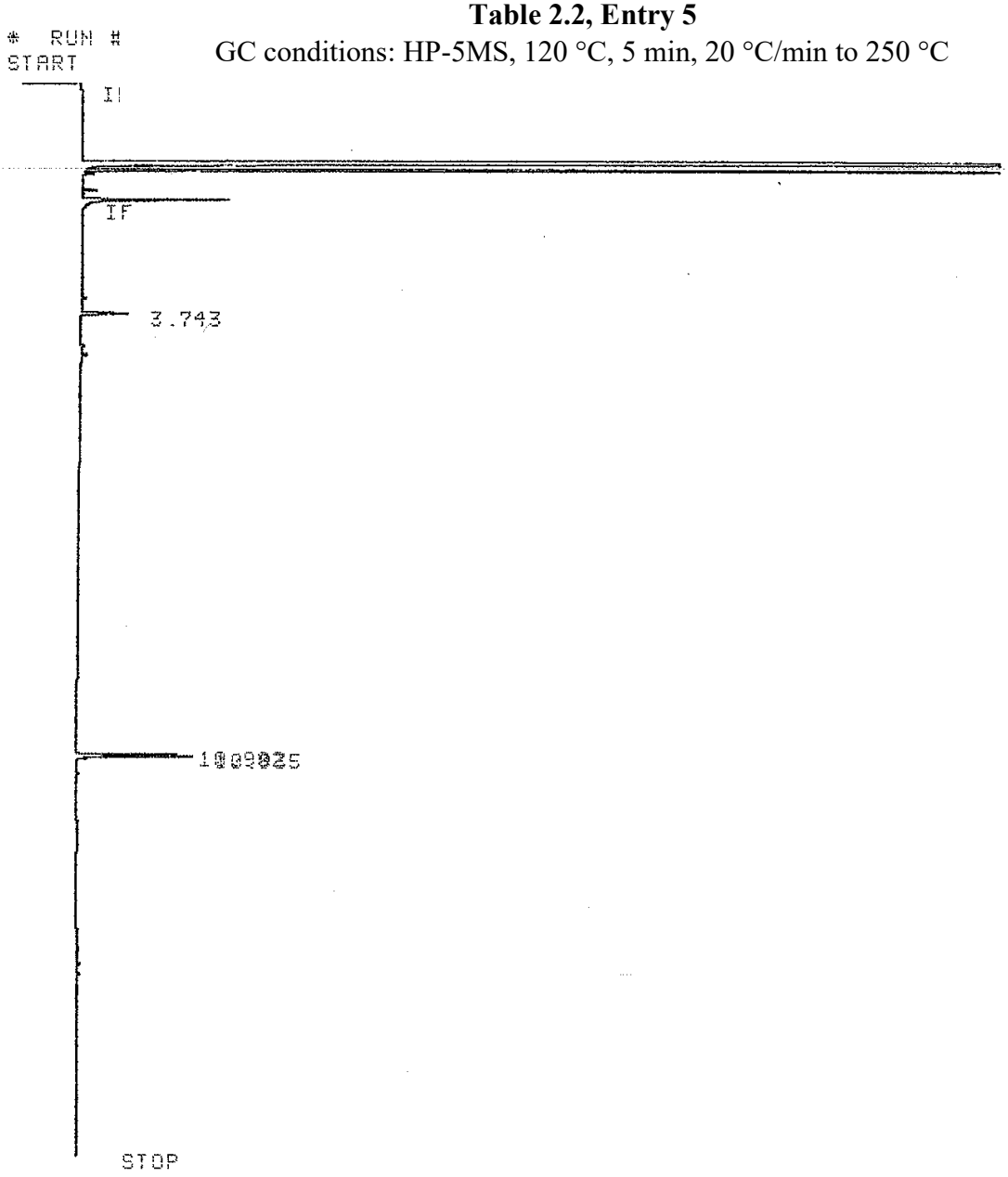

Closing signal file M:SIGNAL .BNC

RUN# 1203 JUN 16, 1901 21:22:09

SIGNAL FILE: M:SIGNAL.BNC
AREA%

RT	AREA	TYPE	WIDTH	AREA%
3.743	1495	VB	.030	23.92000
10.902	2080	PU	.020	33.28000
10.935	2675	VB	.022	42.80000

Table 2.2, Entry 6

GC conditions: HP-5MS, 120 °C, 5 min, 20 °C/min to 250 °C

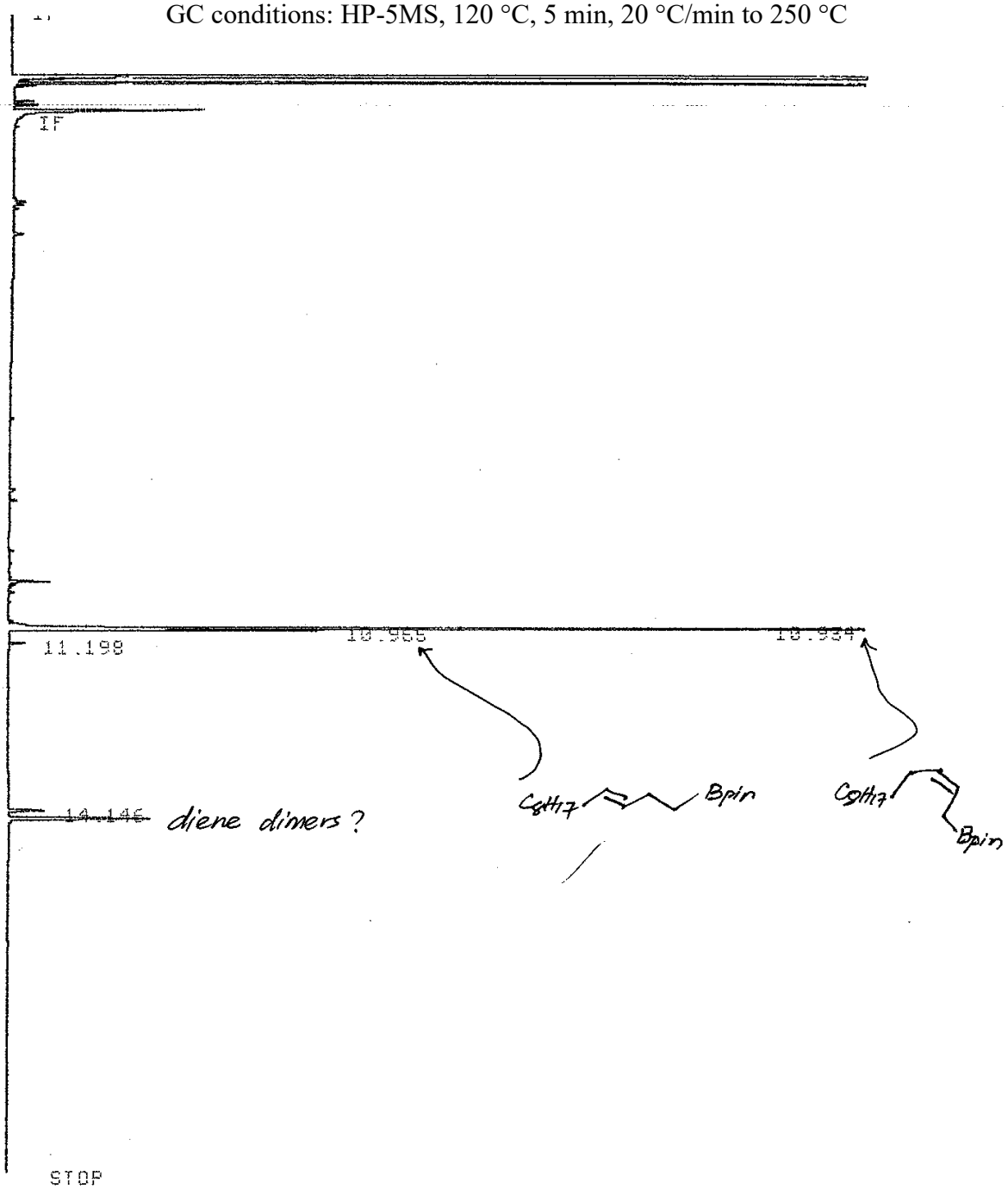

Closing signal file M:SIGNAL .BNC

RUN# 1204 JUN 16, 1901 21:50:54

SIGNAL FILE: M:SIGNAL.BNC
AREA%

RT	AREA	TYPE	WIDTH	AREA%
10.125	1239	VV	.026	2.40615
10.934	37189	VV	.020	72.22147
10.965	6439	VB	.018	12.50462
14.146	1358	BB	.033	2.63725
14.285	5268	PB	.033	10.23052

Table 2.2, Entry 7

GC conditions: HP-5MS, 120 °C, 5 min, 20 °C/min to 250 °C

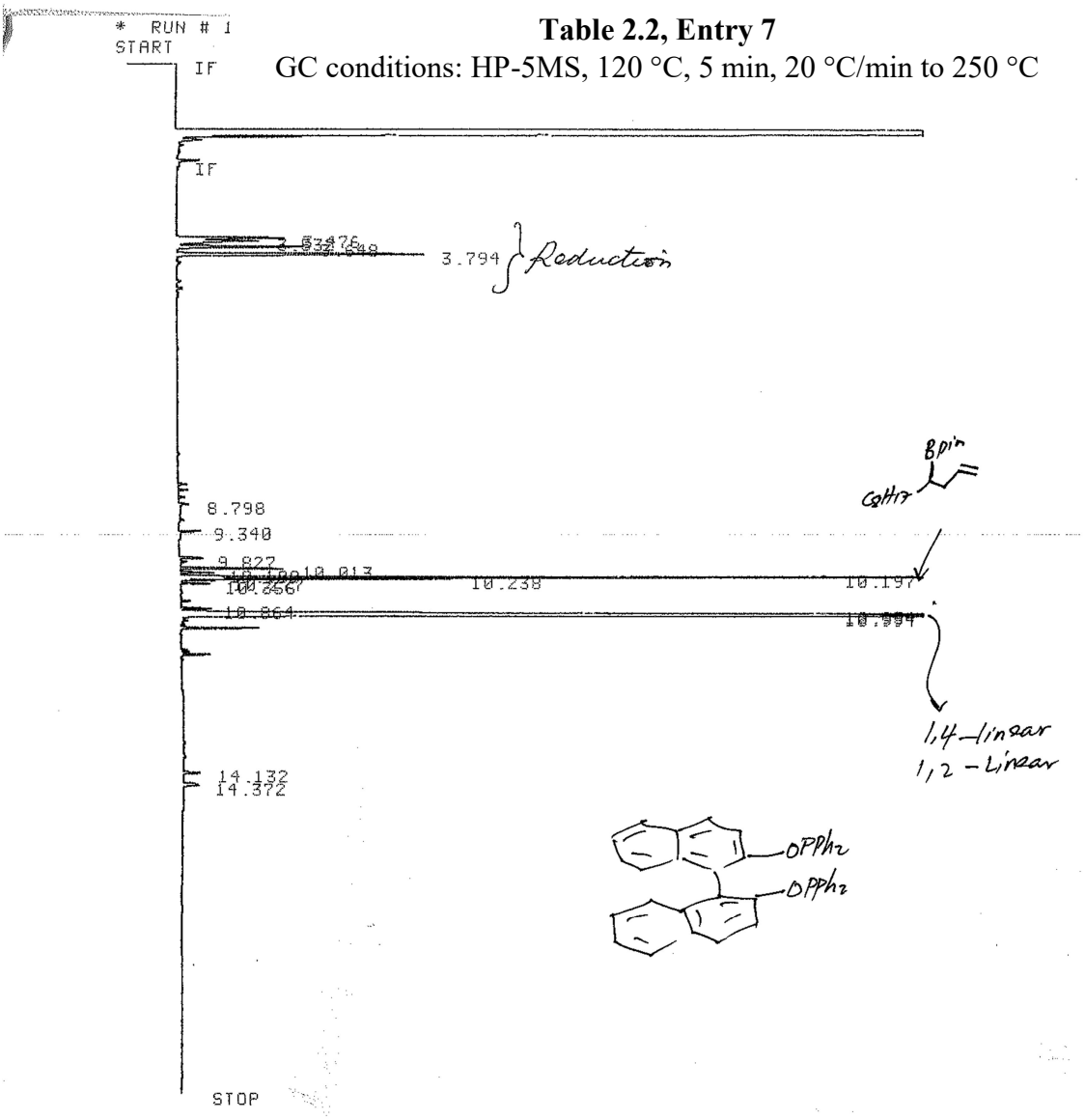

Closing signal file M:SIGNAL .BNC

RUN# 1578. AUG 16, 1901 20:08:37

SIGNAL FILE: M:SIGNAL.BNC
AREA%

RT	AREA	TYPE	WIDTH	AREA%	
3.476	4911	BV	.035	1.51622	
3.532	4767	VV	.045	1.47176	
3.648	5465	VB	.034	1.68726	
3.794	11356	BB	.035	3.50604	
8.798	276	PB	.021	.08521	
9.340	556	PB	.020	.17166	
9.827	794	PP	.024	.24514	
10.013	2768	PB	.020	.85459	
10.100	943	BV	.021	.29114	
10.197	28185	VV	.022	8.70181	✓
10.238	6841	VV	.019	2.11208	✓
10.277	900	VB	.019	.27787	
10.356	750	BB	.020	.23155	
10.864	792	PP	.019	.24452	
10.954	39025	PV	.022	12.04854	✓
10.994	210612	VB	.021	65.02416	✓
11.249	2136	PB	.021	.65947	
11.777	833	VB	.022	.25718	
14.132	804	BB	.034	.24823	
14.372	1184	BB	.058	.36555	

TOTAL AREA= 323898
MUL FACTOR=1.0000E+00

Table 2.2, Entry 8

GC conditions: HP-5MS, 120 °C, 5 min, 20 °C/min to 250 °C

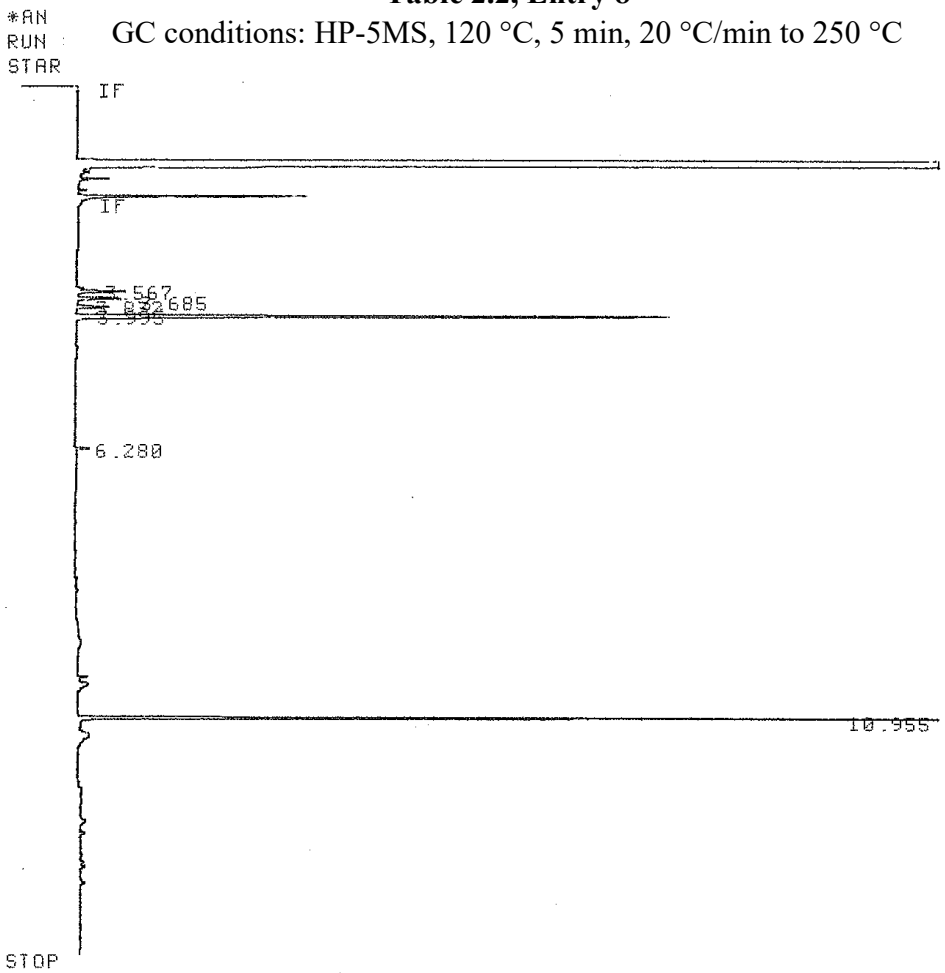


```
Closing signal file M:SIGNAL   .BNA

RUN#  1580           AUG 16, 1901   20:57:43

SIGNAL FILE: M:SIGNAL.BNA
AREA%
      RT       AREA TYPE  WIDTH      AREA%
   3.567       1622   BP    .031    2.99599
   3.685       1608   PB    .033    2.97013
   3.832       1301   BB    .035    2.40307
   3.995      24105   BB    .036   44.52427
   6.280        511   PB    .031     .94387
  10.955      24992   PB    .020   46.16266
```

Appendix A2: Achiral Stationary Phase Gas Chromatograms for Table 2.3

Table 2.3, Entry 1

GC conditions: HP-5MS, 120 °C, 5 min, 20 °C/min to 250 °C

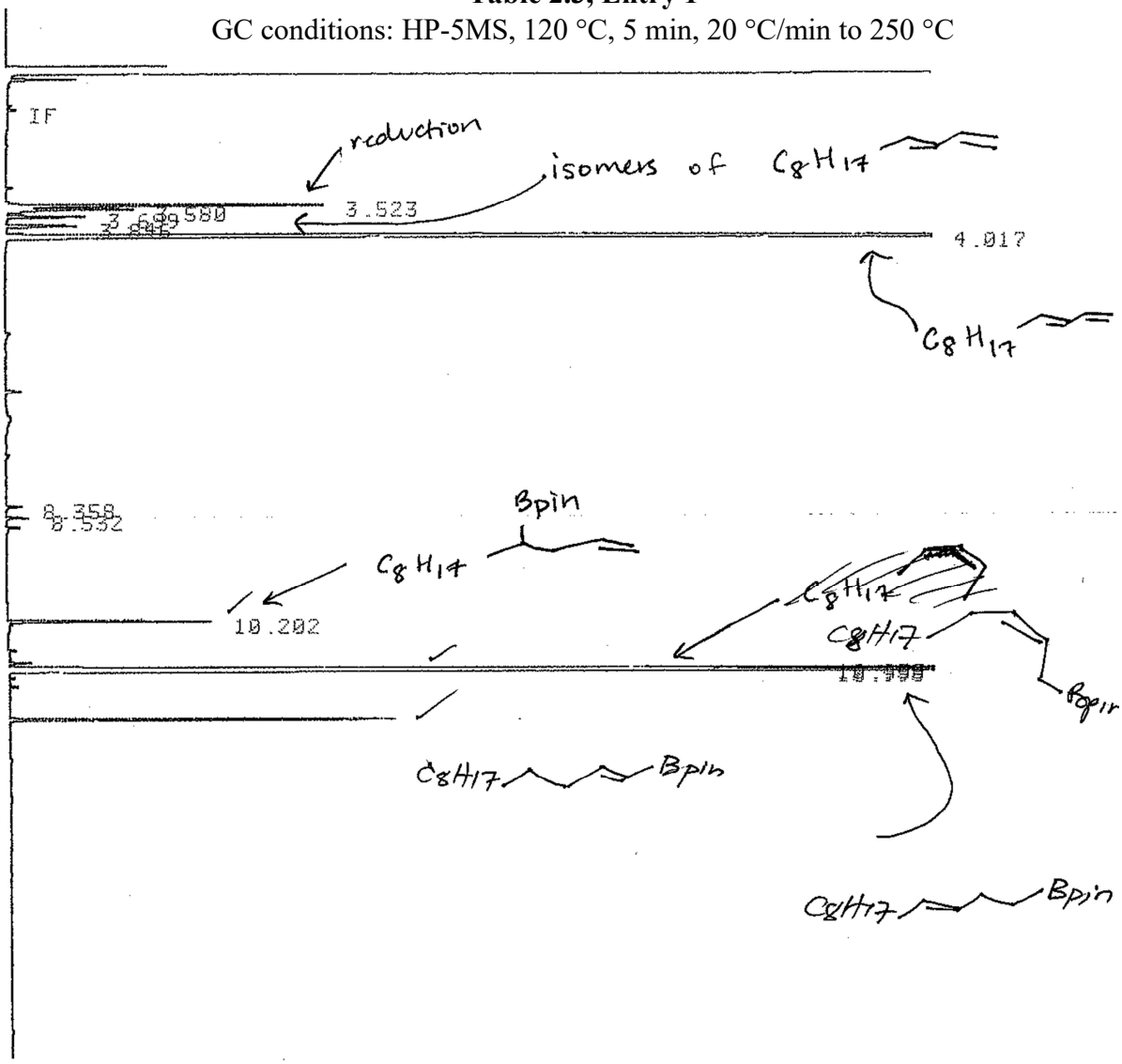

STOP

Closing signal file M:SIGNAL .BNC

RUN# 1693 AUG 29, 1901 22:12:21

Table 2: entry 1

SIGNAL FILE: M:SIGNAL.BNC
AREA%

RT	AREA	TYPE	WIDTH	AREA%
3.523	9739	BV	.029	2.37341
3.580	4374	VP	.033	1.06595
3.699	2326	PB	.028	.56685
3.846	2276	BB	.030	.55466
4.017	133674	PB	.031	32.57658
6.499	483	BB	.027	.11771
8.358	376	BB	.022	.09163
8.532	487	PB	.021	.11868
10.202	4173	PV	.020	1.01697
10.870	510	BB	.020	.12429
10.958	37449	PV	.020	9.12637
10.998	205807	VB	.021	50.15549
11.780	8664	BB	.021	2.11143

Table 2.3, Entry 2

GC conditions: HP-5MS, 120 °C, 5 min, 20 °C/min to 250 °C

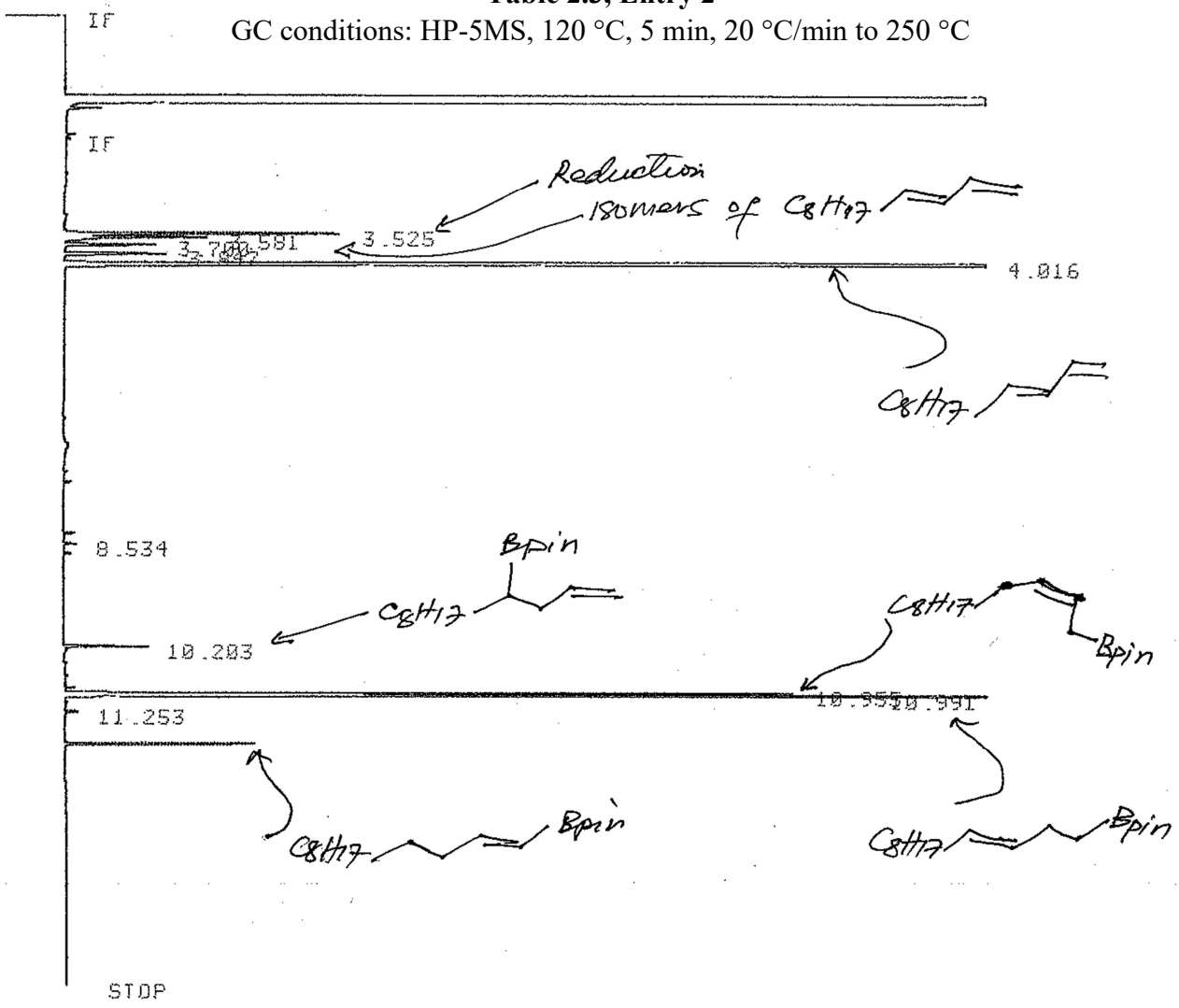


```
Closing signal file M:SIGNAL   .BNC

RUN#  1692           AUG 29, 1901  21:54:35

SIGNAL FILE: M:SIGNAL.BNC
AREA%
      RT       AREA TYPE  WIDTH      AREA%
   3.525       8622   BV    .030    3.82866
   3.581       4776   VV    .032    2.12082
   3.700       2707   VB    .028    1.20206
   3.847       3185   PB    .030    1.41432
   4.016     100594   PB    .032   44.66954
   8.534        320   PB    .021     .14210
  10.203       1719   BV    .019     .76334
  10.955      14863   BV    .020    6.60003
  10.991      83779   VB    .020   37.20270
  11.253        335   PB    .022     .14876
  11.780       4296   PB    .021    1.90767
```

Table 2
Entry 2

MM013+
7.027
(2mg?)
dapp dd Br

Table 2.3, Entry 3

GC conditions: HP-5MS, 120 °C, 5 min, 20 °C/min to 250 °C

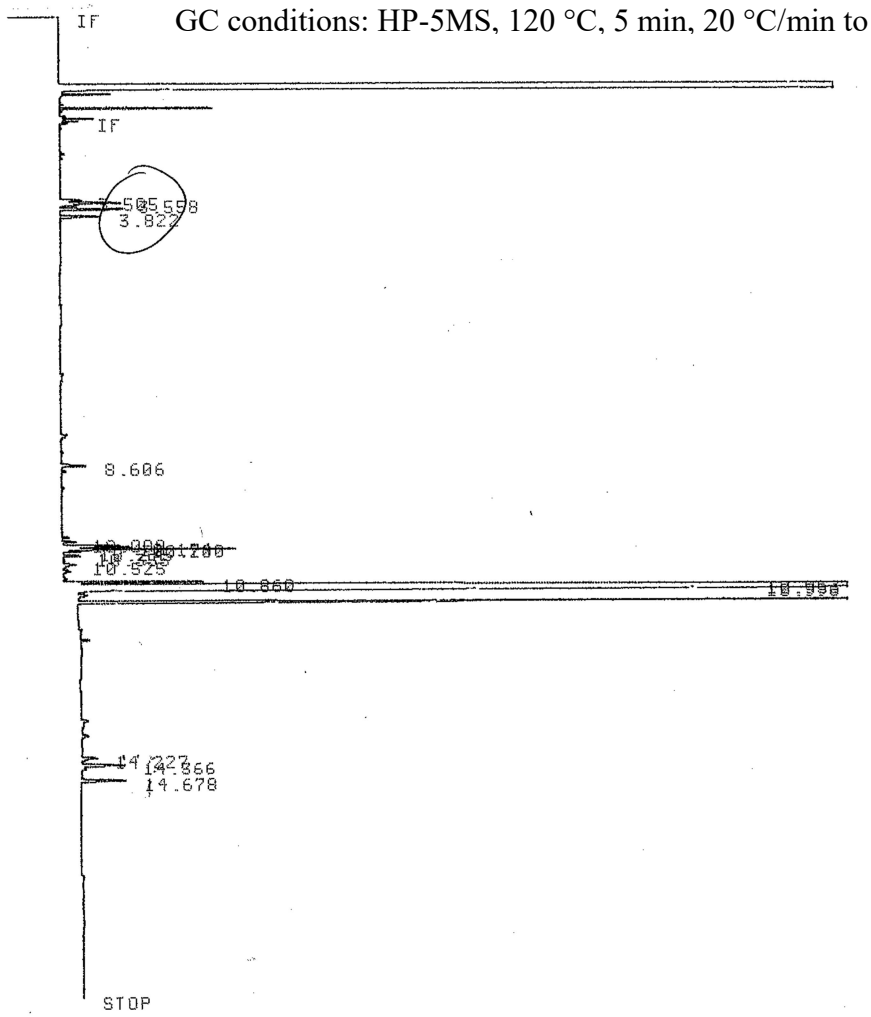

Closing signal file M:SIGNAL .BNC

RUN# 1570 AUG 15, 1901 00:45:03

SIGNAL FILE: M:SIGNAL.BNC

AREA%

RT	AREA	TYPE	WIDTH	AREA%
3.505	960	BV	.036	.19422
3.558	2332	VV	.031	.47178
3.675	2348	VB	.029	.47502
3.822	1570	PB	.031	.31762
8.606	1087	BB	.034	.21991
10.099	373	BV	.021	.07546
10.174	1560	VV	.021	.31560
10.200	1728	VV	.019	.34959
10.235	4231	VV	.019	.85597
10.275	456	VB	.019	.09225
10.355	606	BP	.027	.12260
10.525	662	VV	.038	.13393
10.860	3532	PV	.020	.71455
10.953	75401	VV	.030	15.25428
10.996	363830	VB	.025	73.60598
11.246	28556	VB	.020	5.77713
14.227	847	BV	.042	.17136
14.366	2004	VV	.037	.40543
14.678	2211	PB	.039	.44730

TOTAL AREA= 494294

MUL FACTOR=1.0000E+00

Table 2
Entry 3
dppp Co(COTE)

dppp + H_2O_2 + DMF
120°C
30mins
(30 mins)
MW 01.54

Table 2.3, Entry 4

GC conditions: HP-5MS, 120 °C, 5 min, 20 °C/min to 250 °C

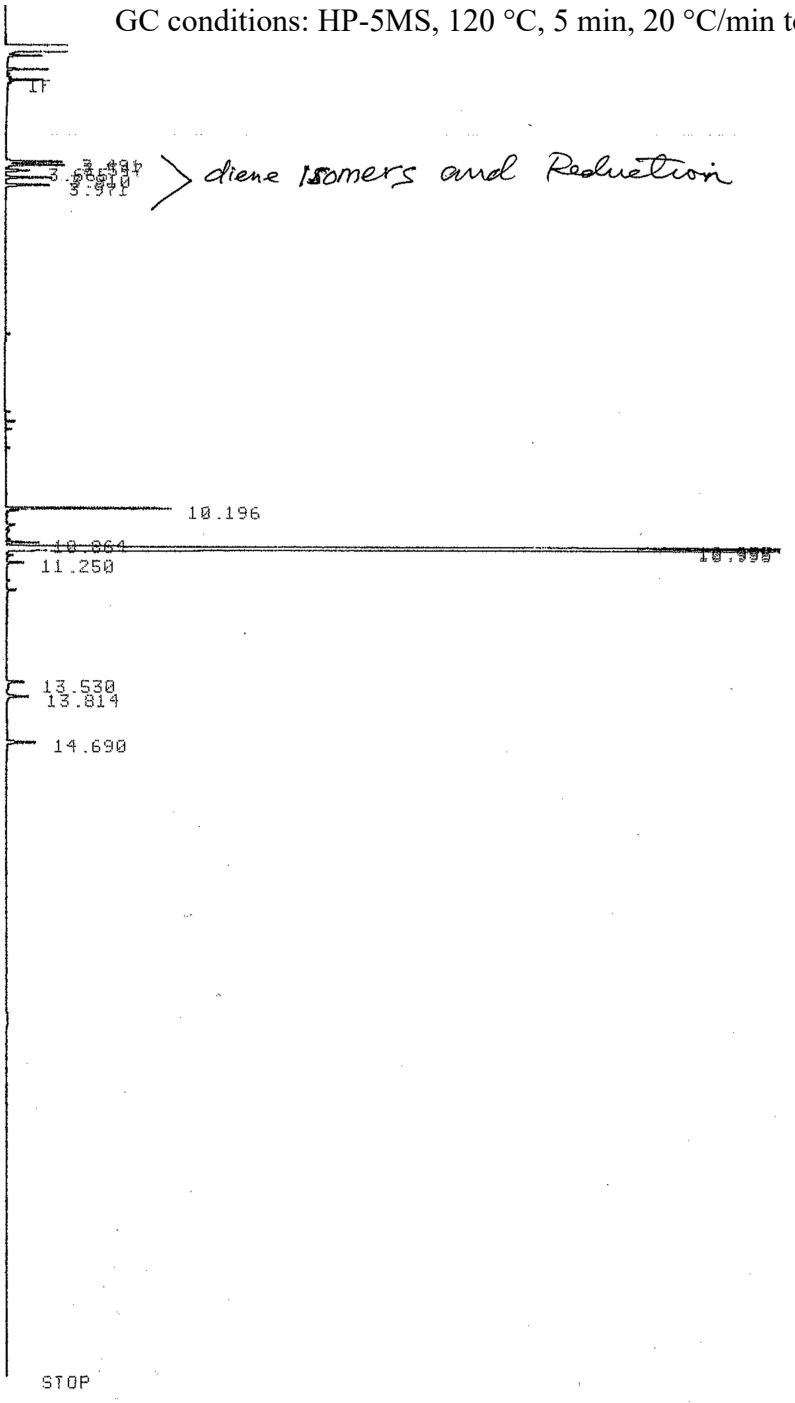

Closing signal file M:SIGNAL .BNC

RUN# 1642 AUG 25, 1901 23:08:19

SIGNAL FILE: M:SIGNAL.BNC
AREA%

RT	AREA	TYPE	WIDTH	AREA%
3.491	2117	PU	.030	.77047
3.547	2216	VB	.030	.80650
3.665	874	BB	.029	.31809
3.810	1776	BB	.030	.64636
3.971	1906	BB	.034	.69367
10.196	4211	BV	.020	1.53256
10.864	826	PP	.019	.30062
10.955	39713	PV	.021	14.45323
10.995	217420	VB	.021	79.12829
11.250	517	PB	.024	.18816

Table 2.3, Entry 5

GC conditions: HP-5MS, 120 °C, 5 min, 20 °C/min to 250 °C

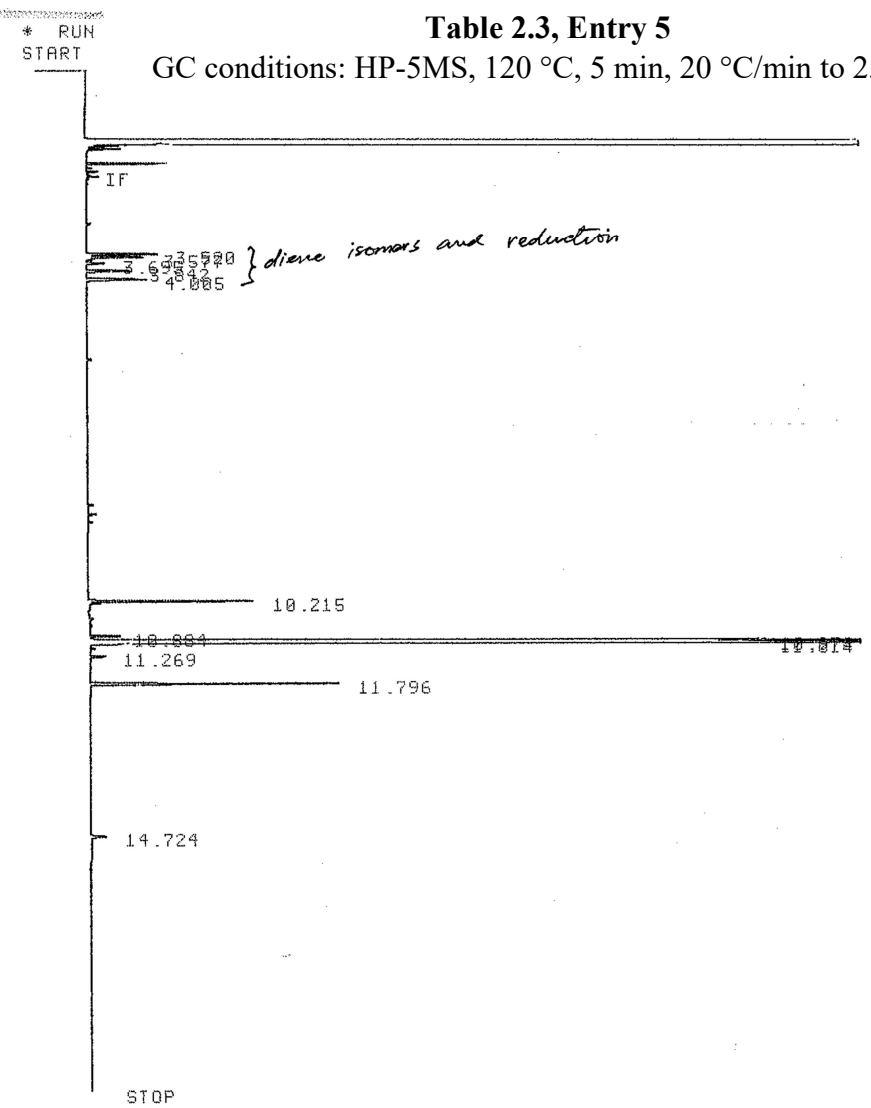

Closing signal file M:SIGNAL .BNC

RUN# 1652 AUG 26, 1901 20:27:00

SIGNAL FILE: M:SIGNAL.BNC
AREA%

RT	AREA	TYPE	WIDTH	AREA%
3.520	2528	PU	.028	.91200
3.577	2029	VV	.028	.73198
3.695	656	BB	.028	.23666
3.842	1662	BB	.029	.59958
4.005	2490	PB	.033	.89829
10.215	4219	PU	.020	1.52204
10.884	770	PP	.019	.27778
10.972	40144	PU	.020	14.48233
11.014	214426	VB	.021	77.35619
11.269	702	PB	.033	.25325
11.796	6767	PB	.022	2.44126
14.724	800	BB	.040	.28861

TOTAL AREA= 277193

MM01.#0.01
dppbcoe2+
Bruker's at
~45°C
(Bonnie)
120°C

Table 2.3, Entry 6

GC conditions: HP-5MS, 120 °C, 5 min, 20 °C/min to 250 °C

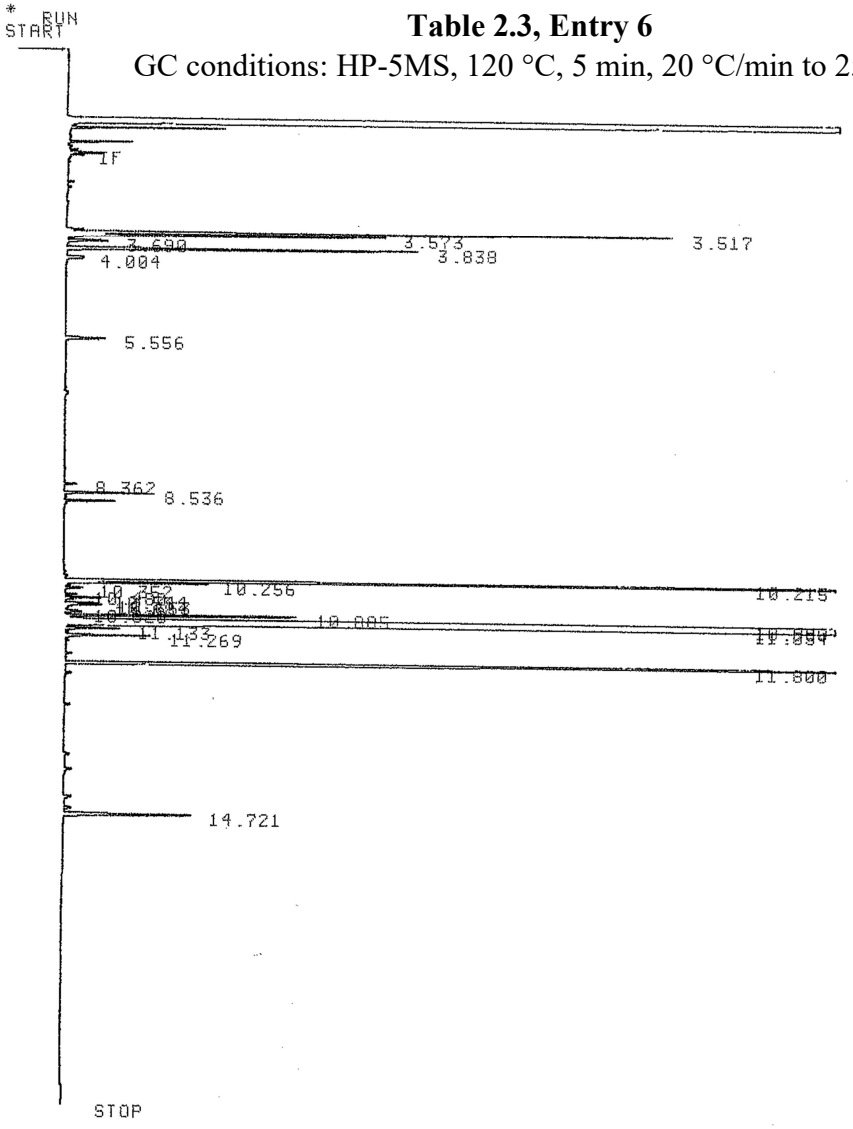

Closing signal file M:SIGNAL .BNC

RUN# 1653 AUG 26, 1901 22:57:15

SIGNAL FILE: M:SIGNAL.BNC
AREA%

RT	AREA	TYPE	WIDTH	AREA%
3.461	502	PV	.025	.02239
3.517	20810	VV	.027	.92805
3.573	10980	VB	.028	.48967
3.690	1460	BB	.029	.06511
3.838	13130	PB	.030	.58555
4.004	1234	BB	.053	.05503
5.556	1654	PB	.033	.07376
8.362	384	PB	.023	.01713
8.536	2160	BB	.021	.09633
8.688	1343	BV	.021	.05989
10.215	46961	VV	.020	2.09430
10.256	3556	VV	.020	.15859
10.352	624	VB	.029	.02783
10.480	384	PV	.022	.01713
10.544	1007	VV	.022	.04491
10.653	850	PV	.020	.03791
10.684	921	VB	.021	.04107
10.820	840	PP	.038	.03746
10.885	6712	PV	.023	.29933
10.989	298884	VV	.030	13.32919
11.054	1766411	VB	.037	78.77578
11.133	1522	PP	.023	.06788
11.269	2414	VP	.022	.10766
11.800	51737	PB	.021	2.30729

MM 9:30
1 mol%
120. C
30m

Table 2.3, Entry 7

GC conditions: HP-5MS, 120 °C, 5 min, 20 °C/min to 250 °C

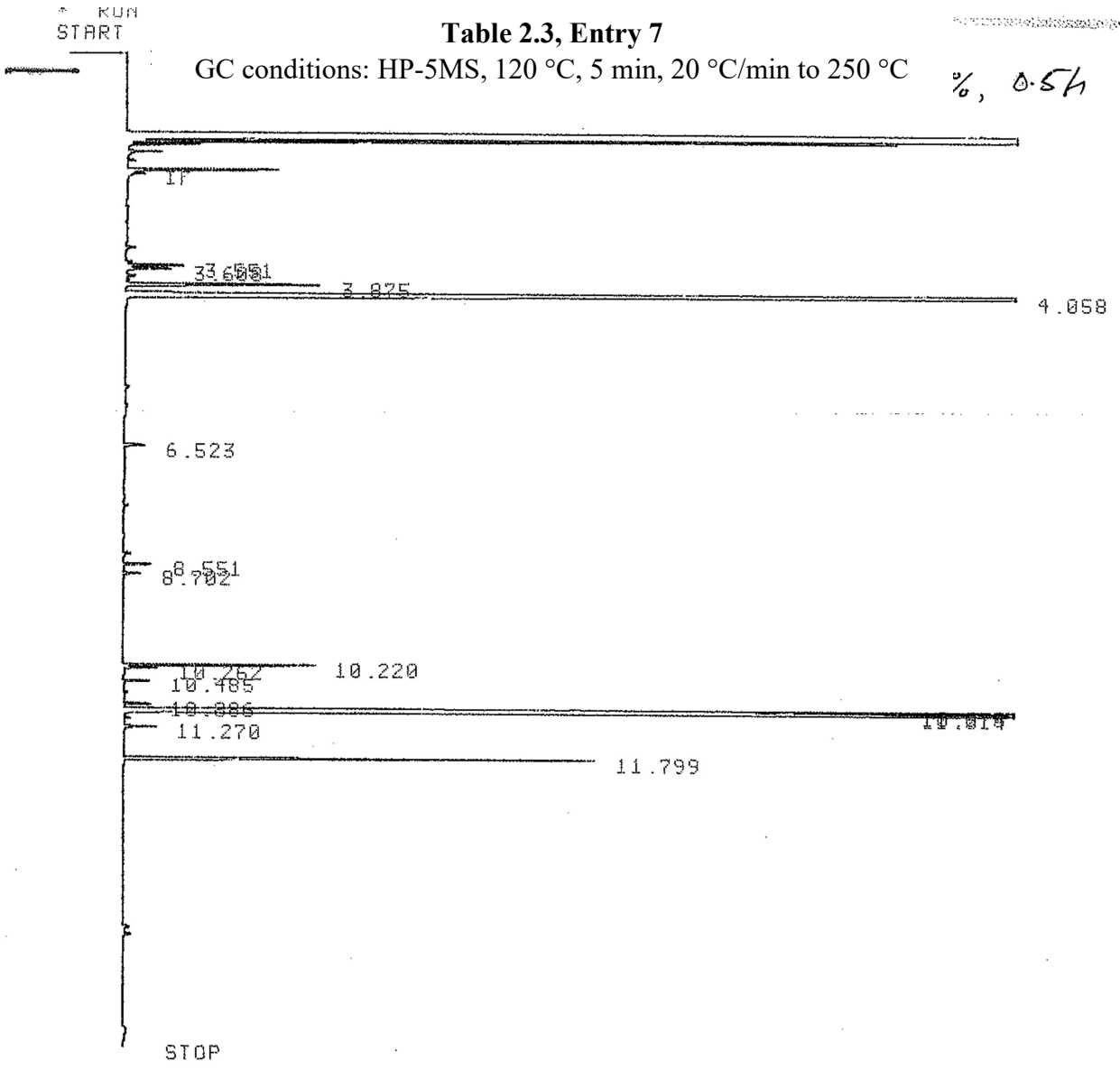


```
Closing signal file M:SIGNAL   .BNC

RUN#  1661           AUG 27, 1901  01:15:04

SIGNAL FILE: M:SIGNAL.BNC
AREA%
      RT       AREA TYPE  WIDTH       AREA%
   3.551       1750   VV    .028      .32608
   3.608       1377   VB    .028      .25658
   3.875       6602   BB    .031     1.23017
   4.058     301348   PB    .034    56.15102
   6.523        631   BB    .027      .11758
   8.551        666   PB    .021      .12410
   8.702        369   PB    .020      .06876
  10.220       4135   PV    .020      .77049
  10.262        710   VB    .019      .13230
  10.485        578   PB    .020      .10770
  10.886        643   PP    .022      .11981
  10.975      38290   PV    .020     7.13468
  11.014     168201   VB    .021    31.34137
  11.270        726   BB    .020      .13528
  11.799      10648   PB    .021     1.98407
```

Table 2.3, Entry 8

GC conditions: HP-5MS, 120 °C, 5 min, 20 °C/min to 250 °C

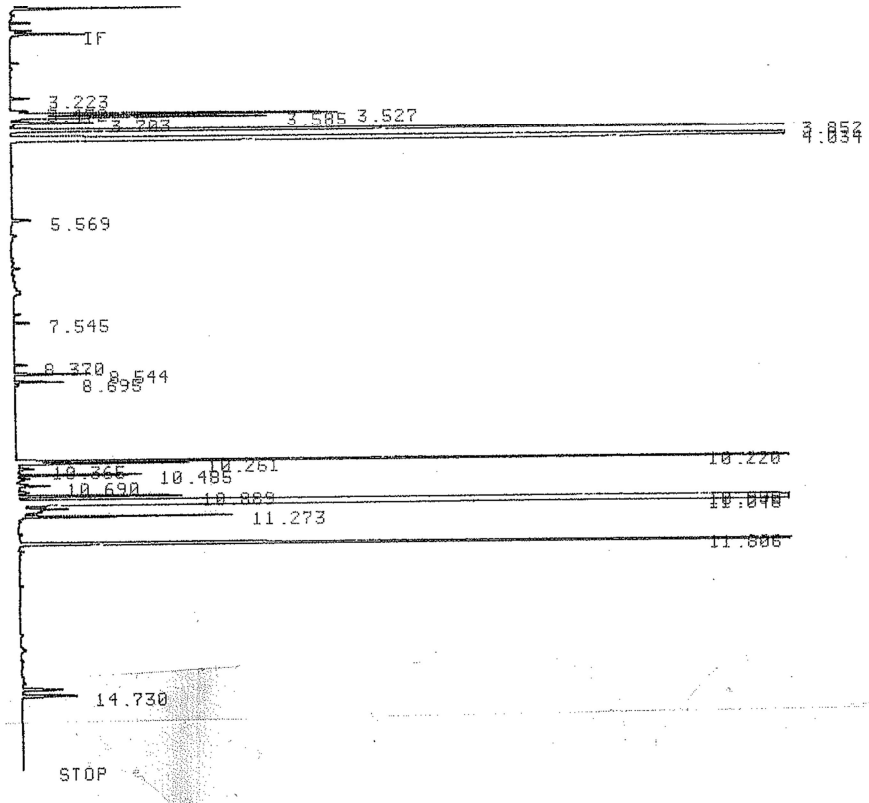

Closing signal file M:SIGNAL .BNC

RUN# 1669 AUG 27, 1901 18:40:50

SIGNAL FILE: M:SIGNAL.BNC

AREA%

RT	AREA	TYPE	WIDTH	AREA%
3.223	730	BB	.027	.03674
3.472	668	PU	.029	.03362
3.527	12025	VV	.030	.60520
3.585	9589	VB	.030	.48260
3.703	3193	BB	.031	.16070
3.852	39382	BB	.033	1.98204
4.034	351033	PB	.036	17.66701
5.569	889	PB	.034	.04474
7.545	505	BB	.024	.02542
8.370	451	PB	.025	.02270
8.544	2081	PB	.022	.10473
8.695	1286	BV	.021	.06472
10.220	29696	PV	.020	1.49456
10.261	4147	VV	.019	.20871
10.365	767	VV	.034	.03860
10.485	3304	VV	.021	.16629
10.550	440	VV	.024	.02214
10.659	287	PV	.019	.01444
10.690	977	VB	.024	.04917
10.889	4647	PP	.022	.23388
10.990	250003	PV	.028	12.58230
11.048	1183627	VB	.032	59.57032
11.134	1424	BV	.025	.07167
11.273	5093	VB	.019	.25632
11.806	76222	BB	.022	3.83615
14.609	1870	BB	.036	.09411
14.730	2605	PB	.037	.13111

(20.0 C
0.1 mol% Al
15 hrs

Table 2.3, Entry 9

GC conditions: HP-5MS, 120 °C, 5 min, 20 °C/min to 250 °C

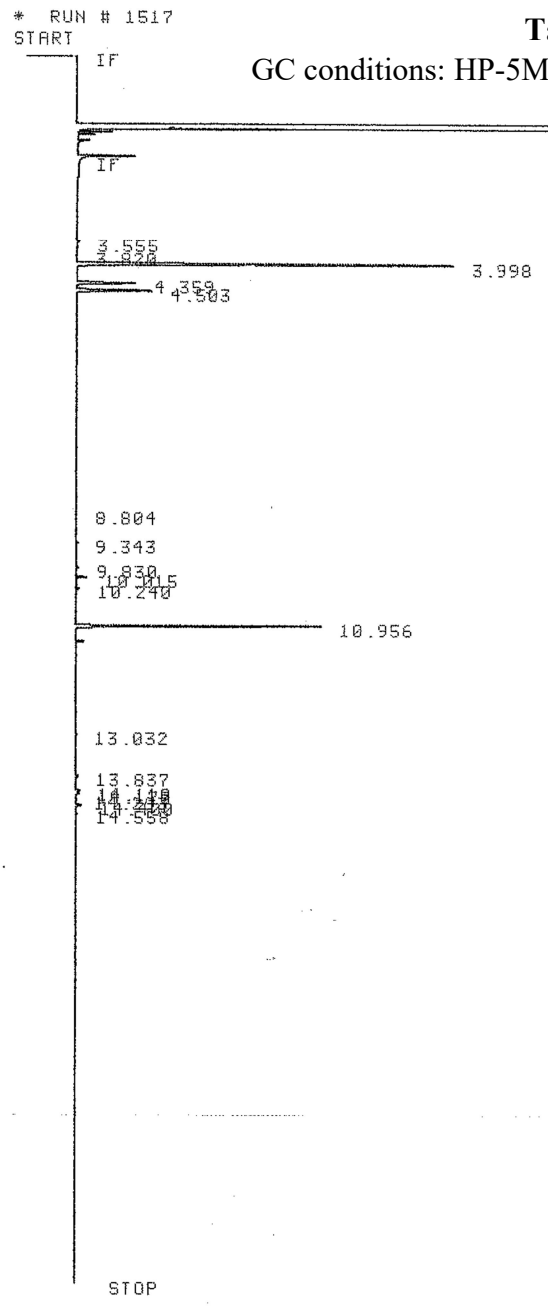

Closing signal file M:SIGNAL .BNC

RUN# 1517 AUG 8, 1901 16:17:21

SIGNAL FILE: M:SIGNAL.BNC
AREA%

RT	AREA	TYPE	WIDTH	AREA%
3.555	1883	VB	.027	.39247
3.673	975	PP	.028	.20322
3.820	982	VB	.030	.20468
3.998	244487	PB	.033	50.95826
4.359	39694	PB	.034	8.27339
4.503	52105	BV	.035	10.86021
5.700	1701	BB	.034	.35454
8.804	765	BB	.024	.15945
9.343	978	PB	.020	.20384
9.830	1686	PB	.024	.35141
10.015	4503	PB	.019	.93856
10.240	1710	VB	.021	.35641
10.956	106907	VV	.022	22.28254
11.249	3999	BB	.021	.83351
13.032	1240	PB	.028	.25845
13.837	2675	PB	.040	.55755
14.119	3200	VV	.036	.66697

Appendix A3: Achiral Stationary Phase Gas Chromatograms for Table 2.4

Table 2.4, Entry 1

GC conditions: HP-5MS, 120 °C, 5 min, 20 °C/min to 250 °C

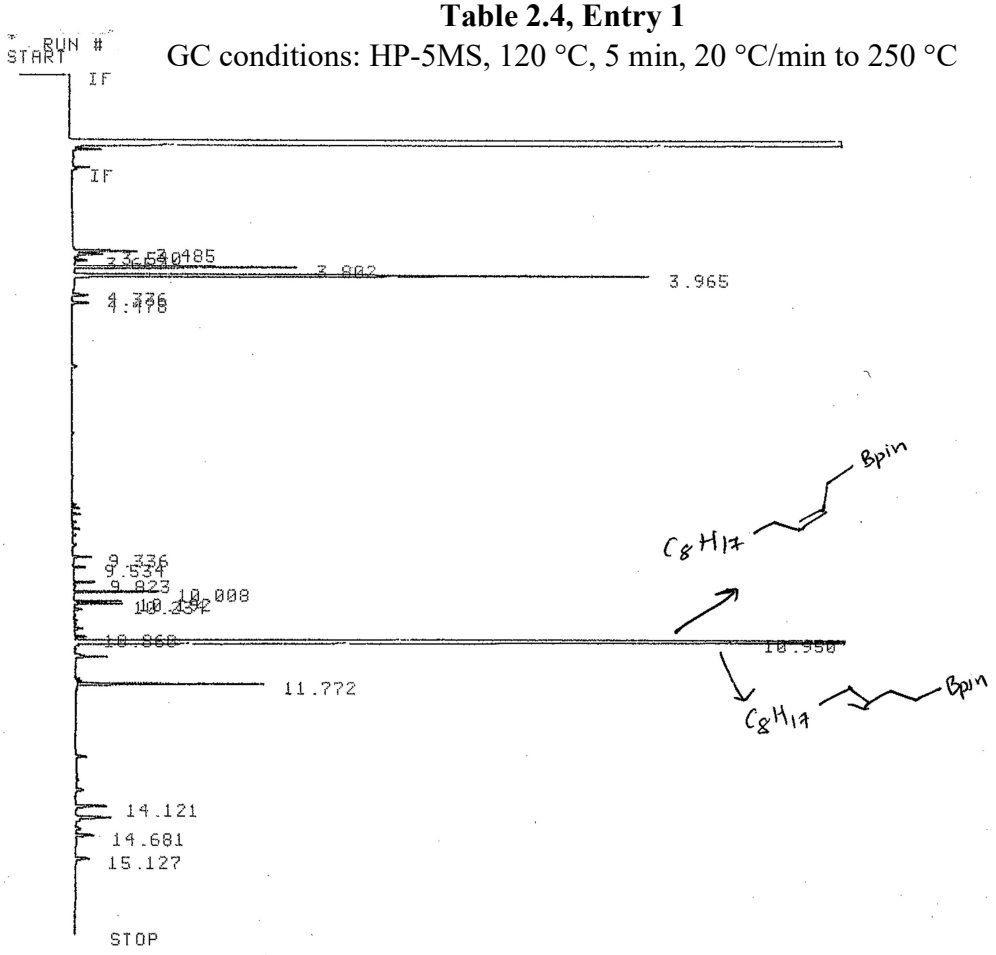


```
Closing signal file M:SIGNAL   .BNC

RUN#  1536          AUG 11, 1901  22:27:53

SIGNAL FILE: M:SIGNAL.BNC
AREA%
      RT       AREA TYPE  WIDTH       AREA%
   3.485       2337   PV    .029     1.25791
   3.540       1231   VP    .033      .66259
   3.657        490   PB    .028      .26375
   3.802       8477   BB    .030     4.56280
   3.965      22885   BB    .032    12.31800
   4.336        780   BB    .037      .41984
   4.478        798   BB    .035      .42953
   9.336        437   PB    .019      .23522
   9.534        355   PB    .021      .19108
   9.823        604   BB    .022      .32511
  10.008       2092   BB    .020     1.12603
  10.192       1179   PV    .020      .63460
  10.234       1171   VB    .019      .63030
  10.860        308   PV    .020      .16578
→10.950      95661   VV    .021    51.49018 → 1,2
→10.981      36187   VV    .019    19.47789 → 1,4
  11.245        883   VB    .021      .47528
  11.772       4951   VB    .021     2.66491
  14.121       1408   VB    .035      .75787
  14.340       1920   BB    .042     1.03345
  14.681        871   PB    .036      .46882
  15.127        760   PB    .041      .40908

TOTAL AREA= 185785
MUL FACTOR=1.0000E+00
```

dppm Col\MM01.SO (after 2 hrs) w/ BLF 120°C

Table 2.4, Entry 2

GC conditions: HP-5MS, 120 °C, 5 min, 20 °C/min to 250 °C

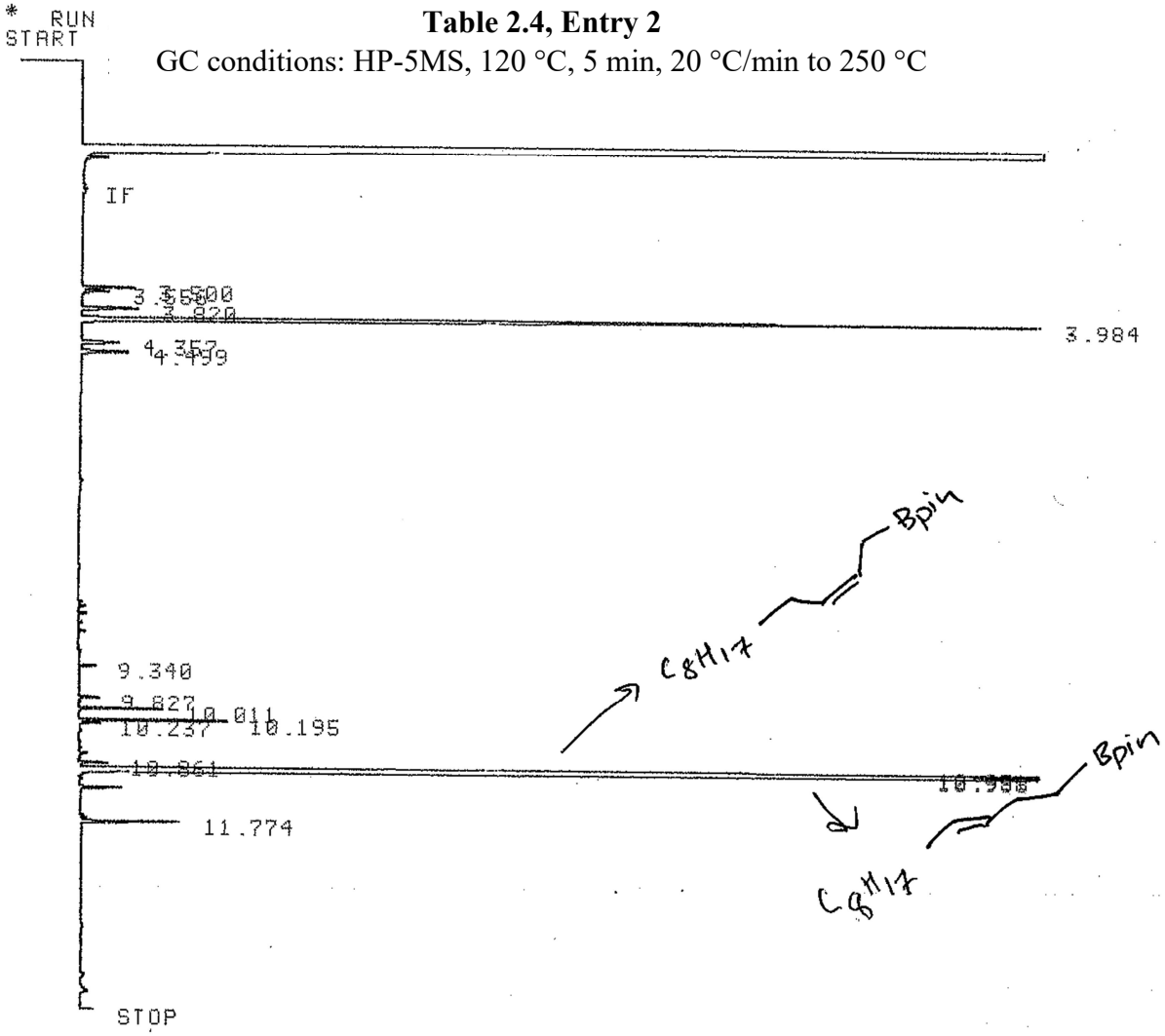


```
Closing signal file M:SIGNAL   .BNC

RUN#  1537          AUG 11, 1901  22:47:36

SIGNAL FILE: M:SIGNAL.BNC
AREA%
      RT       AREA TYPE  WIDTH     AREA%
   3.500       1513   VV    .028      .61371
   3.556        794   VB    .028      .32207
   3.820       1847   BB    .032      .74919
   3.984      32549   BB    .033    13.20270
   4.357       1351   BB    .035      .54800
   4.499       1714   PB    .035      .69524
   9.340        373   PB    .019      .15130
   9.827        475   BP    .021      .19267
  10.011       1702   PB    .020      .69037
  10.195       2881   PV    .019     1.16861
  10.237        466   VB    .020      .18902
  10.861        641   PV    .021      .26001
  10.951      61753   VV    .020    25.04858
  10.988     135472   VV    .020    54.95086
  11.246        910   PB    .021      .36912
  11.774       2092   VB    .021      .84857

TOTAL AREA= 246533
MUL FACTOR=1.0000E+00
```

dupe. 1Mmol.S1
126°C
(2hrs)

Table 2.4, Entry 3

GC conditions: HP-5MS, 120 °C, 5 min, 20 °C/min to 250 °C

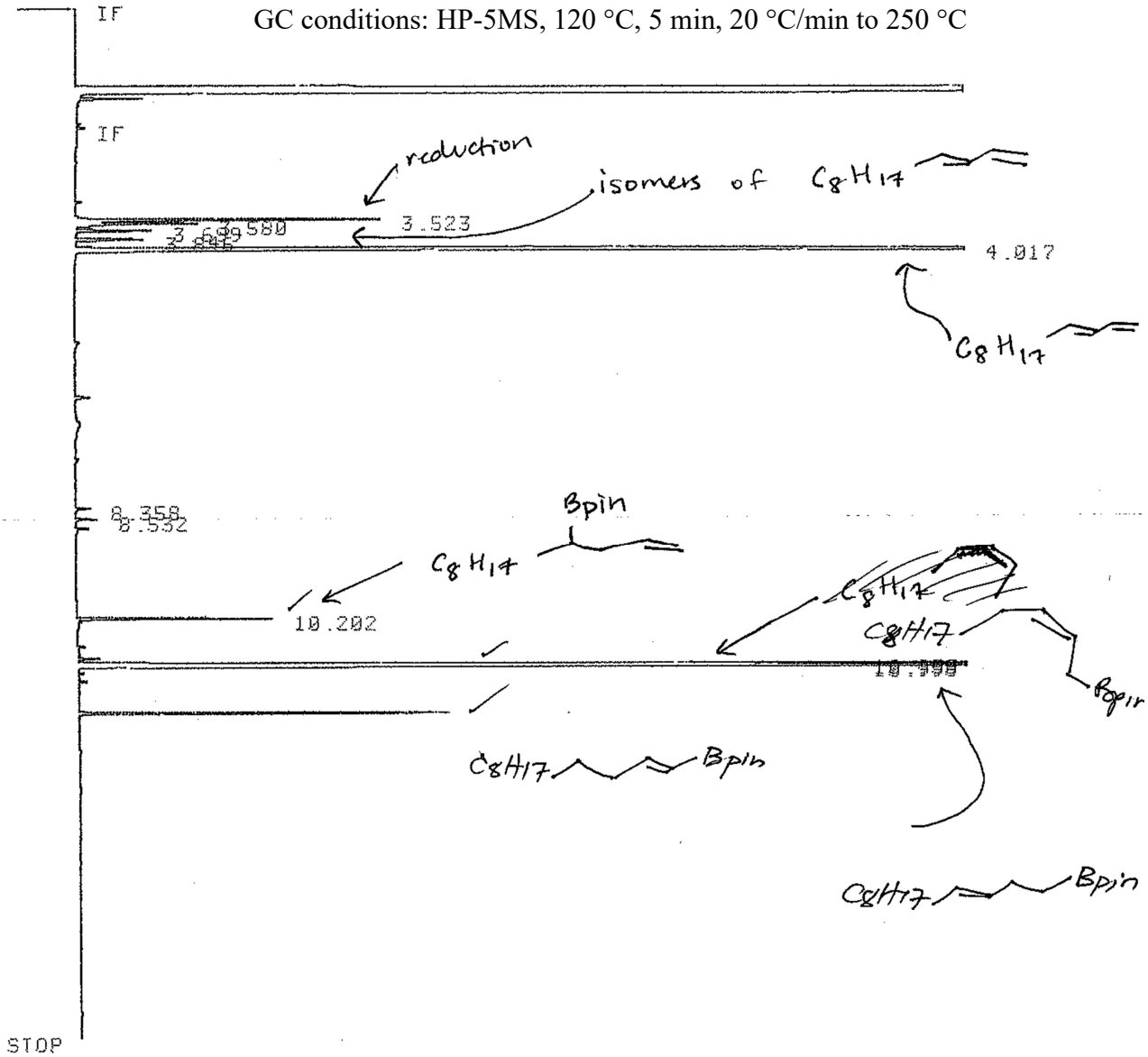


```
Closing signal file M:SIGNAL   .BNC

RUN#  1693          AUG 29, 1901  22:12:21

SIGNAL FILE: M:SIGNAL.BNC
AREA%
      RT       AREA TYPE  WIDTH      AREA%
   3.523       9739   BV    .029    2.37341
   3.580       4374   VP    .033    1.06595
   3.699       2326   PB    .028     .56685
   3.846       2276   BB    .030     .55466
   4.017     133674   PB    .031   32.57658
   6.499        483   BB    .027     .11771
   8.358        376   BB    .022     .09163
   8.532        487   PB    .021     .11868
  10.202       4173   PV    .020    1.01697
  10.870        510   BB    .020     .12429
  10.958      37449   PV    .020    9.12637
  10.998     205807   VB    .021   50.15549
  11.780       8664   BB    .021    2.11143
```

Table 2: entry 1

Apple Ch 30 mm MM01-74

Table 2.4, Entry 4

GC conditions: HP-5MS, 120 °C, 5 min, 20 °C/min to 250 °C

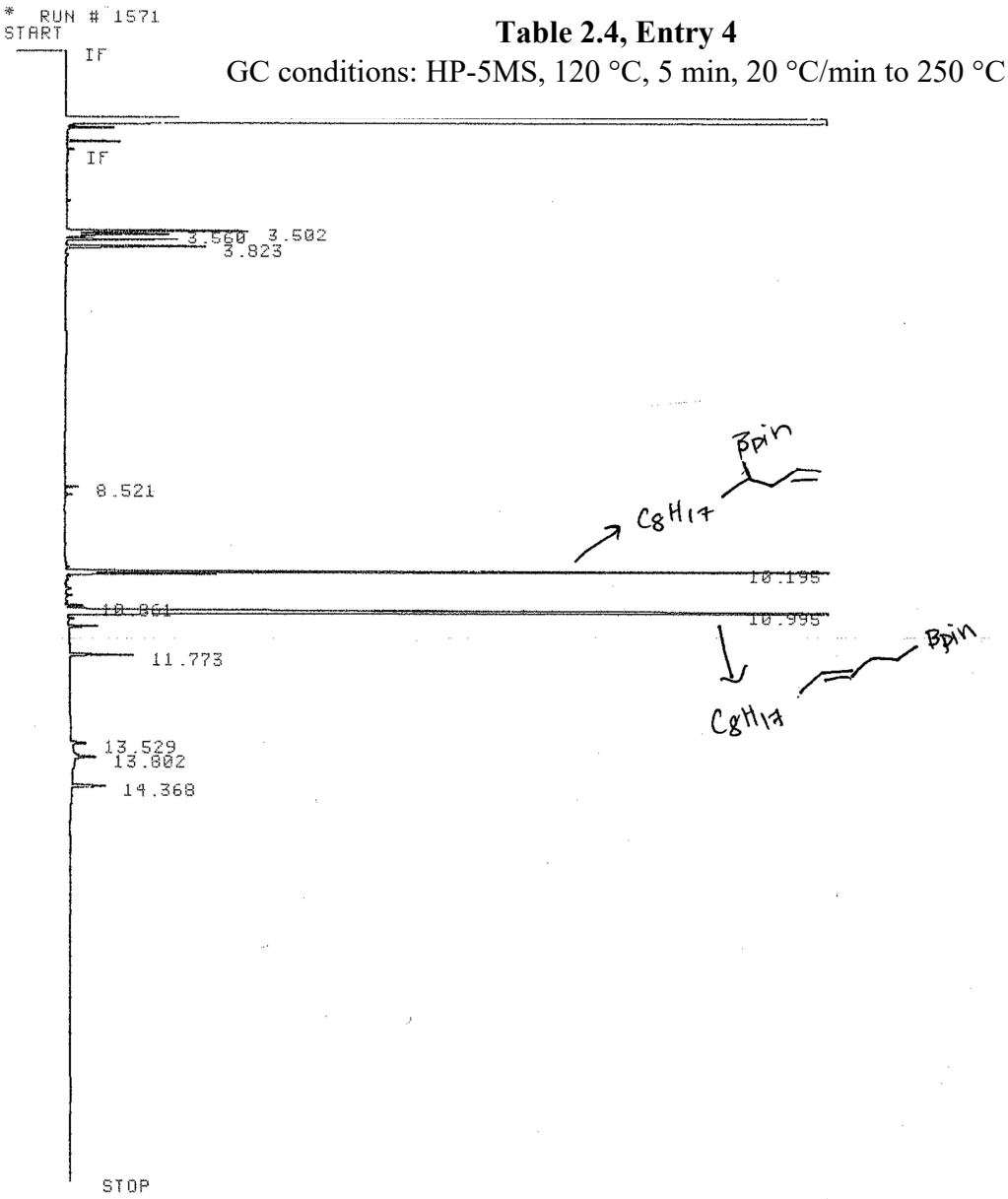

Closing signal file M:SIGNAL .BNC

RUN# 1571 AUG 15, 1901 01:07:16

SIGNAL FILE: M:SIGNAL.BNC
AREA%

RT	AREA	TYPE	WIDTH	AREA%
3.502	6481	BV	.028	1.62223
3.560	3764	VV	.029	.94215
3.676	4021	VB	.028	1.00648
3.823	5228	PB	.029	1.30860
8.521	380	BB	.021	.09512
10.195	31197	BV	.021	7.80878
10.236	3798	VV	.020	.95066
10.861	470	PV	.020	.11764
10.995	337732	VB	.024	84.53613
11.245	945	PB	.025	.23654
11.773	1744	BB	.021	.43653
13.529	642	PV	.035	.16070
13.802	1468	VB	.053	.36745
14.368	1642	BB	.038	.41100

dppbz
H(OCH2)2 BARF
120 °C
(30 min)
NM01.s8

Table 2.4, Entry 5

GC conditions: HP-5MS, 120 °C, 5 min, 20 °C/min to 250 °C

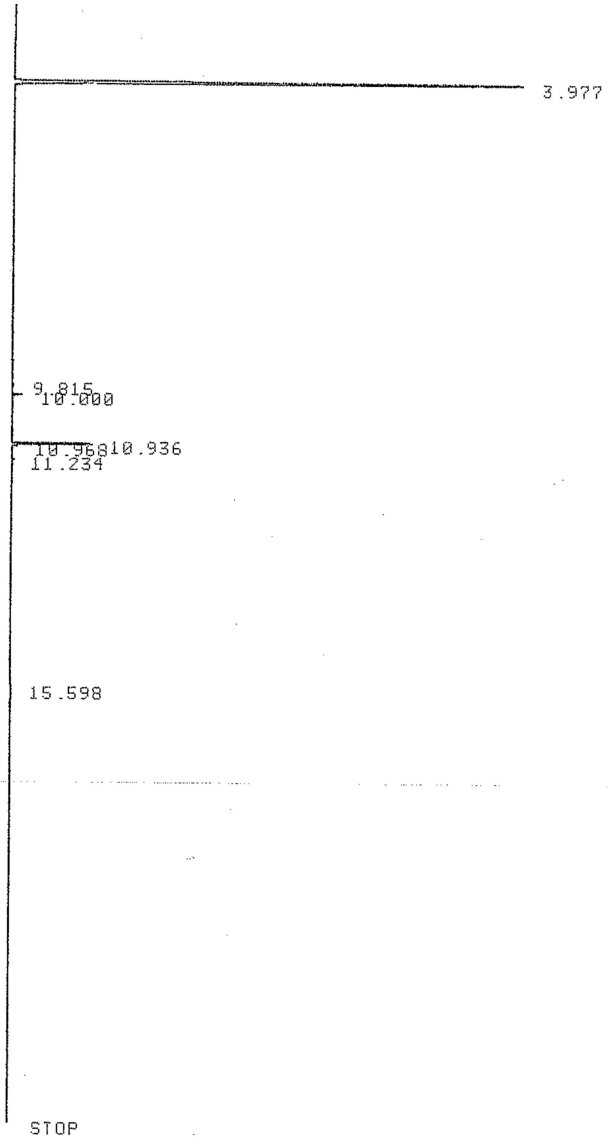

Closing signal file M:SIGNAL .BNC

RUN# 1512 AUG 7, 1901 22:16:03

SIGNAL FILE: M:SIGNAL.BNC
AREA%

RT	AREA	TYPE	WIDTH	AREA%
3.977	346779	PB	.034	87.07875
9.329	1126	BB	.021	.28275
9.815	1471	PB	.023	.36938
10.000	4330	PB	.019	1.08730
10.936	31870	VV	.020	8.00279
10.968	2063	VP	.017	.51803
11.234	1282	PB	.024	.32192
15.598	9315	BP	.248	2.33907

TOTAL AREA= 398236
MUL FACTOR=1.0000E+00

MM01.96
30 mins
120°C

Table 2.4, Entry 6

GC conditions: HP-1MS, 100 °C, 5 min, 20 °C/min to 250 °C

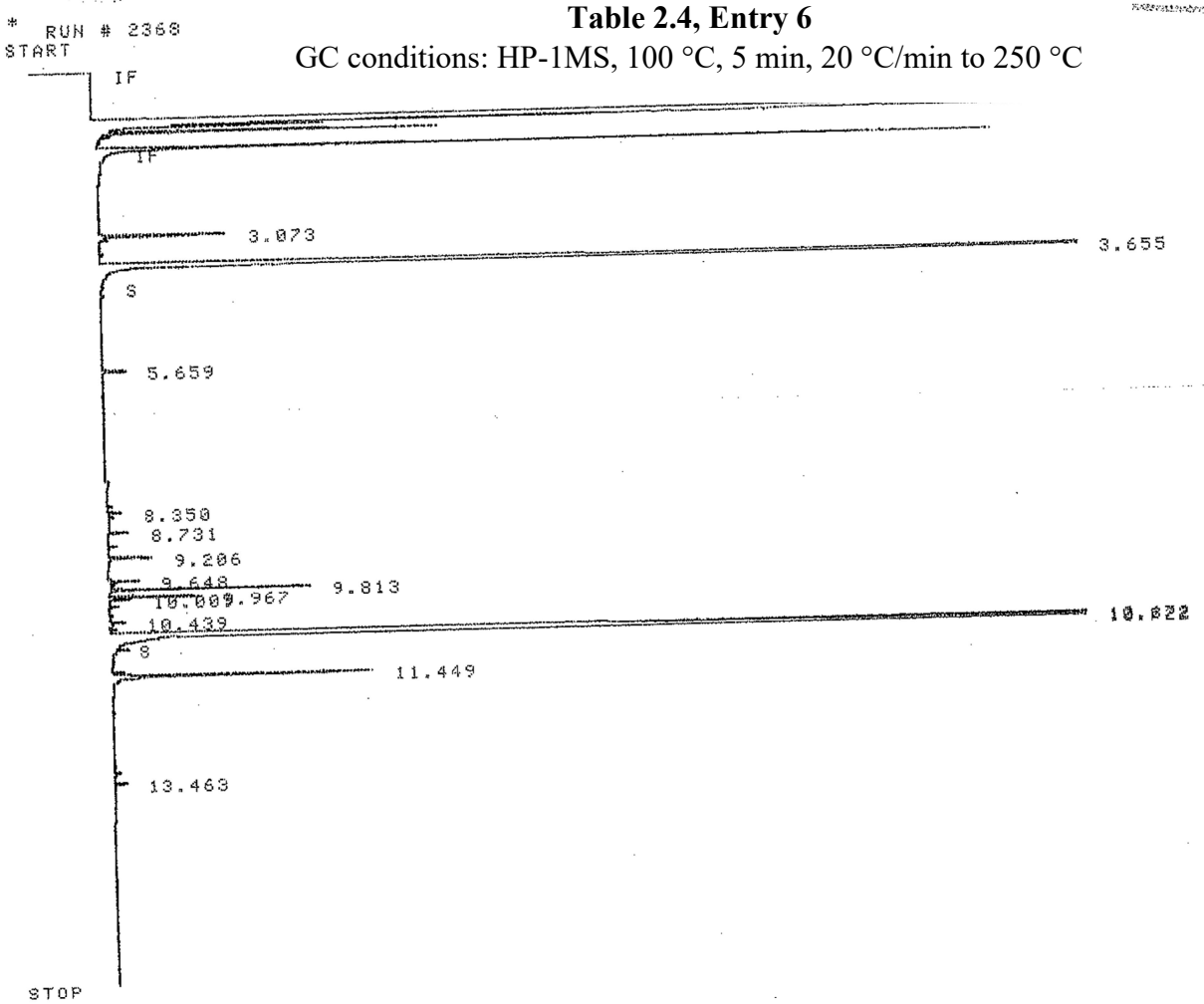

Closing signal file M:SIGNAL .BNC

RUN# 2368 AUG 9, 1901 03:21:28

SIGNAL FILE: M:SIGNAL.BNC

AREA%

RT	AREA	TYPE	WIDTH	AREA%
3.073	490997	PV	.030	1.41236
3.655	12841864	SPB	.042	36.93968
5.659	127509	PB	.038	.36678
9.206	105311	PB	.018	.30293
9.648	70115	BB	.018	.20169
9.813	426174	SPB	.016	1.22589
9.967	213820	BV	.018	.61505
10.672	3676960	SBH	.023	10.57679
10.722	15892912	SHB	.034	45.71602
11.449	918772	SHB	.028	2.64285

(1-5 hours) MM01-48 100°C

Table 2.4, Entry 7

GC conditions: HP-5MS, 120 °C, 5 min, 20 °C/min to 250 °C

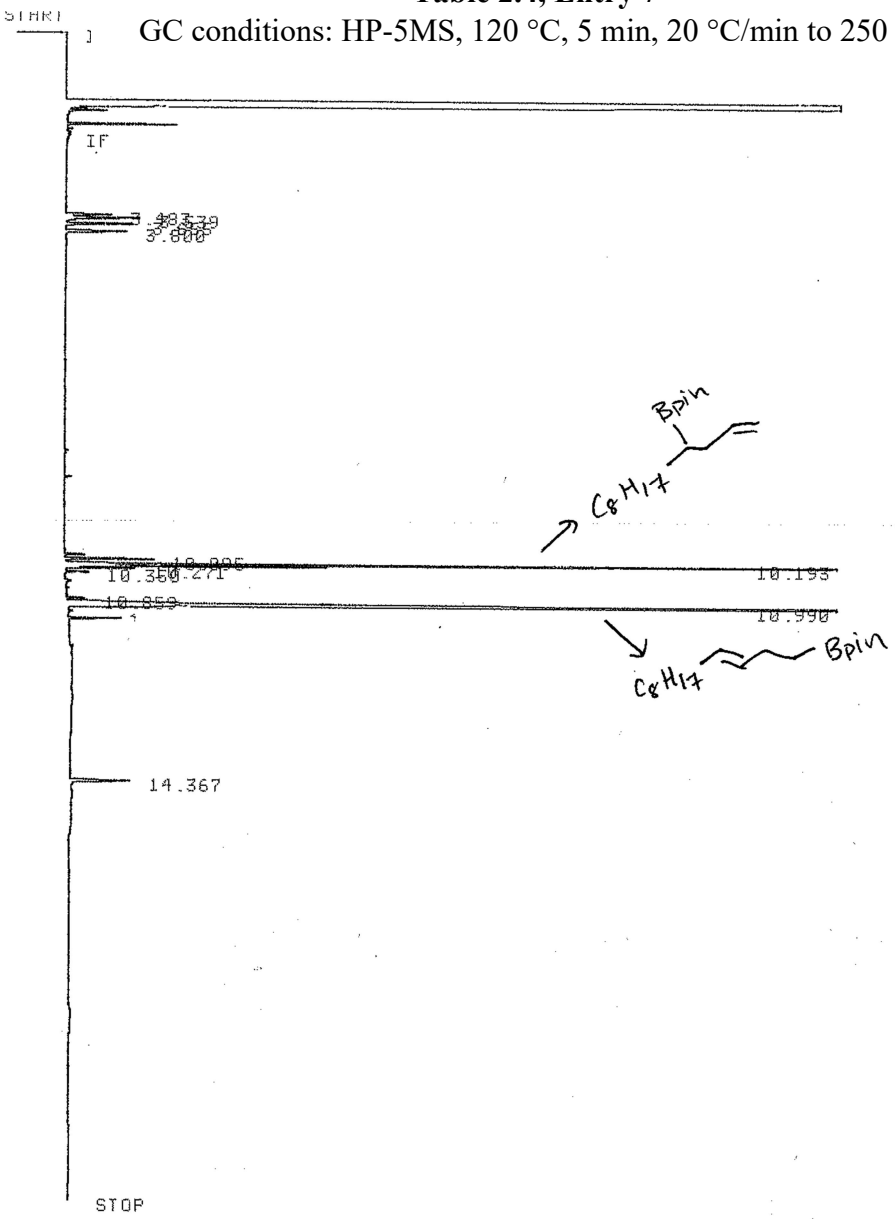

Closing signal file M:SIGNAL .BNC

RUN# 1569 AUG 15, 1901 00:19:51

SIGNAL FILE: M:SIGNAL.BNC
AREA%

RT	AREA	TYPE	WIDTH	AREA%
3.483	1684	PU	.029	.57423
3.539	2995	VV	.032	1.02127
3.655	2426	VB	.029	.82724
3.800	2278	BB	.030	.77678
10.013	526	PB	.020	.17936
10.095	2195	PB	.020	.74847
10.193	22425	BV	.023	7.64672 ✓
10.233	6356	VV	.019	2.16734 ✓
10.271	1684	VB	.019	.57423
10.350	671	BB	.021	.22880
10.859	477	BP	.019	.16265
10.990	245667	PB	.023	03.77021
11.244	1343	BB	.019	.45795
14.367	2536	PB	.034	.86475

TOTAL AREA= 293263
MUL FACTOR=1.0000E+00

DIOP + $H(OAc)_2$ BARF
NMOL. 59
120 °C
(30 mins)

Table 2.4, Entry 8

GC conditions: HP-5MS, 120 °C, 5 min, 20 °C/min to 250 °C

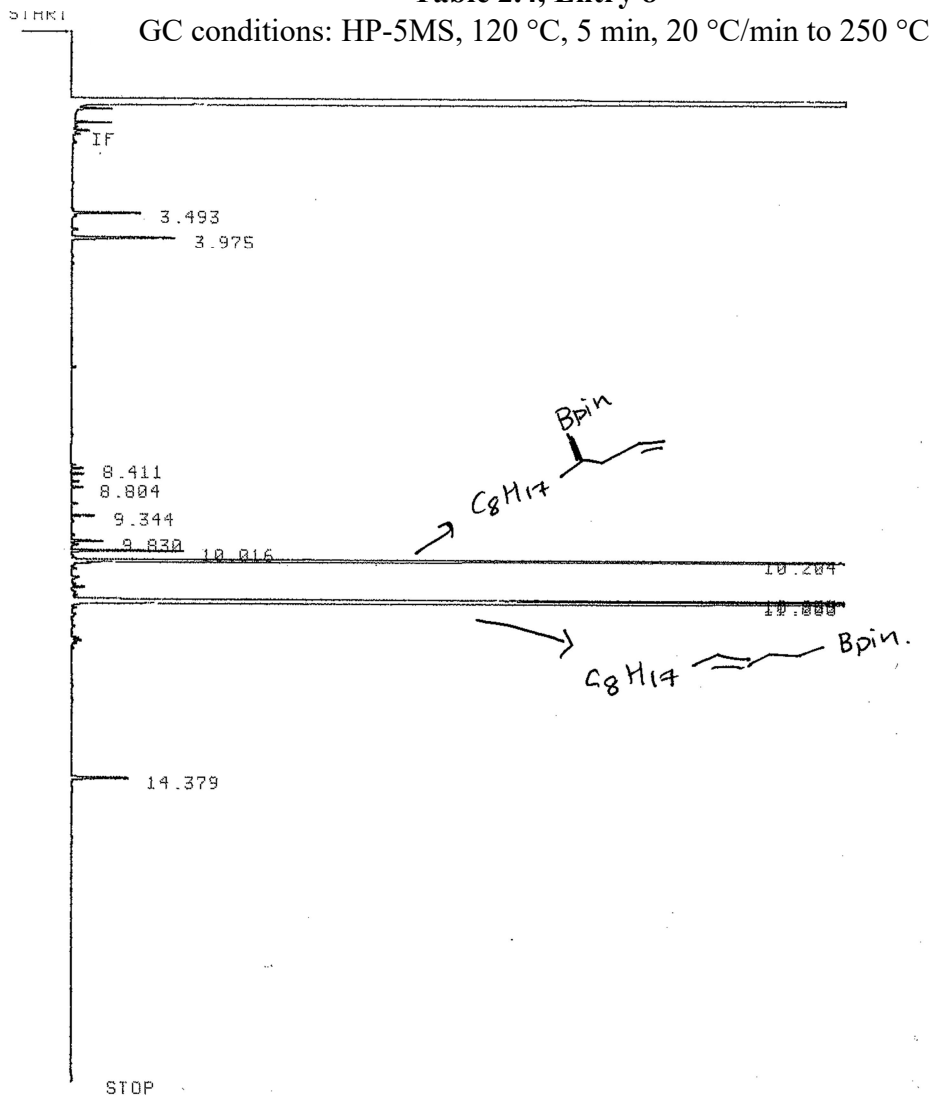


```
Closing signal file M:SIGNAL   .BNC

RUN#  1640          AUG 25, 1901  20:20:37

SIGNAL FILE: M:SIGNAL.BNC
AREA%
      RT       AREA TYPE  WIDTH      AREA%
   3.493       2337   VV    .027      .52663
   3.975       4142   PB    .032      .93337
   8.411        358   PB    .021      .08067
   8.523        366   BB    .021      .08248
   8.804        392   BB    .023      .08833
   9.344        630   BV    .020      .14197
   9.830        897   BP    .022      .20213
  10.016       2698   BB    .019      .60797
  10.204     114940   PV    .020    25.90086
  10.715        419   VB    .024      .09442
  10.955      20452   PV    .020     4.60870
  11.000     293672   VB    .022    66.17677
  14.379       2466   BB    .034      .55569

TOTAL AREA= 443769
MUL FACTOR=1.0000E+00
```

MMOL 67
120°C
(30 mins)
BCF + BPPGCGE

Table 2.4, Entry 9

GC conditions: HP-5MS, 120 °C, 5 min, 20 °C/min to 250 °C

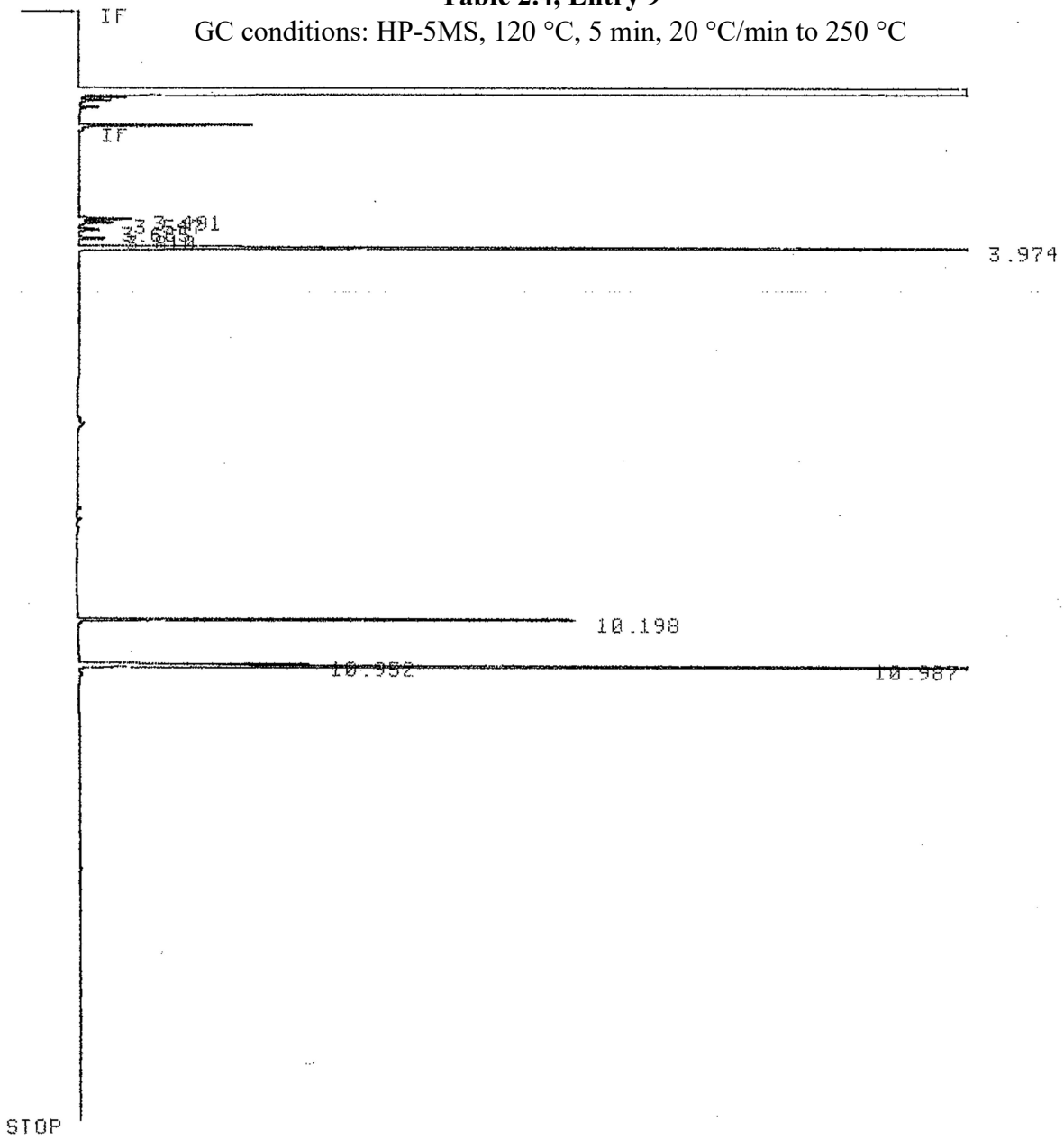

Closing signal file M:SIGNAL .BNC

RUN# 1600 AUG 20, 1901 00:41:03

SIGNAL FILE: M:SIGNAL.BNC
AREA%

RT	AREA	TYPE	WIDTH	AREA%
3.491	1540	PV	.027	1.25822
3.547	1165	VB	.031	.95184
3.665	644	BB	.027	.52617
3.810	858	BB	.029	.70101
3.974	39954	BB	.031	32.64349
10.198	10046	VV	.020	8.86147
10.952	4669	BV	.019	3.81470
10.987	62719	VB	.020	51.24310

TOTAL AREA= 122395
MUL FACTOR=1.0000E+00

BDP MM01-68 (Chris) 120°C

Table 2.4, Entry 10

GC conditions: HP-5MS, 120 °C, 5 min, 20 °C/min to 250 °C

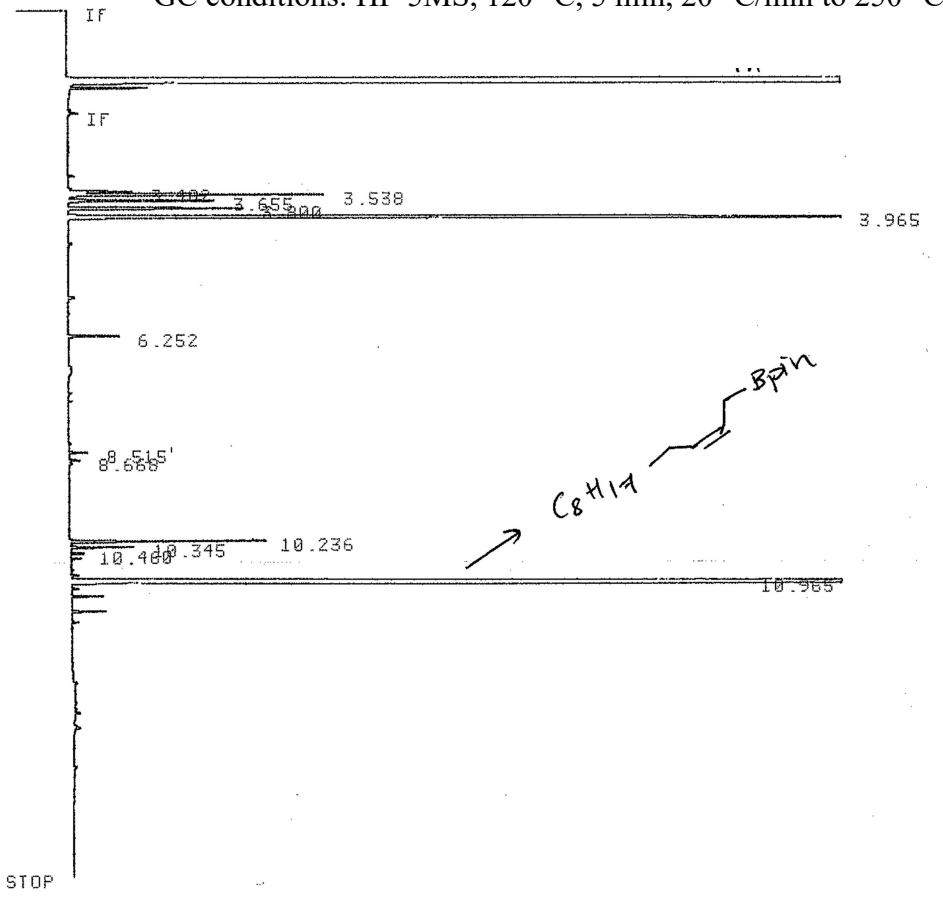

Closing signal file M:SIGNAL .BNC

RUN# 1556 AUG 13, 1901 18:35:11

SIGNAL FILE: M:SIGNAL.BNC
AREA%

RT	AREA	TYPE	WIDTH	AREA%
3.482	2204	PV	.029	.44487
3.538	9374	VB	.030	1.89212
3.655	5475	PB	.030	1.10511
3.800	6852	BB	.031	1.38306
3.965	52356	BB	.033	10.56792
6.252	1822	PB	.028	.36777
8.515	518	BB	.021	.10456
8.668	334	BV	.022	.06742
10.236	4750	VB	.019	.95877
10.345	1553	PB	.019	.31347
10.460	352	BB	.020	.07105
10.965	408137	PB	.025	82.38134
11.246	832	PB	.020	.16794
11.560	865	PB	.020	.17460

TOTAL AREA= 495424
MUL FACTOR=1.0000E+00

(pin)
120°C
MM01-53
(2hrs)

Table 2.4, Entry 11

GC conditions: HP-5MS, 120 °C, 5 min, 20 °C/min to 250 °C

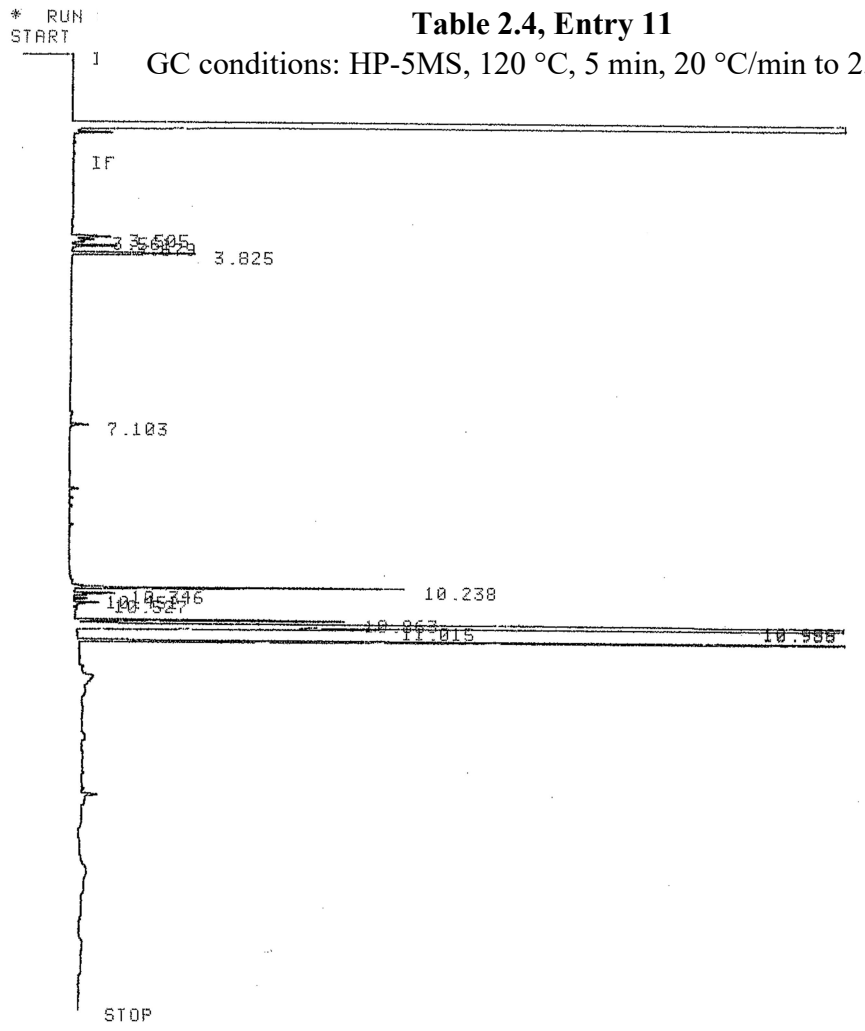

Closing signal file M:SIGNAL .BNC

RUN# 1567 AUG 14, 1901 22:11:45

SIGNAL FILE: M:SIGNAL.BNC
AREA%

RT	AREA	TYPE	WIDTH	AREA%
3.505	1477	BV	.031	.47417
3.561	843	VV	.030	.27063
3.679	1624	PB	.029	.52137
3.825	4889	BB	.032	1.56955
7.103	588	PB	.025	.18877
10.238	6914	PB	.017	2.21965
10.346	1025	PV	.021	.32906
10.451	394	PB	.022	.12649
10.527	727	BV	.023	.23339
10.863	6809	BV	.020	2.18595
10.959	198577	VV	.022	63.75067 ✓
10.986	49329	VV	.018	15.83646 ✓
11.015	6489	VB	.017	2.08321
11.248	31113	VB	.020	9.98845
14.233	692	PB	.035	.22216

TOTAL AREA= 311490
MUL FACTOR=1.0000E+00

ph + NaBARF
120°C
Nimol. 5%
(30 mins)

Table 2.4, Entry 12

GC conditions: HP-5MS, 120 °C, 5 min, 20 °C/min to 250 °C

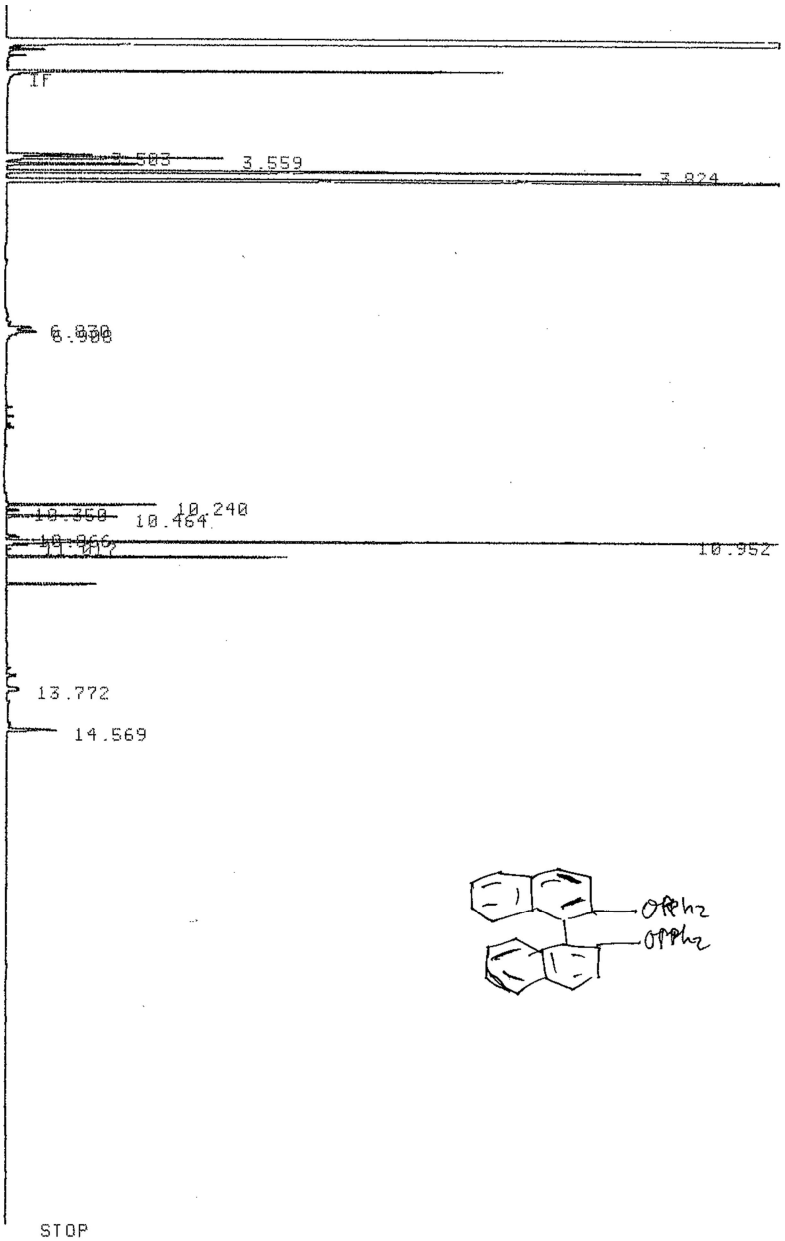

Closing signal file M:SIGNAL .BNC

RUN# 1601 AUG 20, 1901 01:02:34

SIGNAL FILE: M:SIGNAL.BNC
AREA%

RT	AREA	TYPE	WIDTH	AREA%
3.503	3225	BV	.030	1.92945
3.559	8146	VP	.030	4.87358
3.676	4700	PB	.028	2.81191
3.824	23739	PB	.030	14.20255
3.990	82108	PB	.032	49.12352
6.830	1513	VV	.046	.90520
6.908	2403	VB	.065	1.43767
10.240	3859	BV	.020	2.30876
10.350	381	PB	.022	.22794
10.464	2742	PV	.020	1.64048
10.866	677	PV	.035	.40504
10.952	20749	VV	.021	12.41370
11.017	579	VB	.019	.34640
11.250	6929	BB	.019	4.14548
11.778	2440	PB	.021	1.45980
13.772	612	BV	.038	.36615
14.569	2344	VB	.038	1.40237

Bala's
Ugand
MM01.64
2hrs
120°C

Table 2.4, Entry 13

GC conditions: HP-5MS, 120 °C, 5 min, 20 °C/min to 250 °C

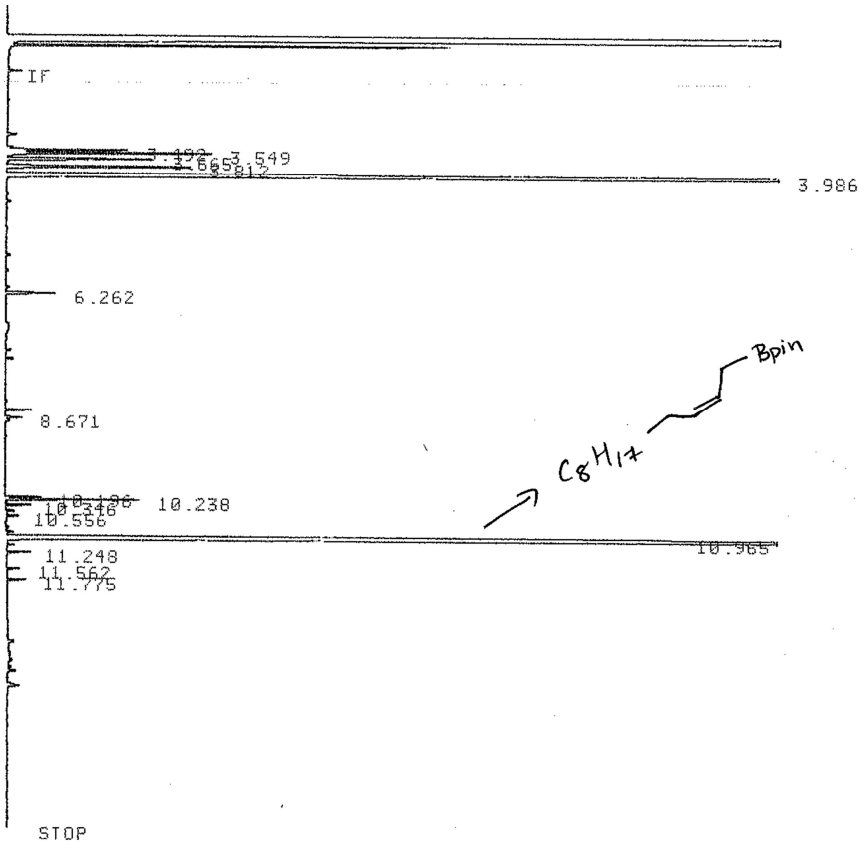

Closing signal file M:SIGNAL .BNC

RUN# 1557 AUG 13, 1901 18:56:49

SIGNAL FILE: M:SIGNAL.BNC
AREA%

RT	AREA	TYPE	WIDTH	AREA%
3.492	4273	VV	.029	.69938
3.549	7348	VB	.029	1.20268
3.665	5392	PB	.030	.88253
3.812	7221	PB	.031	1.18189
3.986	201615	PB	.034	32.99922
6.262	1746	BB	.028	.28578
8.520	725	PB	.022	.11866
8.671	472	BV	.022	.07725
10.196	896	BV	.020	.14665
10.238	3263	VV	.019	.53407
10.346	665	VB	.021	.10884
10.556	344	BB	.020	.05630
10.965	374701	PB	.025	61.32898
11.248	687	PB	.022	.11244
11.562	366	BB	.020	.05990
11.775	520	PB	.021	.08511
13.810	735	BB	.047	.12030

TOTAL AREA= 610969
MUL FACTOR=1.0000E+00

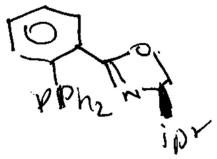

MM01.52 (C24H32NOP)

Appendix B: ^{1}H-NMR and ^{13}C-NMR Spectra for Chapter 2

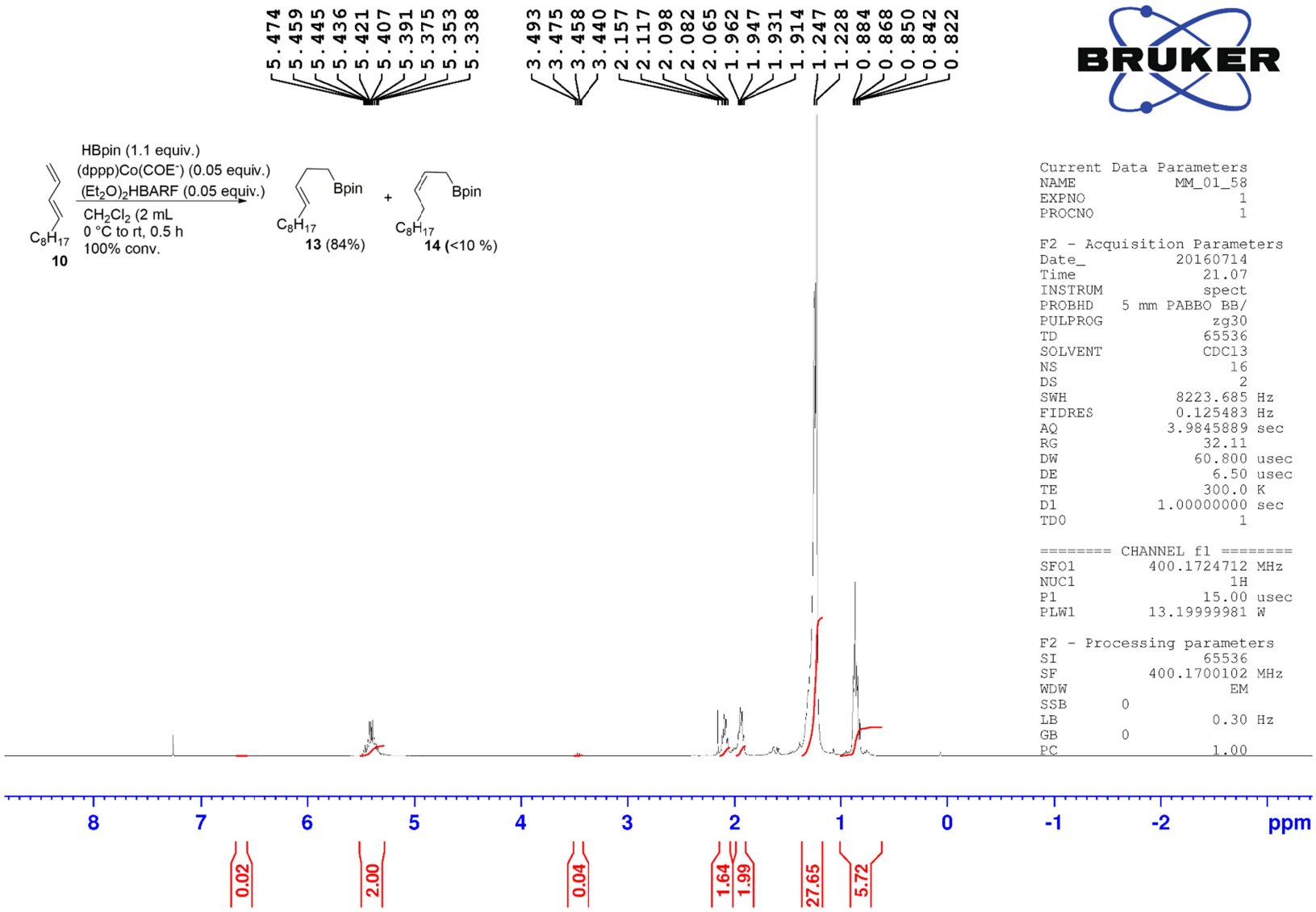
5.474
5.459
5.445
5.436
5.421
5.407
5.391
5.375
5.353
5.338
3.493
3.475
3.458
3.440
2.157
2.117
2.098
2.082
2.065
1.962
1.947
1.931
1.914
1.247
1.228
0.884
0.868
0.850
0.842
0.822
HBpin (1.1 equiv.)
(dppp)Co(COE) (0.05 equiv.)
(Et2O)2HBARF (0.05 equiv.)
CH2Cl2 (2 mL
0 °C to rt, 0.5 h
100% conv.
C8H17
10
Bpin
C8H17
13 (84%)
+
Bpin
C8H17
14 (<10 %)
BRUKER
Current Data Parameters
NAME MM_01_58
EXPNO 1
PROCNO 1
F2 - Acquisition Parameters
Date_ 20160714
Time 21.07
INSTRUM spect
PROBHD 5 mm PABBO BB/
PULPROG zg30
TD 65536
SOLVENT CDCl3
NS 16
DS 2
SWH 8223.685 Hz
FIDRES 0.125483 Hz
AQ 3.9845889 sec
RG 32.11
DW 60.800 usec
DE 6.50 usec
TE 300.0 K
D1 1.00000000 sec
TD0 1
======== CHANNEL f1 ========
SFO1 400.1724712 MHz
NUC1 1H
P1 15.00 usec
PLW1 13.19999981 W
F2 - Processing parameters
SI 65536
SF 400.1700102 MHz
WDW EM
SSB 0
LB 0.30 Hz
GB 0
PC 1.00
8
7
6
5
4
3
2
1
0
-1
-2
ppm
0.02
2.00
0.04
1.64
1.99
27.65
5.72

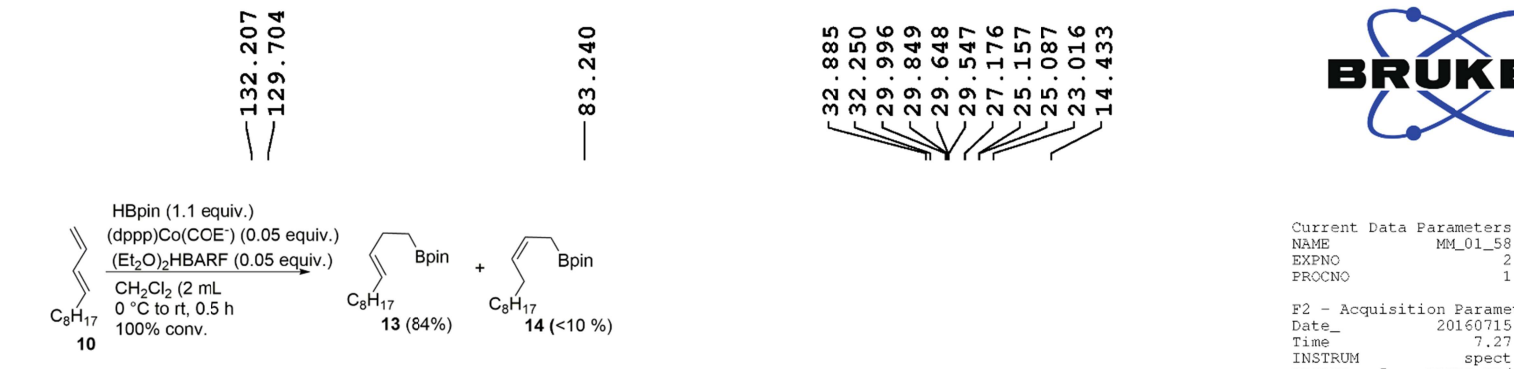

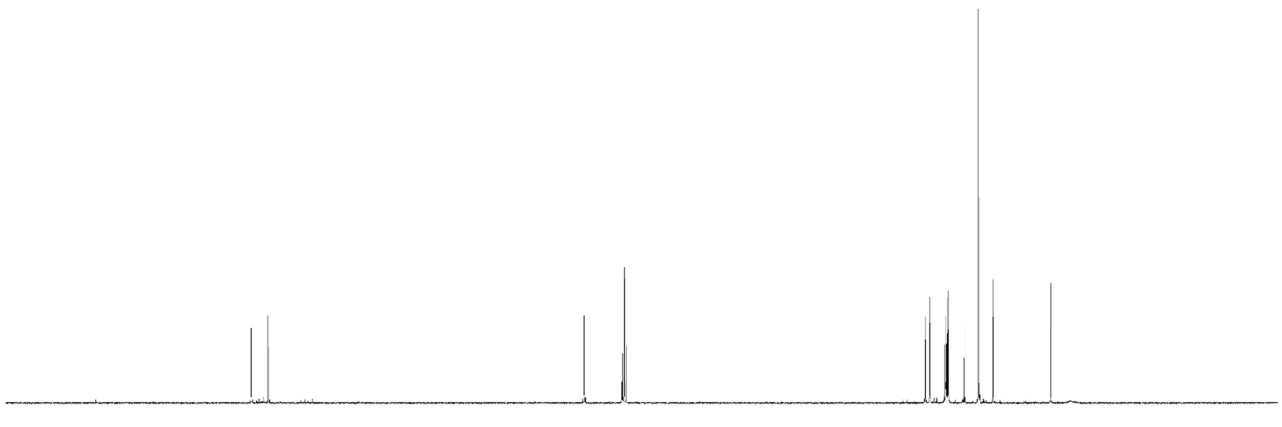

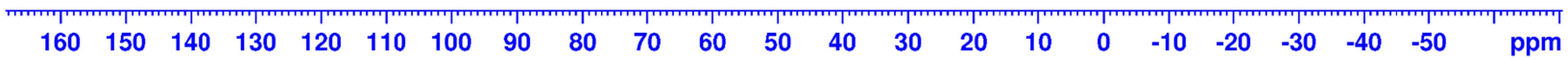


```
Current Data Parameters
NAME                  MM_01_58
EXPNO                        2
PROCNO                       1

F2 - Acquisition Parameters
Date_                20160715
Time                     7.27
INSTRUM                 spect
PROBHD    5 mm PABBO BB/
PULPROG                 zgpg30
TD                       65536
SOLVENT                  CDCl3
NS                        1024
DS                           4
SWH                  24038.461 Hz
FIDRES                0.366798 Hz
AQ                    1.3631488 sec
RG                        1820
DW                      20.800 usec
DE                       6.50 usec
TE                      300.0 K
D1                   2.00000000 sec
D11                  0.03000000 sec
TD0                          1

======== CHANNEL f1 ========
SFO1               100.6328883 MHz
NUC1                       13C
P1                        9.50 usec
PLW1               53.29999924 W

======== CHANNEL f2 ========
SFO2               400.1716007 MHz
NUC2                       1H
CPDPRG[2                waltz16
PCPD2                    80.00 usec
PLW2               14.60000038 W
PLW12               0.51327997 W
PLW13               0.32850000 W

F2 - Processing parameters
SI                       32768
SF                 100.6227916 MHz
WDW                         EM
SSB          0
LB                        1.00 Hz
GB           0
PC                        1.40
```

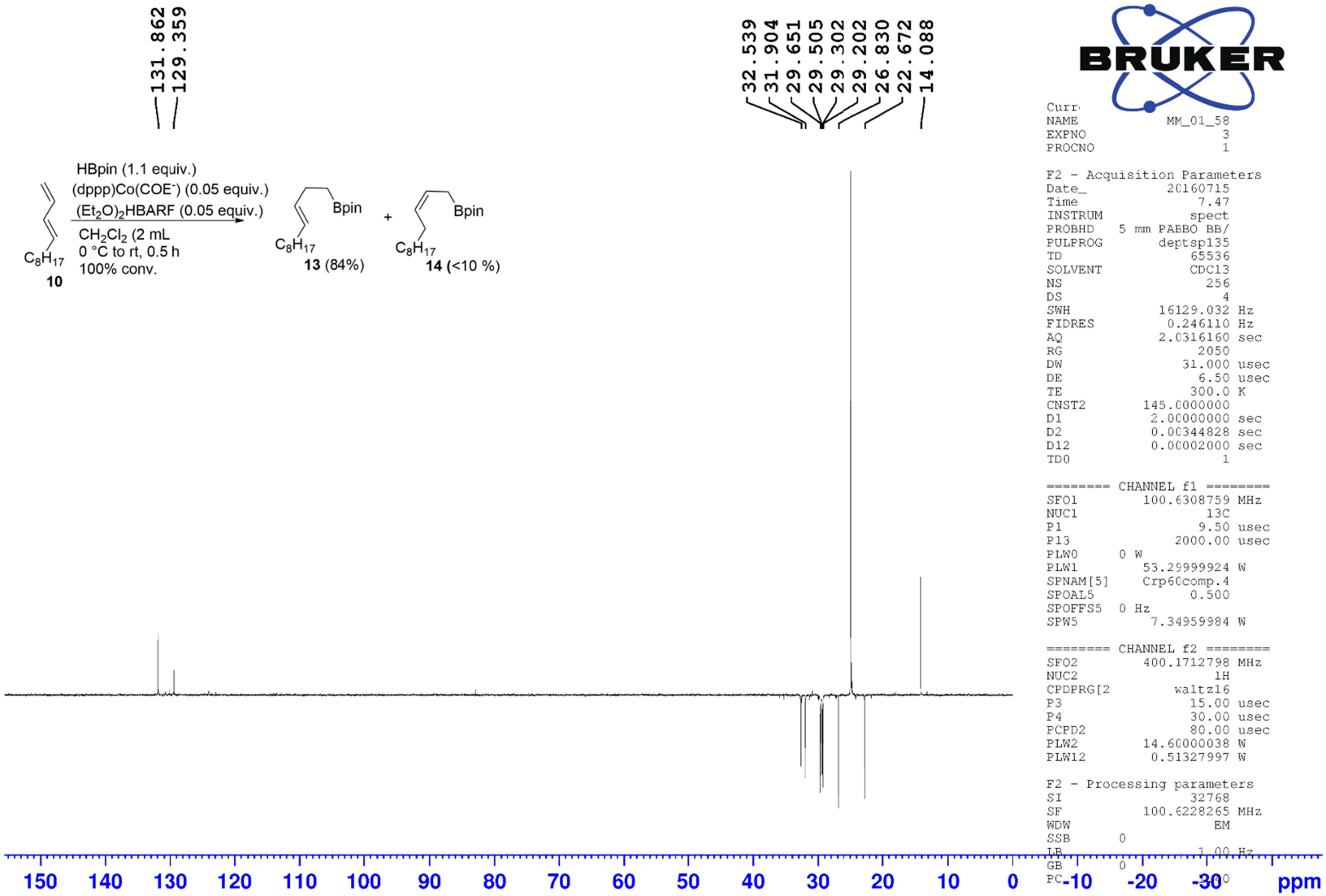


```
Curr
NAME                MM_01_58
EXPNO                      3
PROCNO                     1

F2 - Acquisition Parameters
Date_              20160715
Time                   7.47
INSTRUM               spect
PROBHD    5 mm PABBO BB/
PULPROG          deptsp135
TD                   65536
SOLVENT              CDCl3
NS                     256
DS                       4
SWH              16129.032 Hz
FIDRES           0.246110 Hz
AQ               2.0316160 sec
RG                    2050
DW                  31.000 usec
DE                   6.50 usec
TE                  300.0 K
CNST2           145.0000000
D1               2.00000000 sec
D2               0.00344828 sec
D12              0.00002000 sec
TD0                        1

======== CHANNEL f1 ========
SFO1            100.6308759 MHz
NUC1                    13C
P1                     9.50 usec
P13                 2000.00 usec
PLW0        0 W
PLW1           53.29999924 W
SPNAM[5]       Crp60comp.4
SPOAL5                0.500
SPOFFS5     0 Hz
SPW5            7.34959984 W

======== CHANNEL f2 ========
SFO2            400.1712798 MHz
NUC2                    1H
CPDPRG[2             waltz16
P3                    15.00 usec
P4                    30.00 usec
PCPD2                 80.00 usec
PLW2            14.60000038 W
PLW12            0.51327997 W

F2 - Processing parameters
SI                     32768
SF              100.6228265 MHz
WDW                       EM
SSB         0
LB                      1.00 Hz
GB          0
PC                      1.00
```

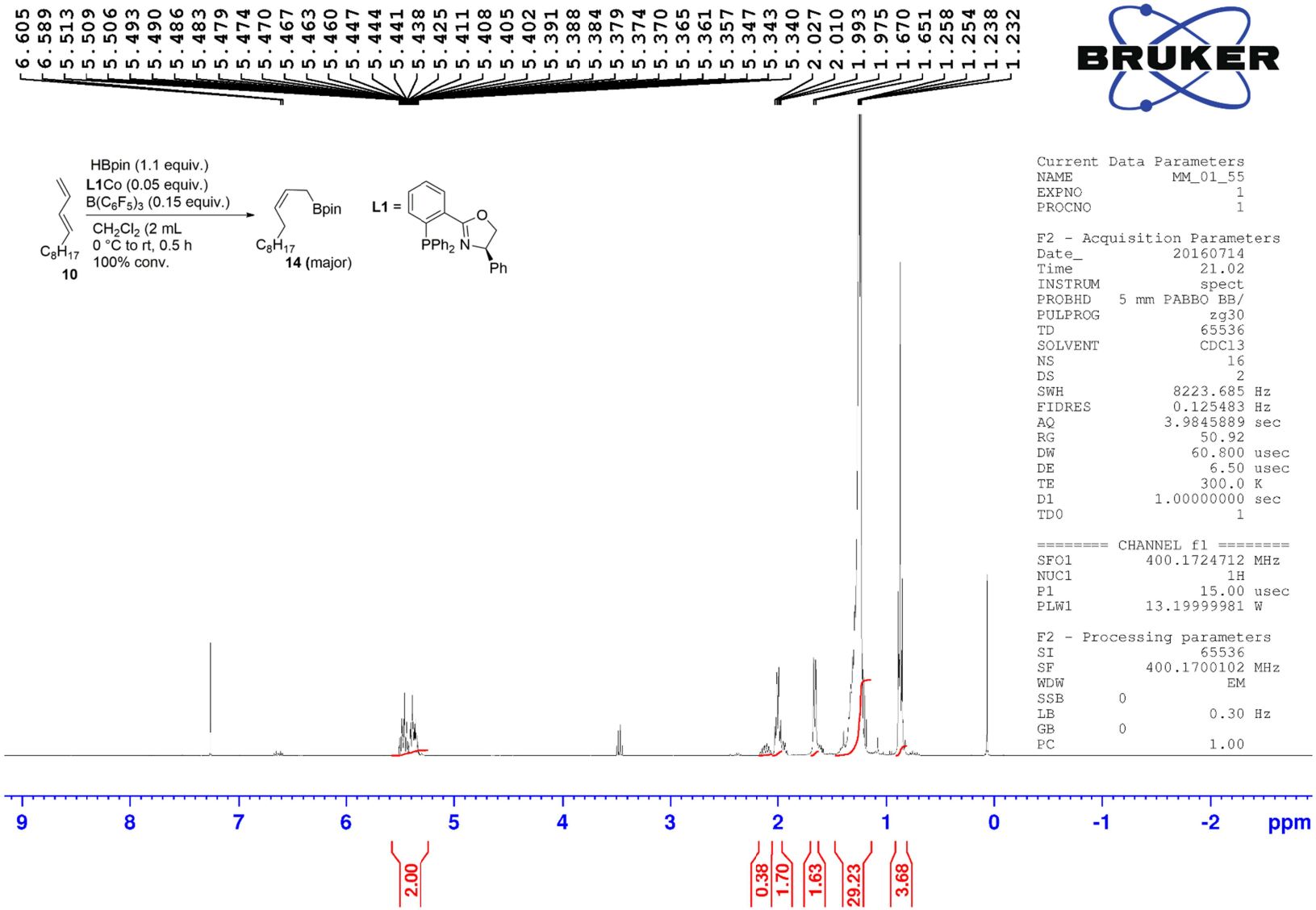
6.605 6.589 5.513 5.509 5.506 5.493 5.490 5.486 5.483 5.479 5.474 5.470 5.467 5.463 5.460 5.447 5.444 5.441 5.438 5.425 5.411 5.408 5.405 5.402 5.391 5.388 5.384 5.379 5.374 5.370 5.365 5.361 5.357 5.347 5.343 5.340 2.027 2.010 1.993 1.975 1.670 1.651 1.258 1.254 1.238 1.232
HBpin (1.1 equiv.)
L1Co (0.05 equiv.)
B(C6F5)3 (0.15 equiv.)
CH2Cl2 (2 mL
0 °C to rt, 0.5 h
100% conv.
C8H17
10
Bpin
C8H17
14 (major)
L1 =
PPh2
O
N
Ph
Current Data Parameters
NAME MM_01_55
EXPNO 1
PROCNO 1
F2 - Acquisition Parameters
Date_ 20160714
Time 21.02
INSTRUM spect
PROBHD 5 mm PABBO BB/
PULPROG zg30
TD 65536
SOLVENT CDCl3
NS 16
DS 2
SWH 8223.685 Hz
FIDRES 0.125483 Hz
AQ 3.9845889 sec
RG 50.92
DW 60.800 usec
DE 6.50 usec
TE 300.0 K
D1 1.00000000 sec
TD0 1
======== CHANNEL f1 ========
SFO1 400.1724712 MHz
NUC1 1H
P1 15.00 usec
PLW1 13.19999981 W
F2 - Processing parameters
SI 65536
SF 400.1700102 MHz
WDW EM
SSB 0
LB 0.30 Hz
GB 0
PC 1.00
9 8 7 6 5 4 3 2 1 0 -1 -2 ppm
2.00
0.38
1.70
1.63
29.23
3.68

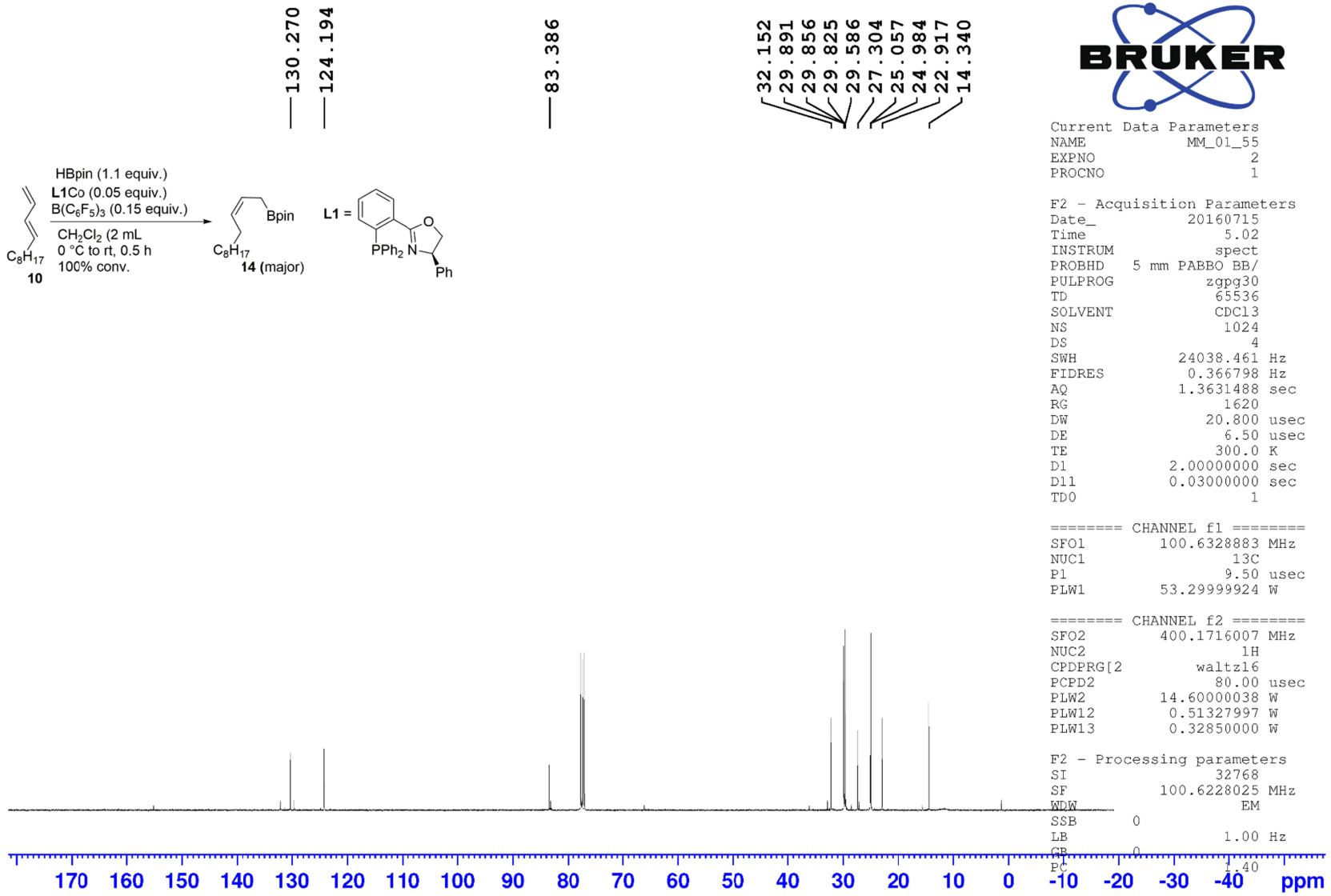
130.270
124.194
83.386
32.152
29.891
29.856
29.825
29.586
27.304
25.057
24.984
22.917
14.340
HBpin (1.1 equiv.)
L1Co (0.05 equiv.)
B(C6F5)3 (0.15 equiv.)
CH2Cl2 (2 mL
0 °C to rt, 0.5 h
100% conv.
C8H17
10
Bpin
C8H17
14 (major)
L1 =
PPh2
N
O
Ph
BRUKER
Current Data Parameters
NAME MM_01_55
EXPNO 2
PROCNO 1
F2 - Acquisition Parameters
Date_ 20160715
Time 5.02
INSTRUM spect
PROBHD 5 mm PABBO BB/
PULPROG zgpg30
TD 65536
SOLVENT CDCl3
NS 1024
DS 4
SWH 24038.461 Hz
FIDRES 0.366798 Hz
AQ 1.3631488 sec
RG 1620
DW 20.800 usec
DE 6.50 usec
TE 300.0 K
D1 2.00000000 sec
D11 0.03000000 sec
TD0 1
======== CHANNEL f1 ========
SFO1 100.6328883 MHz
NUC1 13C
P1 9.50 usec
PLW1 53.29999924 W
======== CHANNEL f2 ========
SFO2 400.1716007 MHz
NUC2 1H
CPDPRG[2 waltz16
PCPD2 80.00 usec
PLW2 14.60000038 W
PLW12 0.51327997 W
PLW13 0.32850000 W
F2 - Processing parameters
SI 32768
SF 100.6228025 MHz
WDW EM
SSB 0
LB 1.00 Hz
GB 0
PC 1.40
170 160 150 140 130 120 110 100 90 80 70 60 50 40 30 20 10 0 -10 -20 -30 -40 ppm

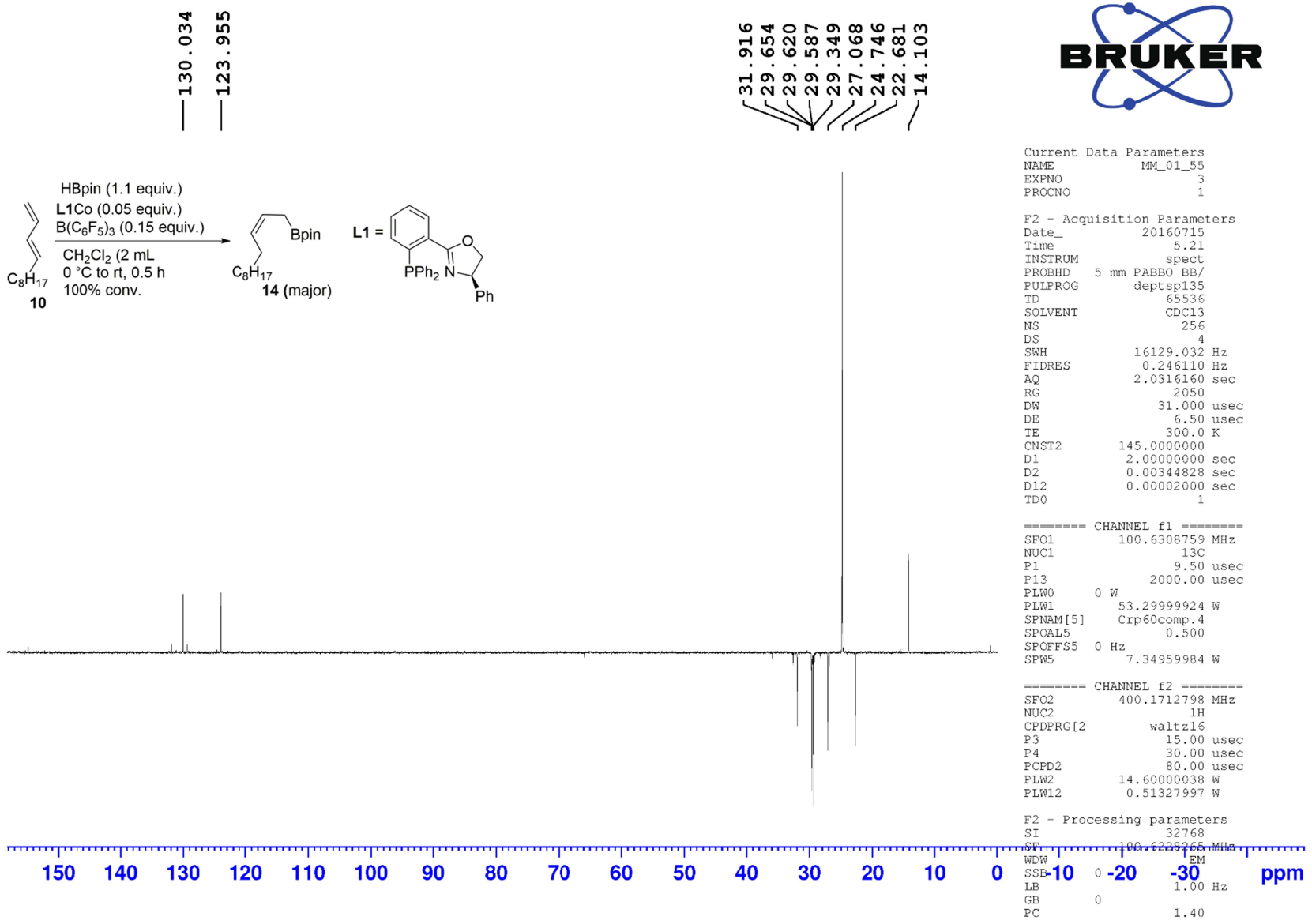


```
Current Data Parameters
NAME                  MM_01_55
EXPNO                        3
PROCNO                       1

F2 - Acquisition Parameters
Date_                 20160715
Time                      5.21
INSTRUM                  spect
PROBHD    5 mm PABBO BB/
PULPROG              deptsp135
TD                       65536
SOLVENT                  CDCl3
NS                         256
DS                           4
SWH                  16129.032 Hz
FIDRES                0.246110 Hz
AQ                    2.0316160 sec
RG                        2050
DW                      31.000 usec
DE                       6.50 usec
TE                      300.0 K
CNST2               145.0000000
D1                    2.00000000 sec
D2                    0.00344828 sec
D12                   0.00002000 sec
TD0                          1

======== CHANNEL f1 ========
SFO1                100.6308759 MHz
NUC1                        13C
P1                        9.50 usec
P13                    2000.00 usec
PLW0          0 W
PLW1               53.29999924 W
SPNAM[5]           Crp60comp.4
SPOAL5                   0.500
SPOFFS5       0 Hz
SPW5                7.34959984 W

======== CHANNEL f2 ========
SFO2                400.1712798 MHz
NUC2                        1H
CPDPRG[2                waltz16
P3                       15.00 usec
P4                       30.00 usec
PCPD2                    80.00 usec
PLW2               14.60000038 W
PLW12               0.51327997 W

F2 - Processing parameters
SI                       32768
SF                  100.6228265 MHz
WDW                         EM
SSB                          1
LB                        1.00 Hz
GB              0
PC                        1.40
```

Appendix C: Achiral Stationary Phase Gas Chromatograms for Table 3.1

Table 3.1, Entry 1

GC Conditions: HP-5MS, 100°C, 5 min, 20°C/min to 250°C

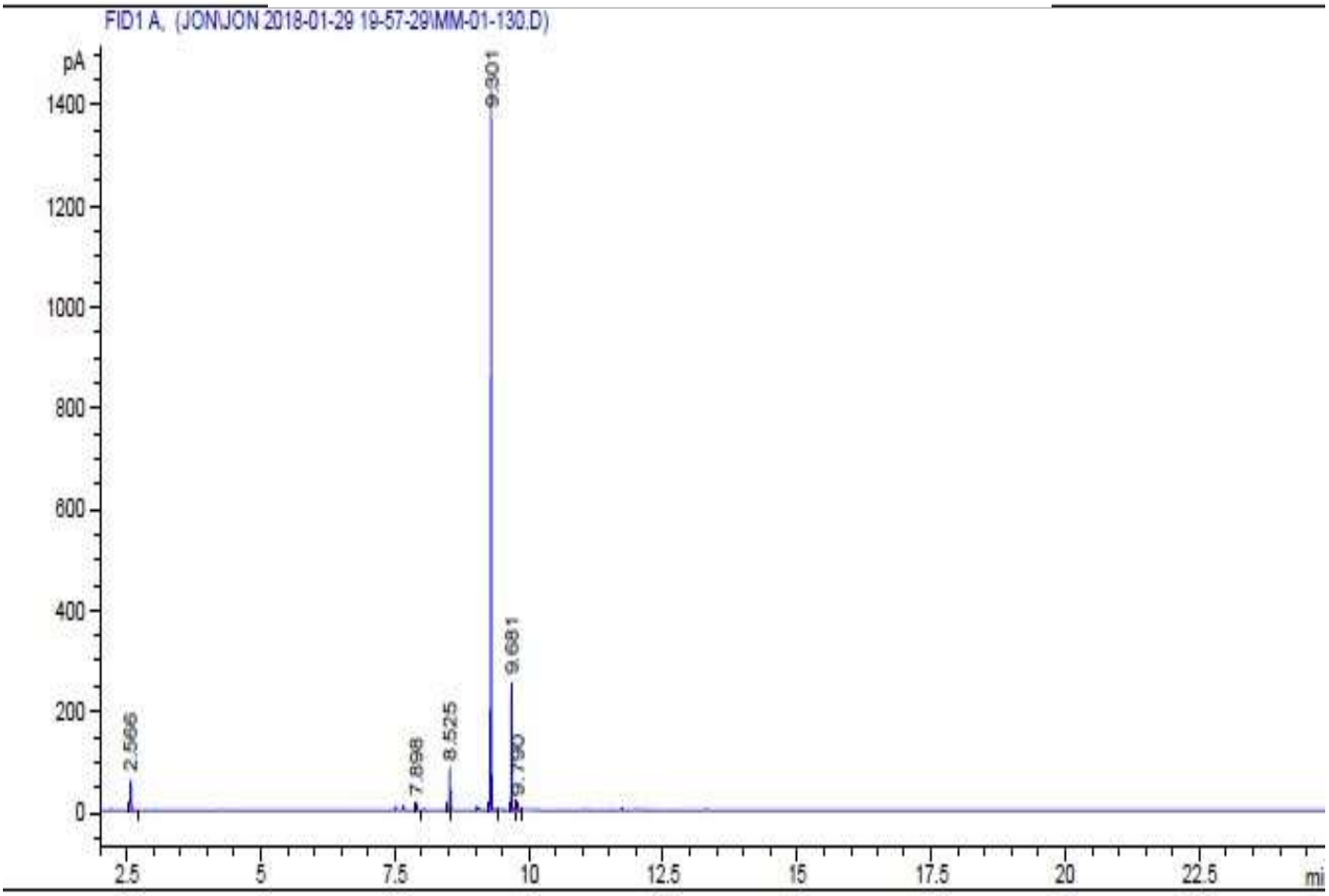

Peak #	RetTime [min]	Type	Width [min]	Area [pA*s]	Height [pA]	Area %
1	2.566	BB	0.0206	81.18777	60.77331	4.25979
2	7.898	BV	0.0175	16.10714	14.41462	0.84512
3	8.525	VV	0.0155	82.87236	83.92336	4.34818
4	9.301	VV	0.0153	1461.07739	1439.24841	76.66037
5	9.681	VV	0.0153	245.12407	253.50044	12.86126
6	9.790	VV	0.0185	19.54097	15.70655	1.02528

Table 3.1, Entry 2
GC Conditions: HP-5MS, 100°C, 5 min, 20°C/min to 250°C

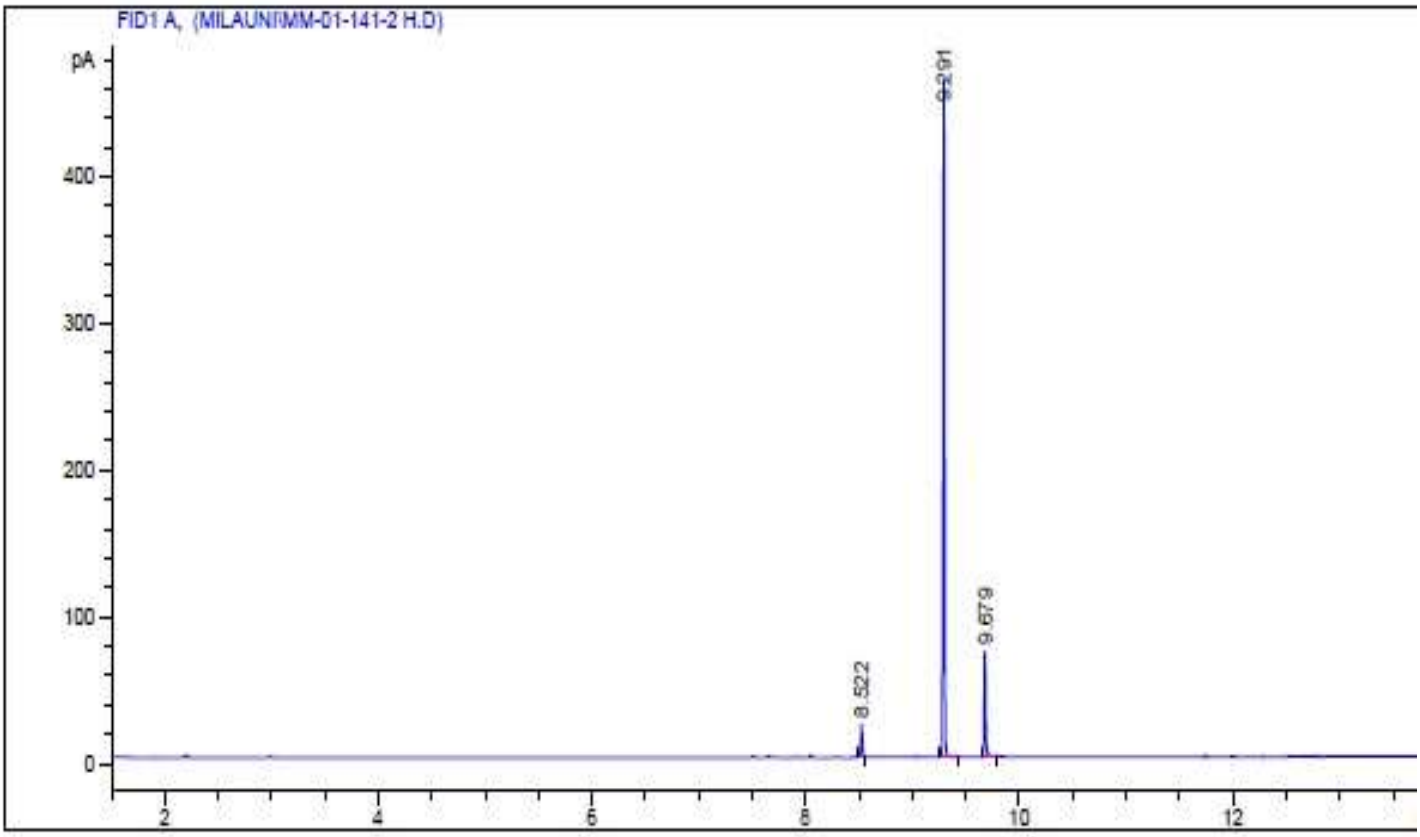


```
================================================================================
                          Area Percent Report
================================================================================

Sorted By             :      Signal
Multiplier:                   :      1.0000
Dilution:                     :      1.0000
Use Multiplier & Dilution Factor with ISTDs


Signal 1: FID1 A,

Peak RetTime Type  Width     Area      Height     Area
  #   [min]        [min]   [pA*s]      [pA]        %
----|-------|----|-------|----------|----------|--------|
   1   8.522 VV    0.0157   22.69189   22.68320  4.16608
   2   9.291 VB    0.0148  446.72842  459.56573 82.01640
   3   9.679 BV    0.0160   75.26148   72.93928 13.81751
```

Table 3.1, Entry 3

GC Conditions: HP-5MS, 100°C, 5 min, 20°C/min to 250°C

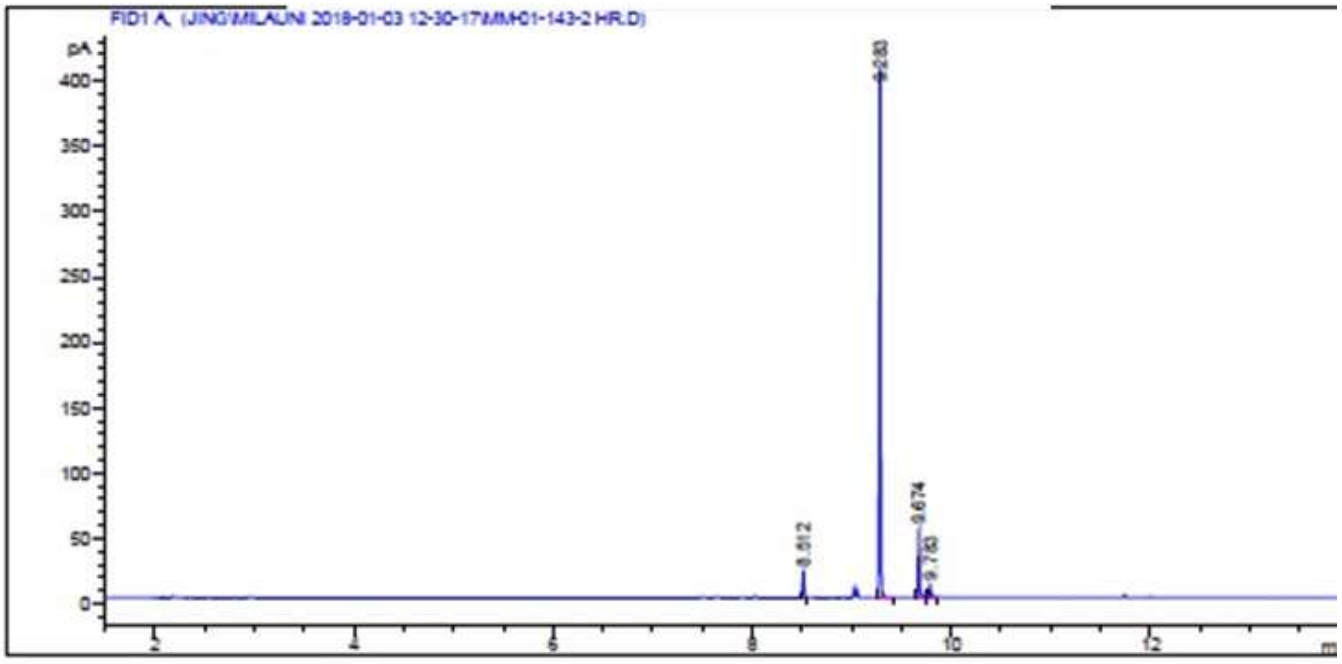


```
=====================================================================
                      Area Percent Report
=====================================================================

Sorted By             :      Signal
Multiplier:                   :      1.0000
Dilution:                     :      1.0000
Use Multiplier & Dilution Factor with ISTDs


Signal 1: FID1 A,

Peak RetTime Type  Width     Area      Height     Area
  #   [min]        [min]    [pA*s]     [pA]       %
----|-------|----|-------|----------|----------|--------|
   1   8.512 VV    0.0159   20.66536   20.19814  4.38431
   2   9.283 VV    0.0150  382.93219  407.21448 81.24192
   3   9.674 VV    0.0156   54.17699   52.10780 11.49405
   4   9.783 VV    0.0195   13.57349   10.20962  2.87972
```

Table 3.1, Entry 4
GC Conditions: HP-5MS, 100°C, 5 min, 20°C/min to 250°C

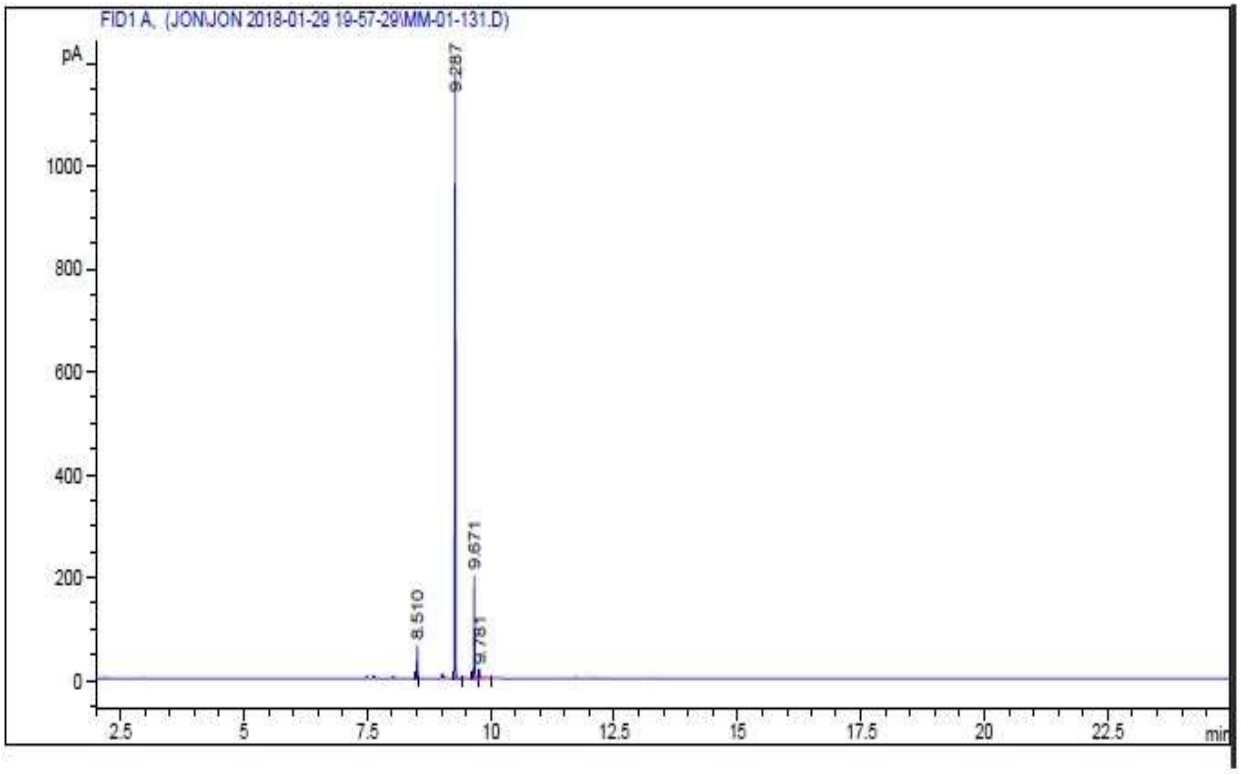

Peak #	RetTime [min]	Type	Width [min]	Area [pA*s]	Height [pA]	Area %
1	8.510	VV	0.0158	63.51426	63.00370	4.40725
2	9.287	VV	0.0155	1164.38989	1177.69531	80.79691
3	9.671	VV	0.0149	194.83632	200.26038	13.51967
4	9.781	VB	0.0198	18.39125	13.53786	1.27617

Table 3. 1, Entry 5

GC Conditions: HP-5MS, 100°C, 5 min, 20°C/min to 250°C

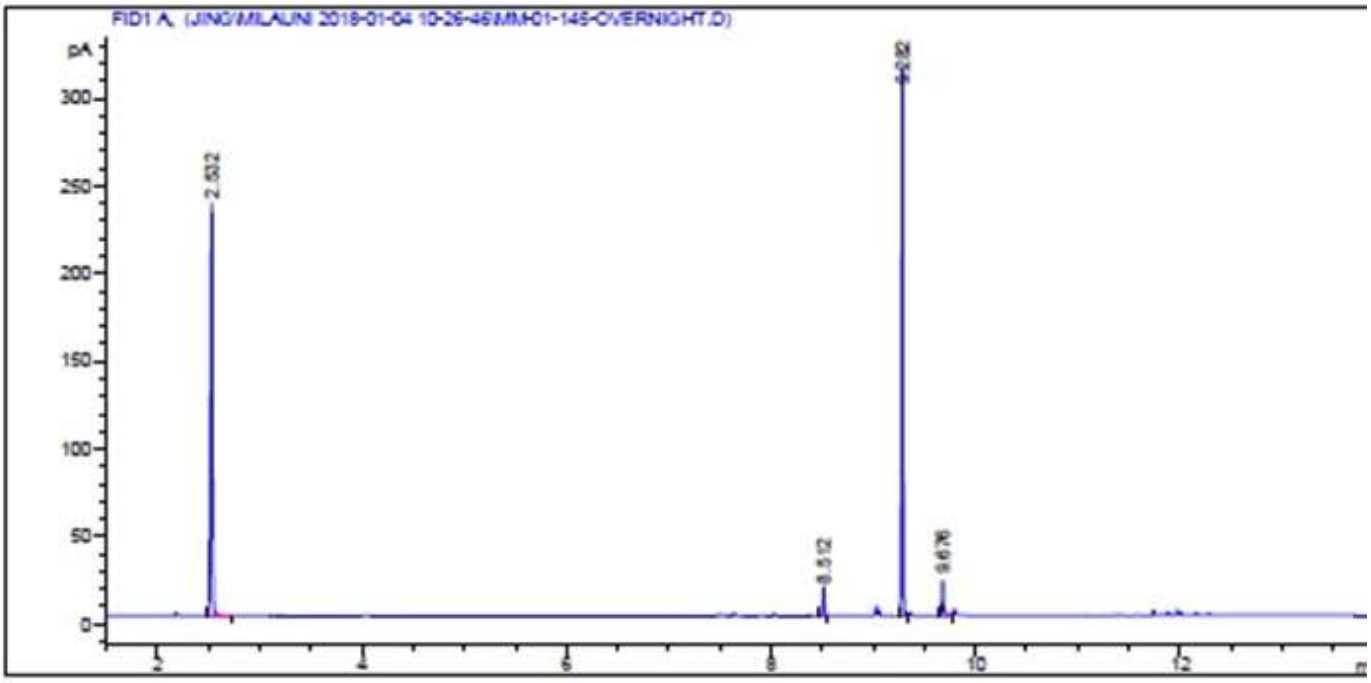

Area Percent Report

Sorted By : Signal
Multiplier: : 1.0000
Dilution: : 1.0000
Use Multiplier & Dilution Factor with ISTDs

Signal 1: FID1 A,

Peak #	RetTime [min]	Type	Width [min]	Area [pA*s]	Height [pA]	Area %
1	2.532	BB	0.0198	298.20065	235.38945	47.32819
2	8.512	VV	0.0158	16.23659	16.02384	2.57695
3	9.282	VV	0.0149	291.72177	313.00113	46.29991
4	9.676	BV	0.0175	23.91084	20.61672	3.79495

Table 3. 1, Entry 6

GC Conditions: HP-5MS, 100°C, 5 min, 20°C/min to 250°C

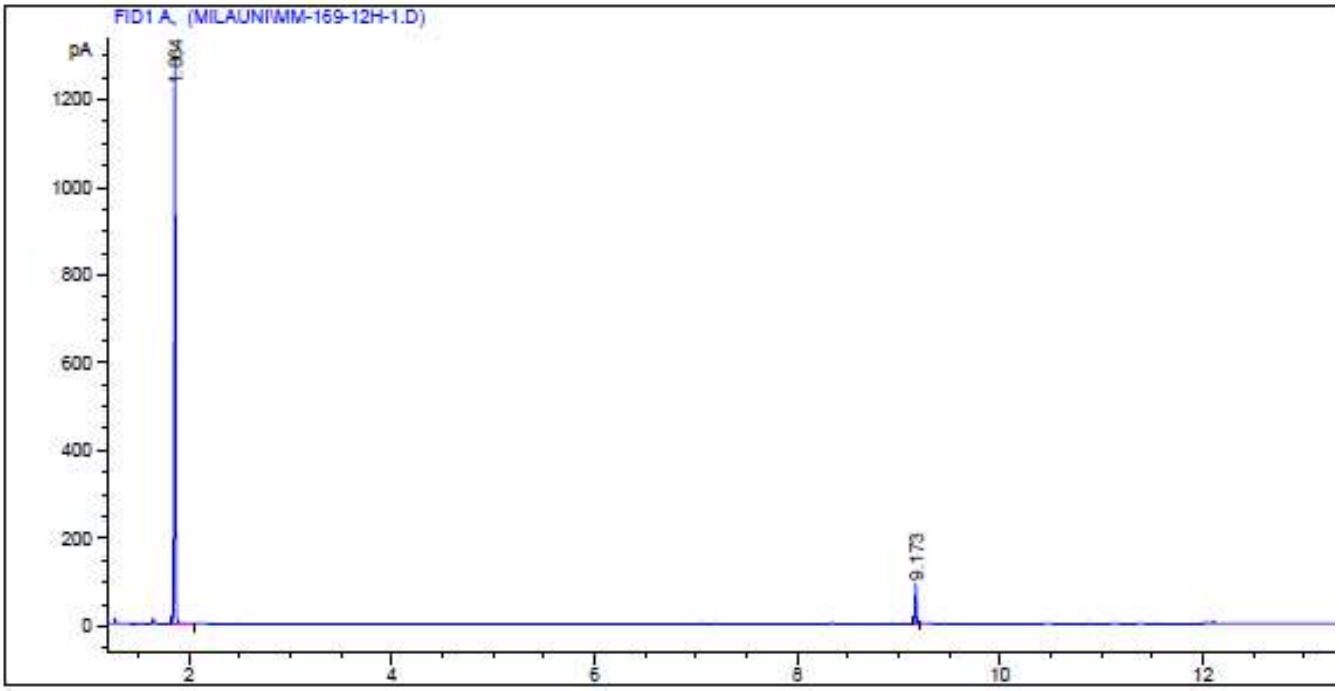


```
=====================================================================
                      Area Percent Report
=====================================================================

Sorted By             :      Signal
Multiplier:                   :      1.0000
Dilution:                     :      1.0000
Use Multiplier & Dilution Factor with ISTDs


Signal 1: FID1 A,

Peak RetTime Type  Width     Area      Height     Area
  #   [min]        [min]   [pA*s]      [pA]        %
----|-------|----|-------|----------|----------|--------|
   1   1.864 VV    0.0140 1140.67578 1267.33057 93.31280
   2   9.173 VV    0.0147   81.74583   89.47720  6.68720
```

Table 3. 1, Entry 7
GC Conditions: HP-5MS, 100°C, 5 min, 20°C/min to 250°C

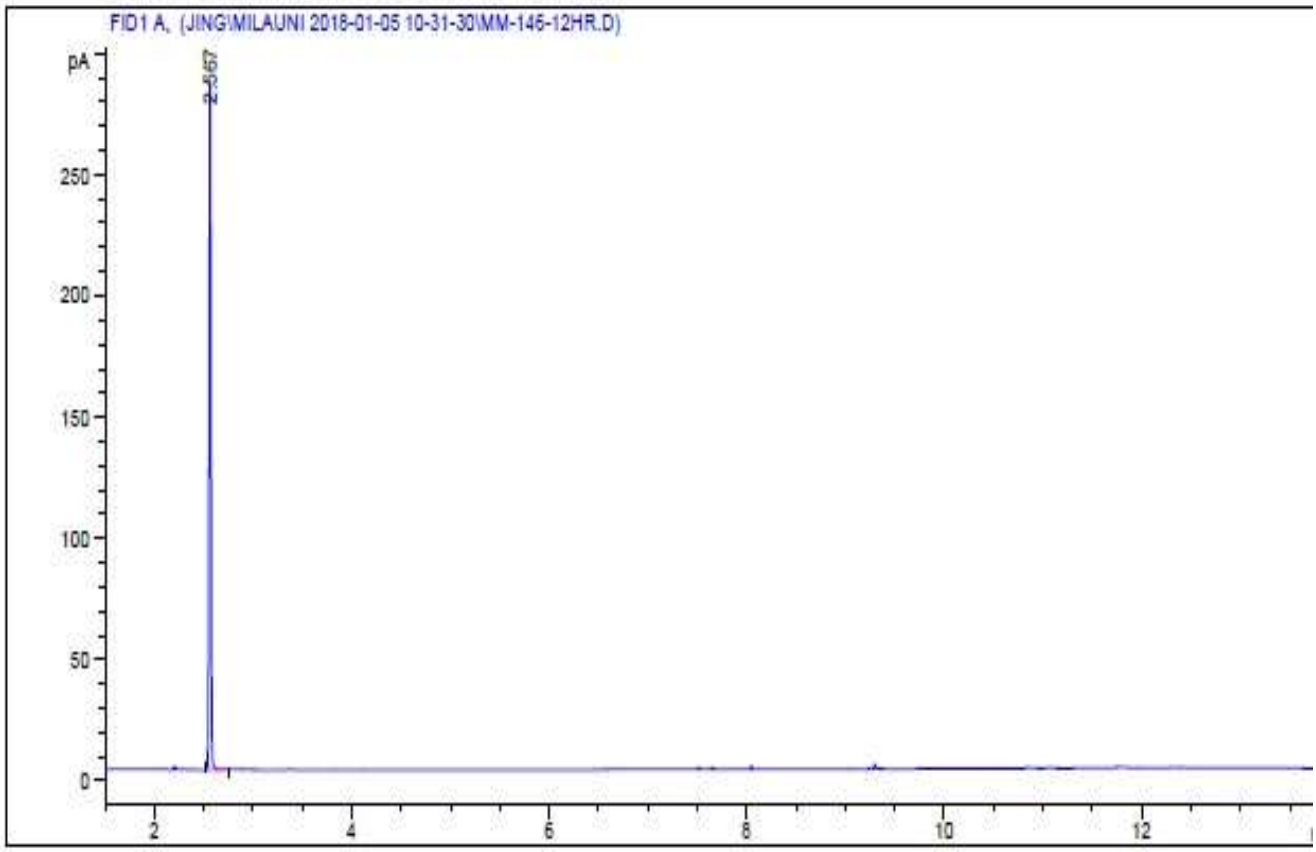


```
=====================================================================
                      Area Percent Report
=====================================================================

Sorted By             :      Signal
Multiplier:                   :      1.0000
Dilution:                     :      1.0000
Use Multiplier & Dilution Factor with ISTDs


Signal 1: FID1 A,

Peak RetTime Type  Width     Area      Height     Area
  #   [min]        [min]   [pA*s]      [pA]        %
----|-------|----|-------|----------|----------|--------|
   1   2.567 BB    0.0198  359.82718  283.22516 1.000e2
```

Table 3. 1, Entry 8

GC Conditions: HP-5MS, 100°C, 5 min, 20°C/min to 250°C

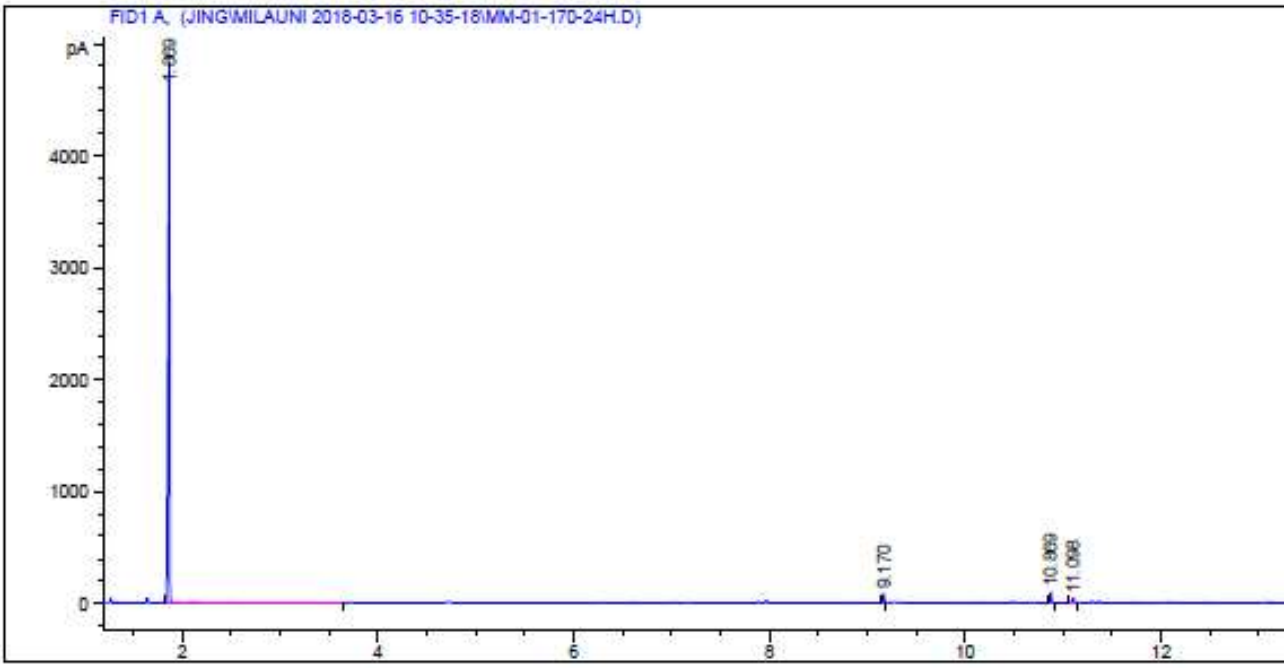


```
=====================================================================
                        Area Percent Report
=====================================================================

Sorted By             :      Signal
Multiplier:                   :      1.0000
Dilution:                     :      1.0000
Use Multiplier & Dilution Factor with ISTDs


Signal 1: FID1 A,

Peak RetTime Type  Width     Area      Height     Area
  #   [min]        [min]   [pA*s]      [pA]        %
----|-------|----|-------|----------|----------|--------|
   1   1.869 VB S  0.0154 4920.25439 4838.00488 95.84056
   2   9.170 VV    0.0143   73.35548   79.55220  1.42888
   3  10.869 VV    0.0152   94.23768   98.41658  1.83564
```

Table 3. 1, Entry 9

GC Conditions: HP-5MS, 100°C, 5 min, 20°C/min to 250°C

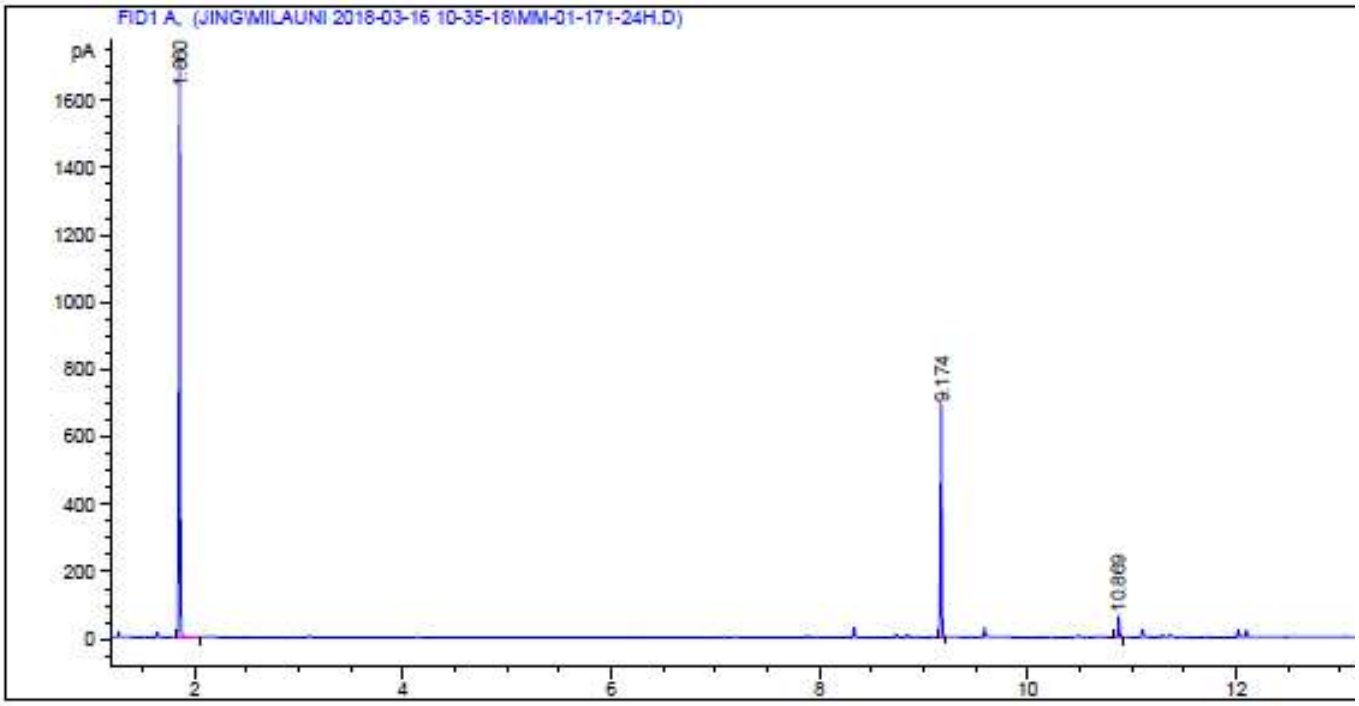


```
=====================================================================
                        Area Percent Report
=====================================================================

Sorted By             :      Signal
Multiplier:                   :      1.0000
Dilution:                     :      1.0000
Use Multiplier & Dilution Factor with ISTDs


Signal 1: FID1 A,

Peak RetTime Type  Width     Area      Height     Area
  #   [min]        [min]    [pA*s]      [pA]        %
----|-------|----|-------|----------|----------|--------|
   1   1.860 VV    0.0139 1506.36890 1689.24109 68.91366
   2   9.174 VV    0.0141  622.42676  681.94080 28.47490
   3  10.869 VV    0.0145   57.08290   60.28089  2.61144
```

Table 3. 1, Entry 10
GC Conditions: HP-5MS, 100°C, 5 min, 20°C/min to 250°C

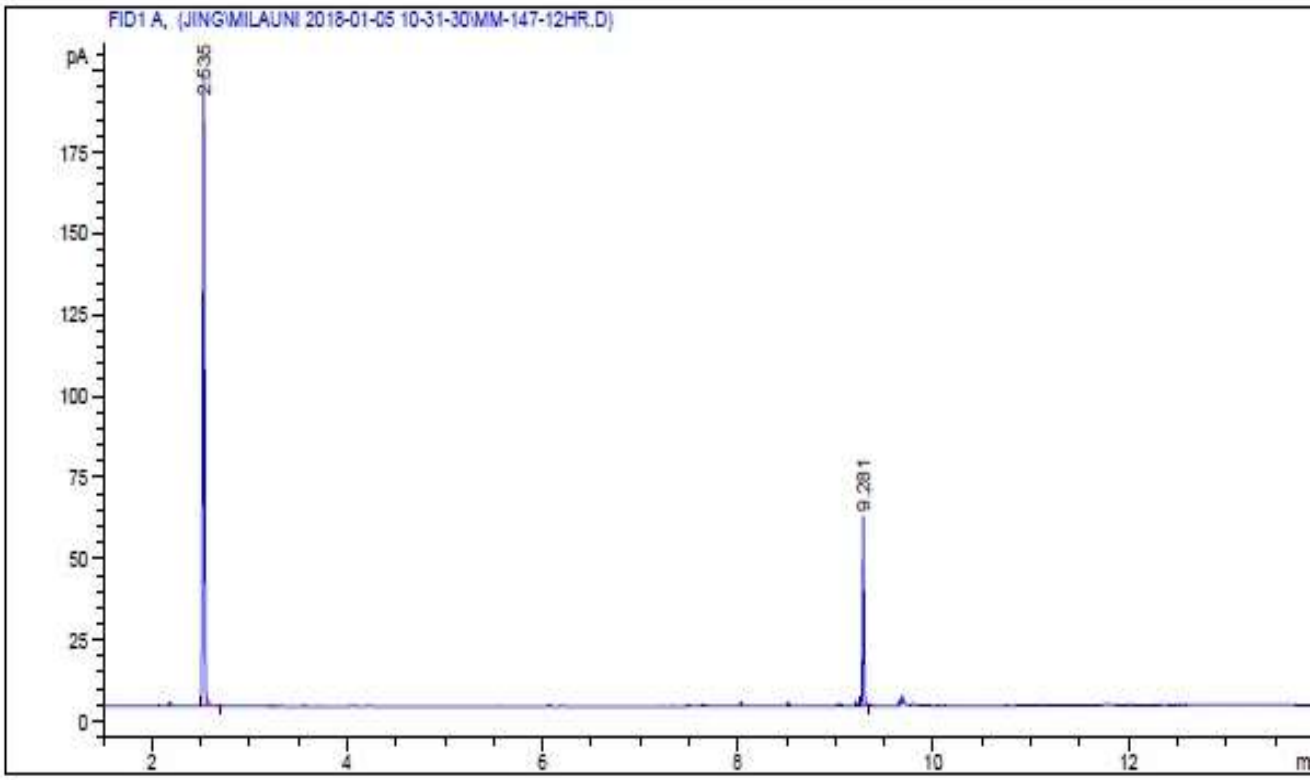


```
=====================================================================
                        Area Percent Report
=====================================================================

Sorted By             :      Signal
Multiplier:                   :      1.0000
Dilution:                     :      1.0000
Use Multiplier & Dilution Factor with ISTDs


Signal 1: FID1 A,

Peak RetTime Type  Width     Area      Height     Area
  #   [min]        [min]   [pA*s]      [pA]        %
----|-------|----|-------|----------|----------|--------|
   1   2.535 BB    0.0193  245.24112  193.92339 81.21001
   2   9.281 VV    0.0149   56.74274   58.15638 18.78999
```

Table 3. 1, Entry 11
GC Conditions: HP-5MS, 100°C, 5 min, 20°C/min to 250°C

```
Last changed     : 1/22/2018 12:24:30 PM by Milauni
                   (modified after loading)
Method Info      : General Higher BP that correlates to Stambuli Group's GCMS - 30 min

Sample Info      : MM-01-144-15 mins track
```

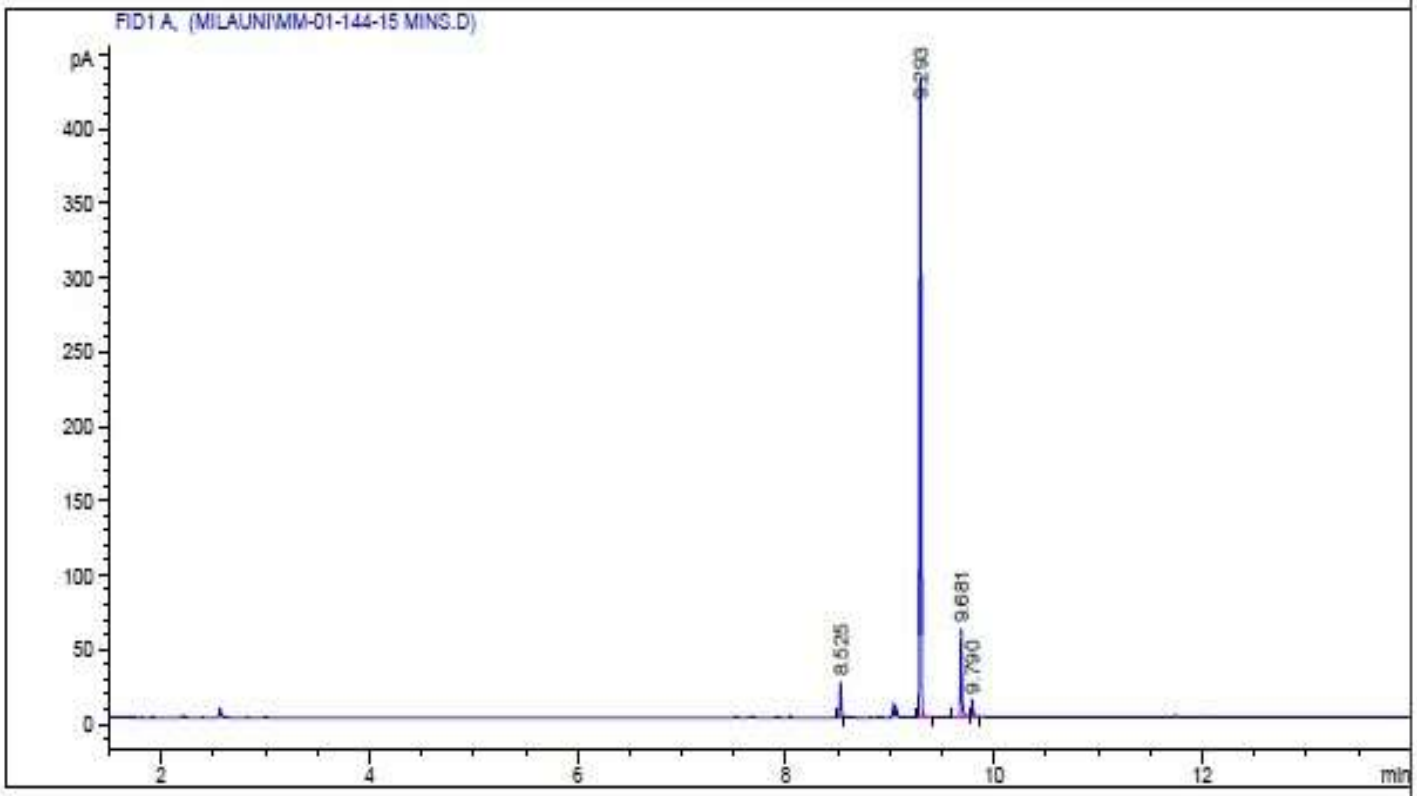


```
Signal 1: FID1 A,

Peak RetTime Type  Width     Area      Height     Area
  #   [min]        [min]   [pA*s]      [pA]        %
----|-------|----|-------|----------|----------|--------|
   1   8.525 VV    0.0156   22.95272   23.15723  4.48649
   2   9.293 VV    0.0152  411.92584  428.89218 80.55358
   3   9.681 VV    0.0156   61.52719   59.30364 12.03186
   4   9.790 VV    0.0187   14.96301   11.84402  2.92607

Totals :                   511.36876  523.19708
```

Table 3. 1, Entry 12

GC Conditions: HP-5MS, 100°C, 5 min, 20°C/min to 250°C

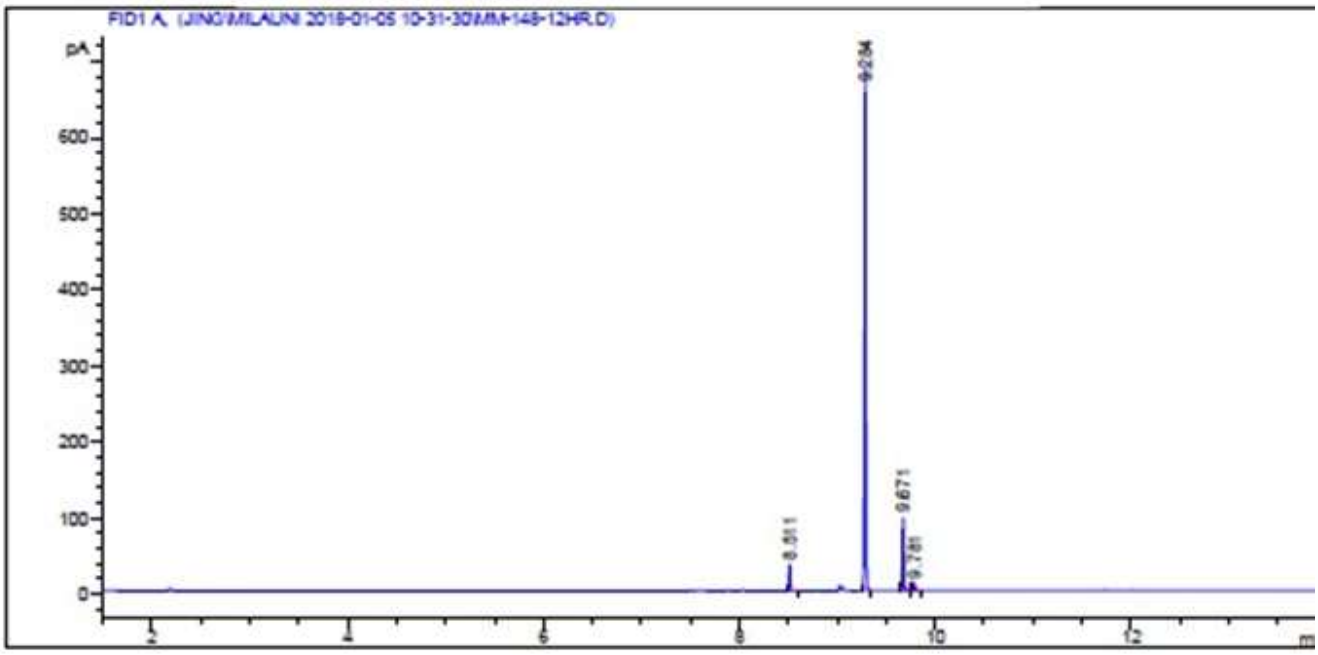

Area Percent Report

Sorted By : Signal
Multiplier: : 1.0000
Dilution: : 1.0000
Use Multiplier & Dilution Factor with ISTDs

Signal 1: FID1 A,

Peak #	RetTime [min]	Type	Width [min]	Area [pA*s]	Height [pA]	Area %
1	8.511	VB	0.0158	34.47852	34.01653	4.36044
2	9.284	VV	0.0145	647.35382	688.18762	81.86978
3	9.671	BV	0.0155	95.80443	96.79131	12.11623
4	9.781	VV	0.0186	13.07480	10.44152	1.65355

Table 3. 1, Entry 13

GC Conditions: HP-5MS, 100°C, 5 min, 20°C/min to 250°C

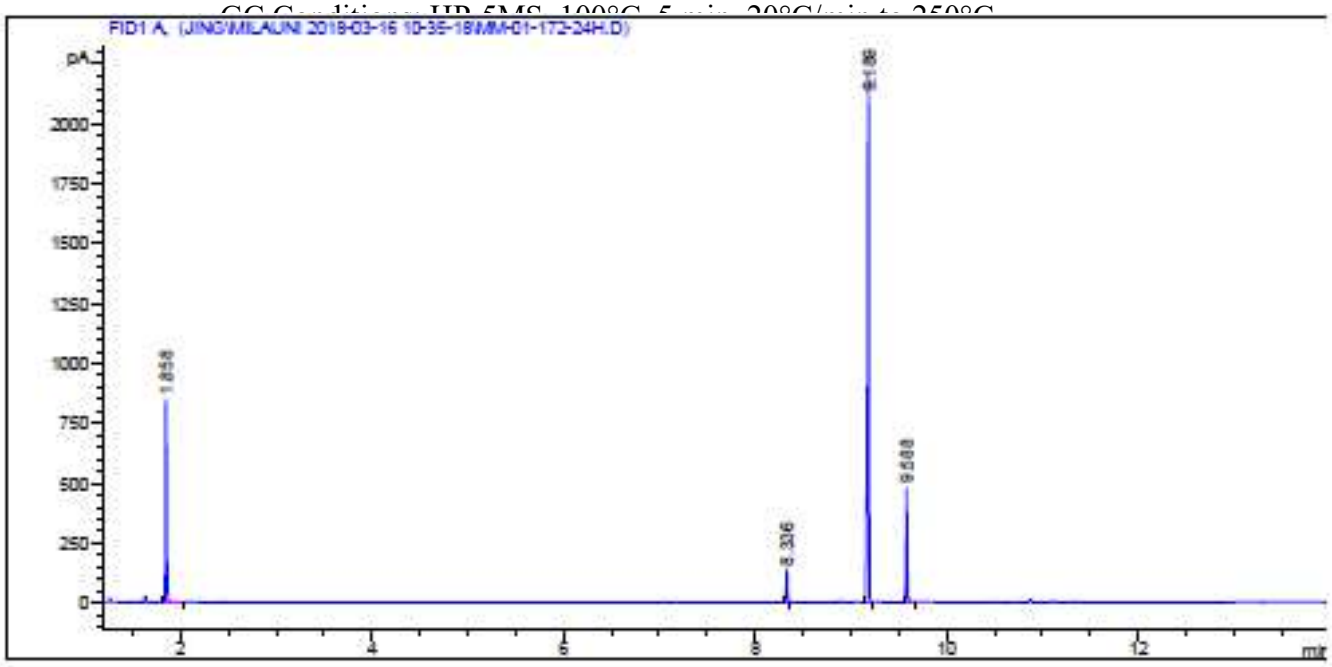

Area Percent Report

Sorted By : Signal
Multiplier: : 1.0000
Dilution: : 1.0000
Use Multiplier & Dilution Factor with ISTDs

Signal 1: FID1 A,

Peak #	RetTime [min]	Type	Width [min]	Area [pA*s]	Height [pA]	Area %
1	1.858	VV	0.0140	758.49481	846.03790	19.88815
2	8.336	BV	0.0151	127.61381	133.54044	3.34610
3	9.189	VV	0.0173	2490.06641	2191.13721	65.29092
4	9.588	VV	0.0142	437.62683	475.69366	11.47482

Table 3. 1, Entry 14

Method Info : GC Conditions: HP-5MS, 100°C, 5 min, 20°C/min to 250°C MS - 30 min

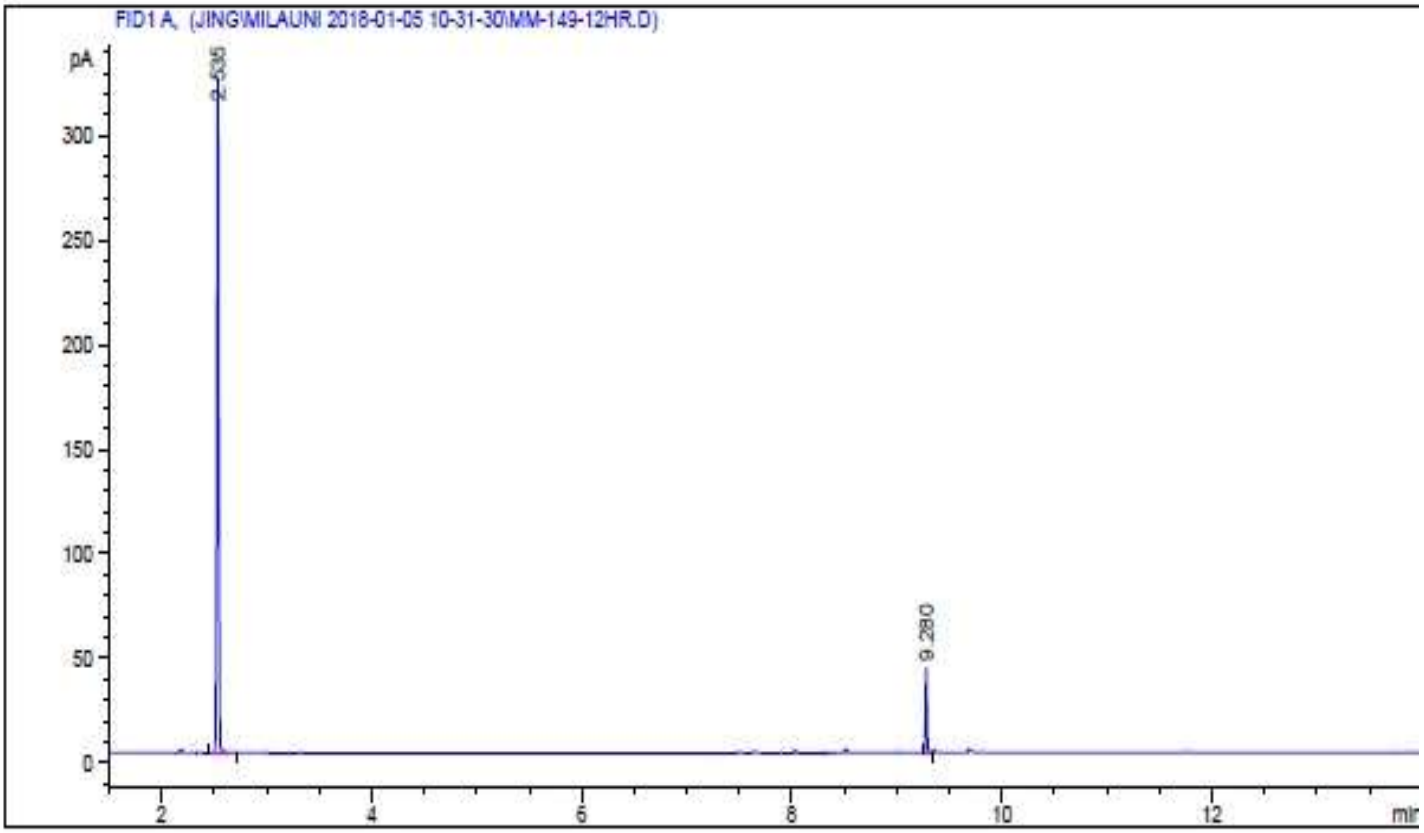


```
=====================================================================
                        Area Percent Report
=====================================================================

Sorted By             :      Signal
Multiplier:                   :      1.0000
Dilution:                     :      1.0000
Use Multiplier & Dilution Factor with ISTDs


Signal 1: FID1 A,

Peak RetTime Type  Width     Area      Height     Area
  #   [min]        [min]   [pA*s]      [pA]        %
----|-------|----|-------|----------|----------|--------|
   1   2.535 BB    0.0192  405.59076  322.39053 90.85677
   2   9.280 VV    0.0155   40.81601   41.23921  9.14323
```

Table 3. 1, Entry 15

GC Conditions: HP-5MS, 100°C, 5 min, 20°C/min to 250°C

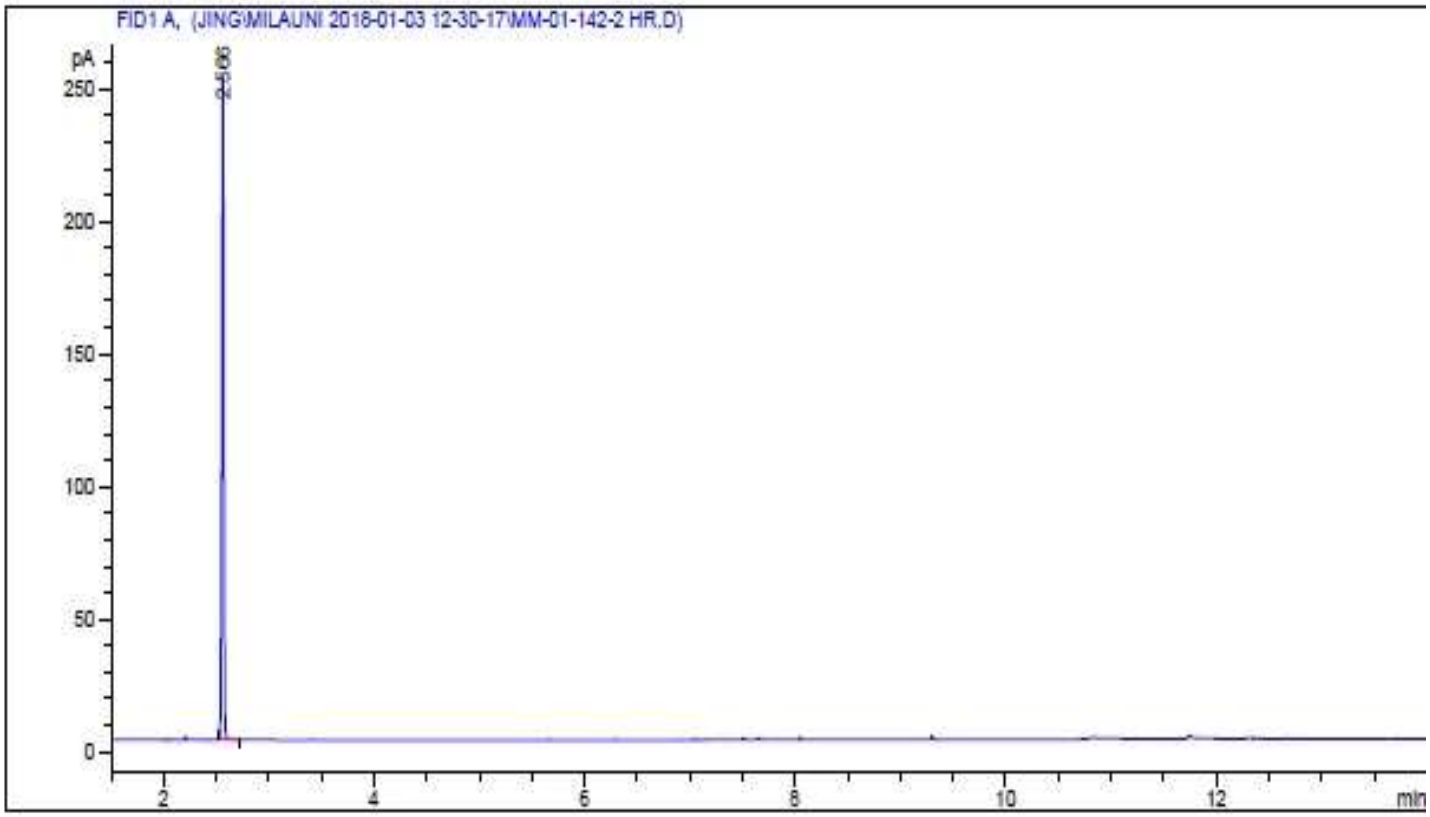


```
=====================================================================
                        Area Percent Report
=====================================================================

Sorted By             :      Signal
Multiplier:                   :      1.0000
Dilution:                     :      1.0000
Use Multiplier & Dilution Factor with ISTDs


Signal 1: FID1 A,

Peak RetTime Type  Width     Area      Height     Area
  #   [min]        [min]   [pA*s]      [pA]        %
----|-------|----|-------|----------|----------|--------|
   1   2.566 BB    0.0198  316.08524  249.83258 1.000e2

Totals :                   316.08524  249.83258
```

Table 3. 1, Entry 16
GC Conditions: HP-5MS, 100°C, 5 min, 20°C/min to 250°C

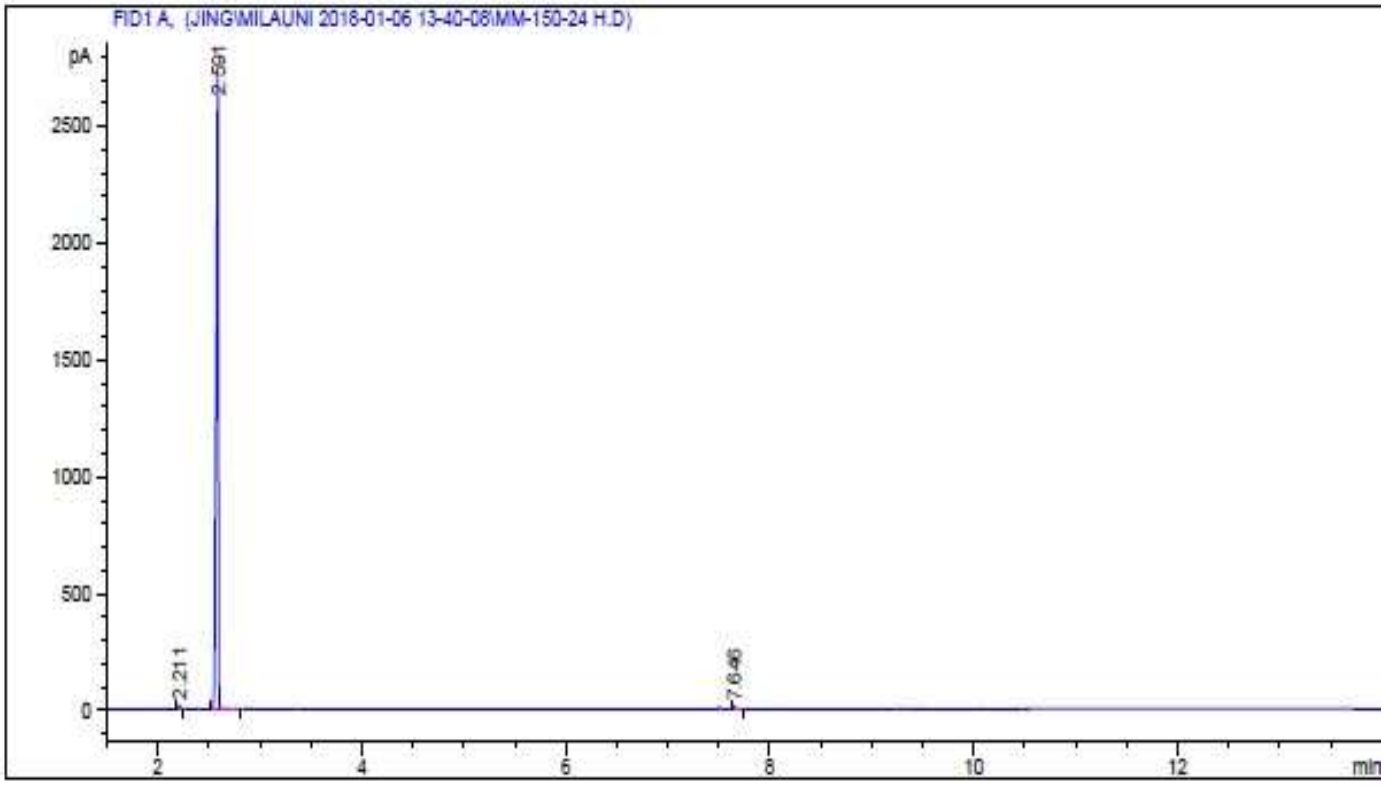


```
=====================================================================
                        Area Percent Report
=====================================================================

Sorted By             :      Signal
Multiplier:                   :      1.0000
Dilution:                     :      1.0000
Use Multiplier & Dilution Factor with ISTDs


Signal 1: FID1 A,

Peak RetTime Type  Width     Area      Height     Area
  #   [min]        [min]   [pA*s]      [pA]        %
----|-------|----|-------|----------|----------|--------|
   1   2.211 BV    0.0175   17.89771   16.04711  0.41438
   2   2.591 VV    0.0224 4287.89111 2722.87476 99.27730
   3   7.646 VB    0.0185   13.31637   11.53614  0.30831
```

Table 3. 1, Entry 17

GC Conditions: HP-5MS, 100°C, 5 min, 20°C/min to 250°C

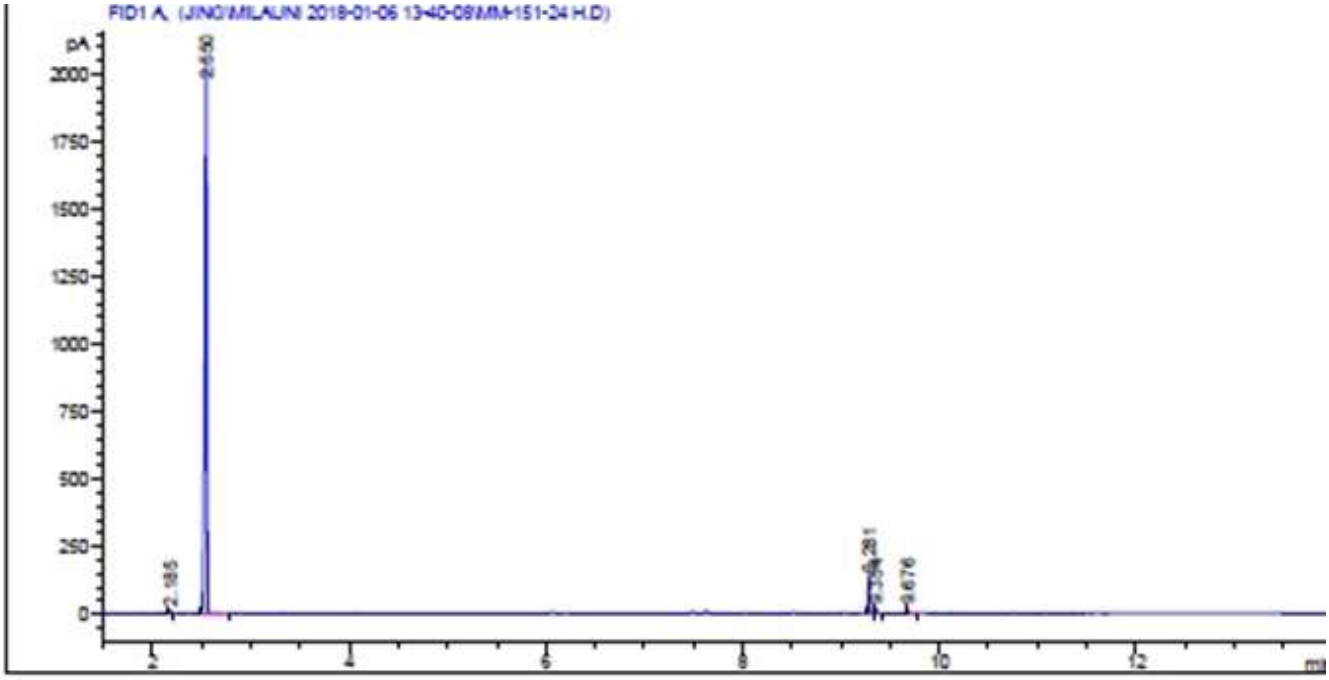

Area Percent Report

Sorted By : Signal
Multiplier: : 1.0000
Dilution: : 1.0000
Use Multiplier & Dilution Factor with ISTDs

Signal 1: FID1 A,

Peak #	RetTime [min]	Type	Width [min]	Area [pA*s]	Height [pA]	Area %
1	2.185	VV	0.0173	11.81232	10.78532	0.38314
2	2.550	VV	0.0217	2914.94604	2039.50952	94.54713
3	9.281	VV	0.0152	125.85725	131.46703	4.08222
4	9.354	VV	0.0165	13.86031	12.93445	0.44956
5	9.676	VV	0.0190	16.58551	12.90822	0.53796

Table 3. 1, Entry 18
GC Conditions: HP-5MS, 100°C, 5 min, 20°C/min to 250°C

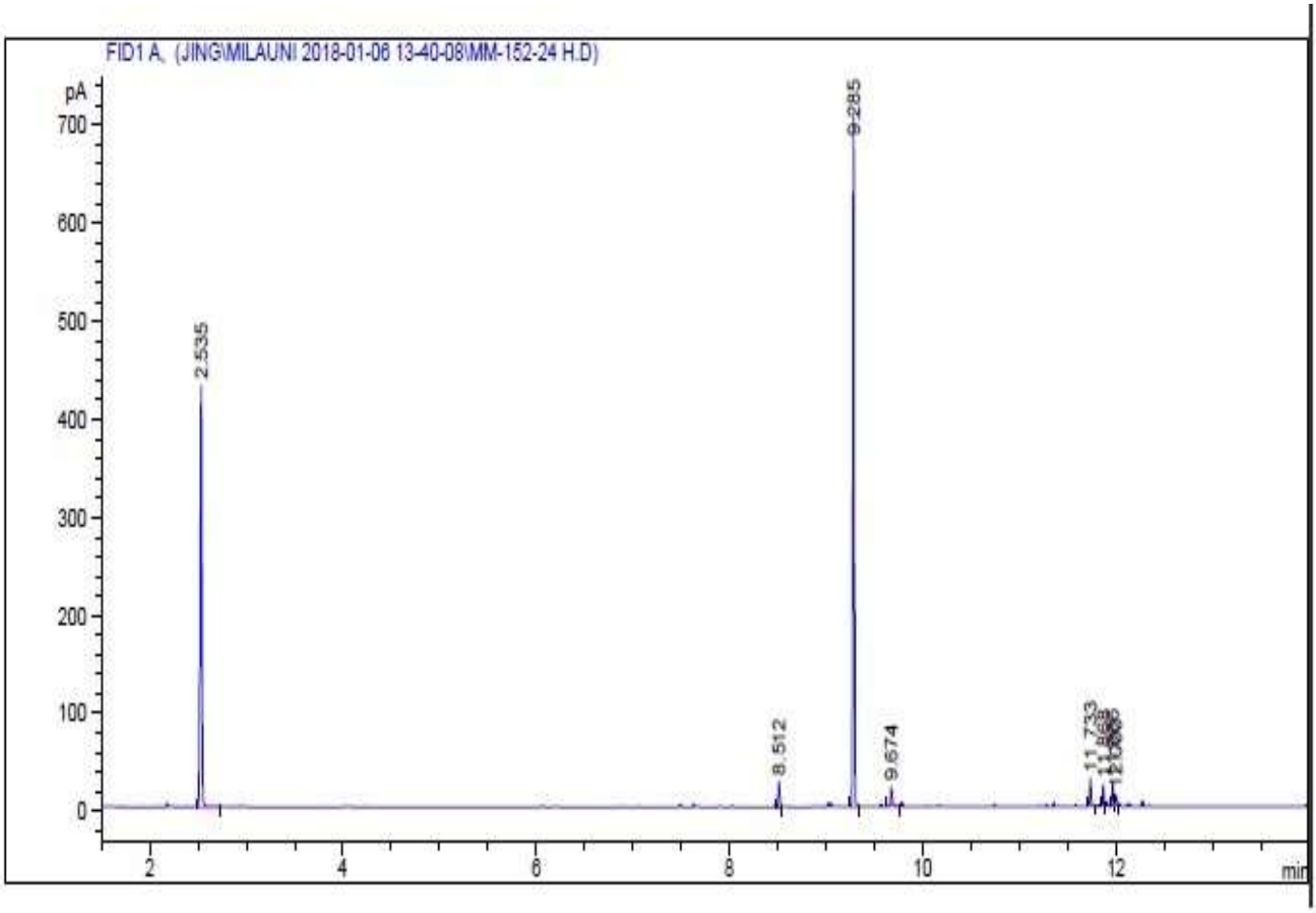

Peak #	RetTime [min]	Type	Width [min]	Area [pA*s]	Height [pA]	Area %
1	2.535	VB	0.0197	541.18756	429.51627	40.35884
2	8.512	VV	0.0156	25.94383	26.01396	1.93475
3	9.285	VV	0.0149	662.01178	707.71265	49.36926
4	9.674	VV	0.0170	21.62362	19.33740	1.61257
5	11.733	VV	0.0162	29.82348	28.61293	2.22407
6	11.868	VV	0.0160	22.83471	22.15430	1.70289
7	11.966	VV	0.0167	25.93523	22.88709	1.93411
8	12.000	VV	0.0150	11.57900	11.76995	0.86350

Table 3. 1, Entry 19
GC Conditions: HP-5MS, 100°C, 5 min, 20°C/min to 250°C

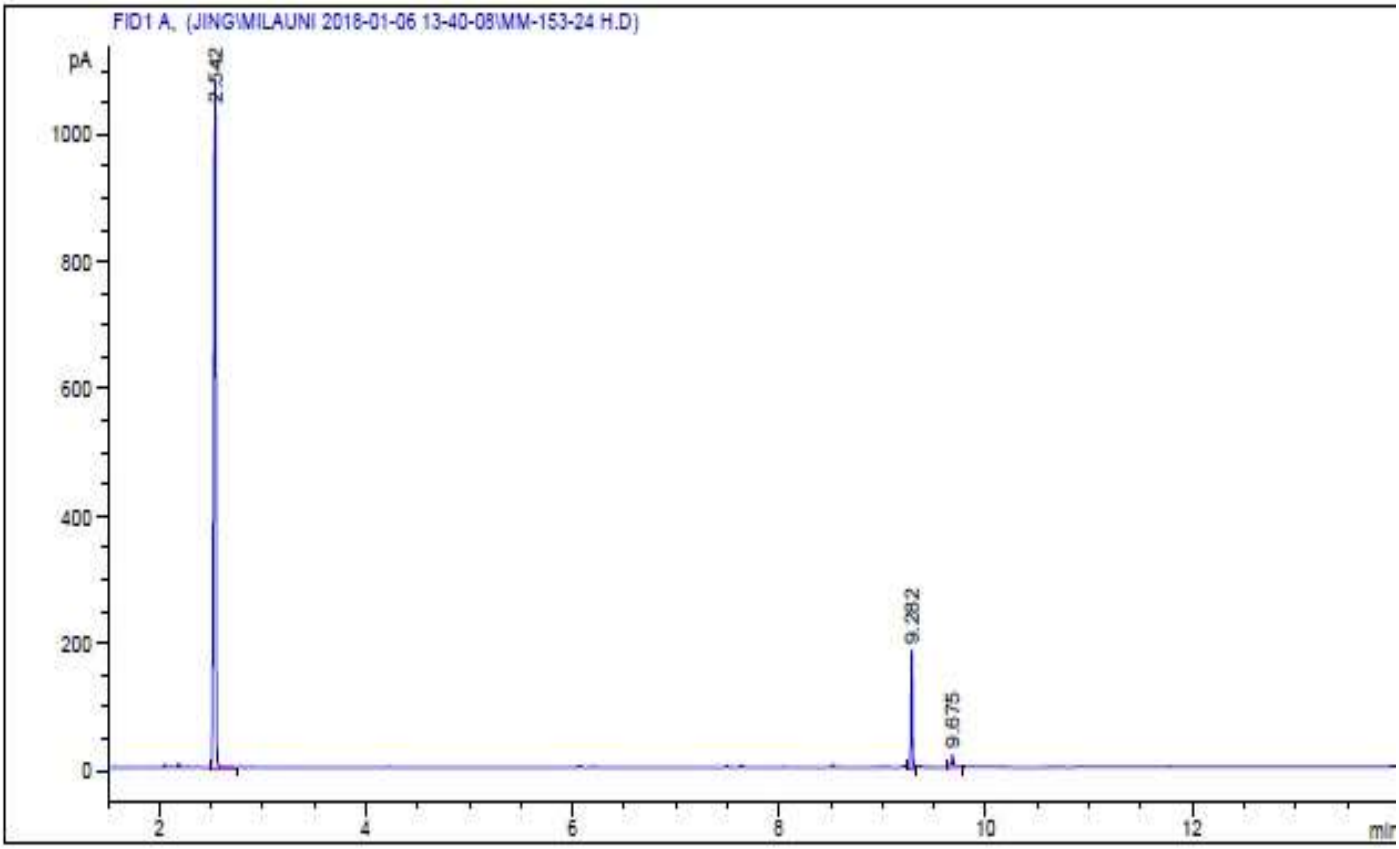


```
=====================================================================
                      Area Percent Report
=====================================================================

Sorted By             :      Signal
Multiplier:                   :      1.0000
Dilution:                     :      1.0000
Use Multiplier & Dilution Factor with ISTDs


Signal 1: FID1 A,

Peak RetTime Type  Width     Area      Height     Area
  #   [min]        [min]   [pA*s]      [pA]        %
----|-------|----|-------|----------|----------|--------|
   1   2.542 VB    0.0201 1398.36731 1078.55029 87.29332
   2   9.282 VV    0.0153  175.99103  182.07333 10.98627
   3   9.675 VV    0.0195   27.55963   20.74852  1.72041
```

Appendix D: ^{1}H-NMR and ^{13}C-NMR Spectra for Chapter 3

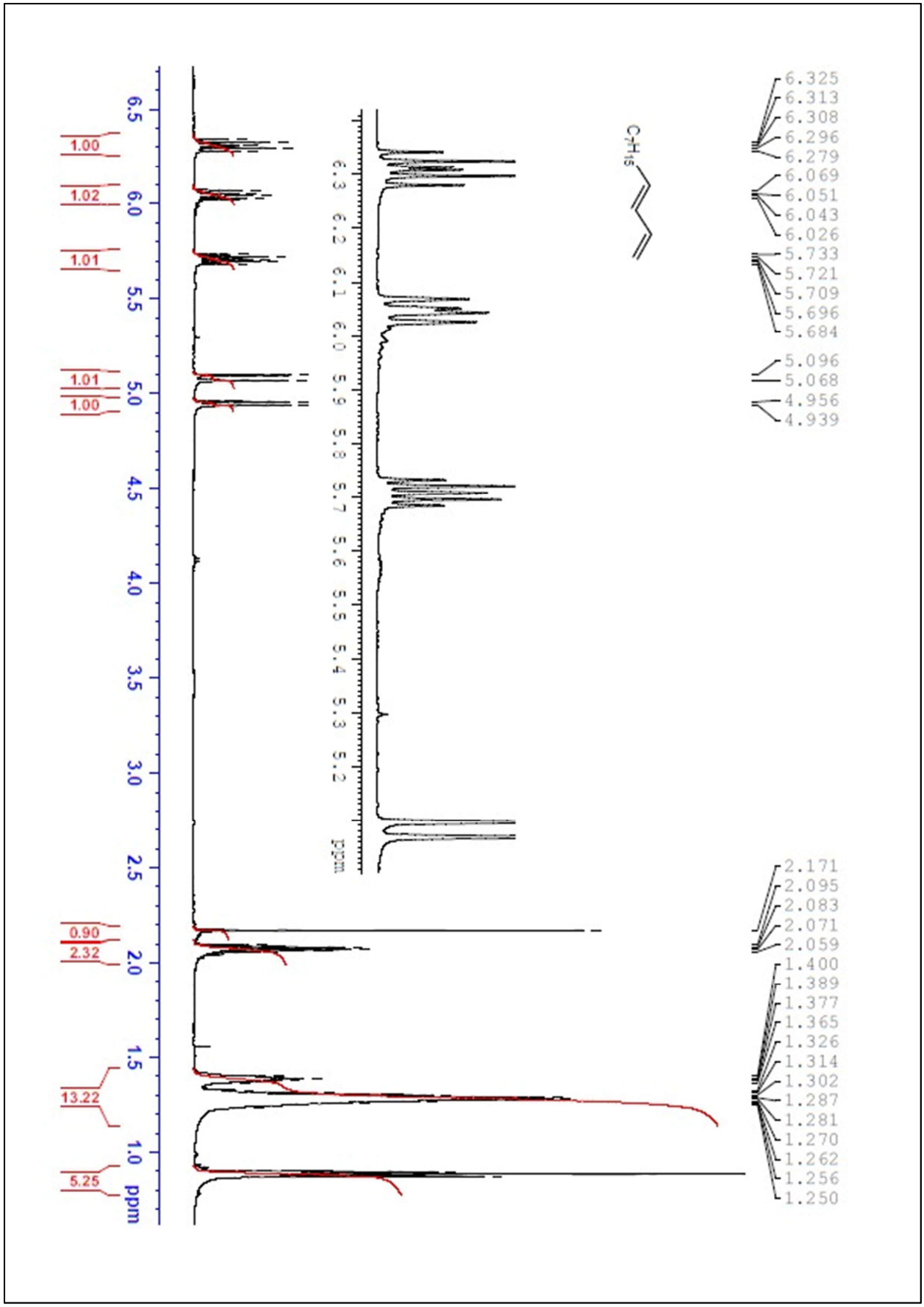
6.325
6.313
6.308
6.296
6.279
6.069
6.051
6.043
6.026
5.733
5.721
5.709
5.696
5.684
5.096
5.068
4.956
4.939
2.171
2.095
2.083
2.071
2.059
1.400
1.389
1.377
1.365
1.326
1.314
1.302
1.287
1.281
1.270
1.262
1.256
1.250
1.00
1.02
1.01
1.01
1.00
0.90
2.32
13.22
5.25
ppm

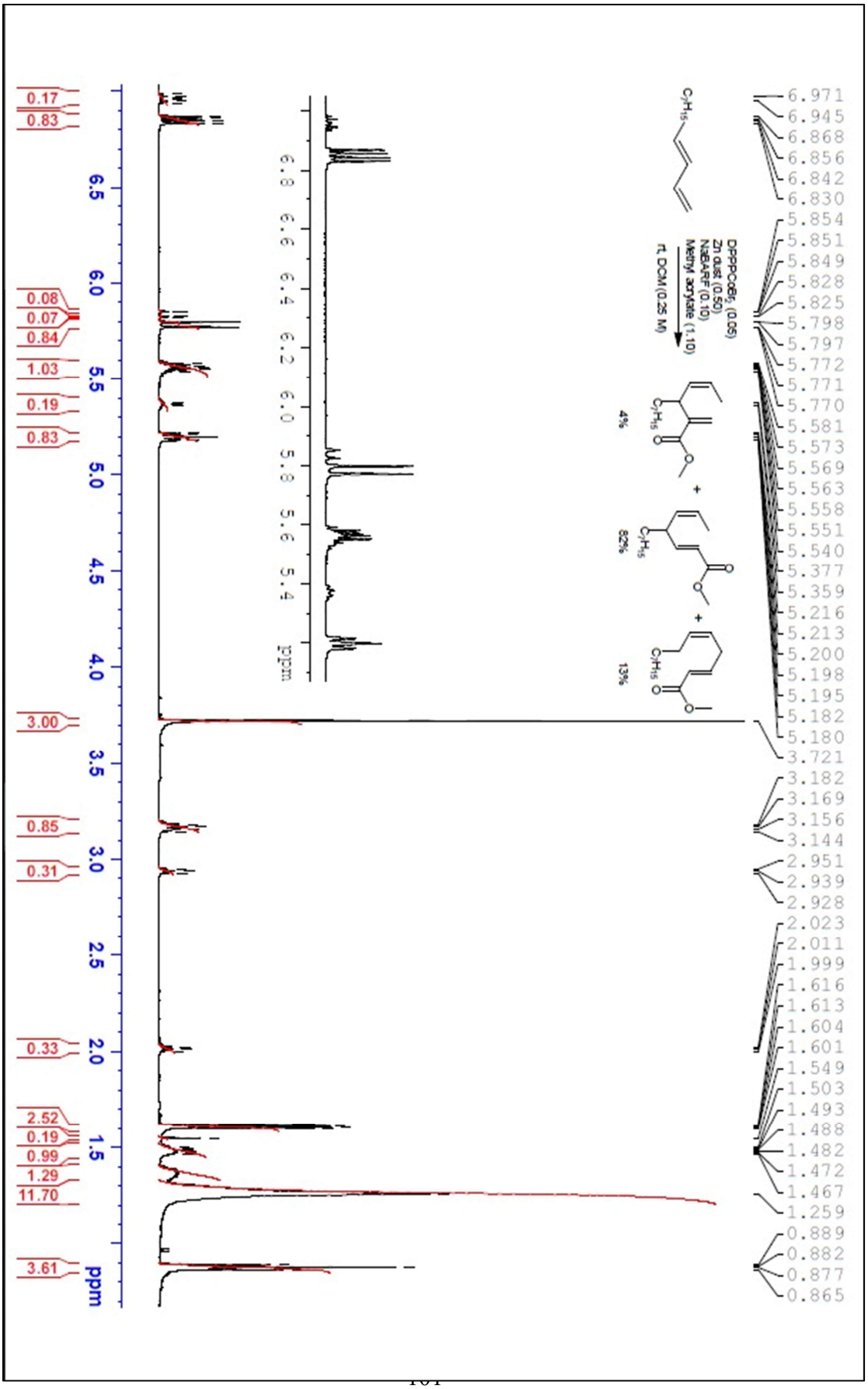
6.971
6.945
6.868
6.856
6.842
6.830
5.854
5.851
5.849
5.828
5.825
5.798
5.797
5.772
5.771
5.770
5.581
5.573
5.569
5.563
5.558
5.551
5.540
5.377
5.359
5.216
5.213
5.200
5.198
5.195
5.182
5.180
3.721
3.182
3.169
3.156
3.144
2.951
2.939
2.928
2.023
2.011
1.999
1.616
1.613
1.604
1.601
1.549
1.503
1.493
1.488
1.482
1.472
1.467
1.259
0.889
0.882
0.877
0.865
DPPPCoBr2 (0.05)
Zn dust (0.50)
NaBArF (0.10)
Methyl acrylate (1.10)
rt, DCM (0.25 M)
4%
82%
13%
0.17
0.83
0.08
0.07
0.84
1.03
0.19
0.83
3.00
0.85
0.31
0.33
2.52
0.19
0.99
1.29
11.70
3.61
ppm

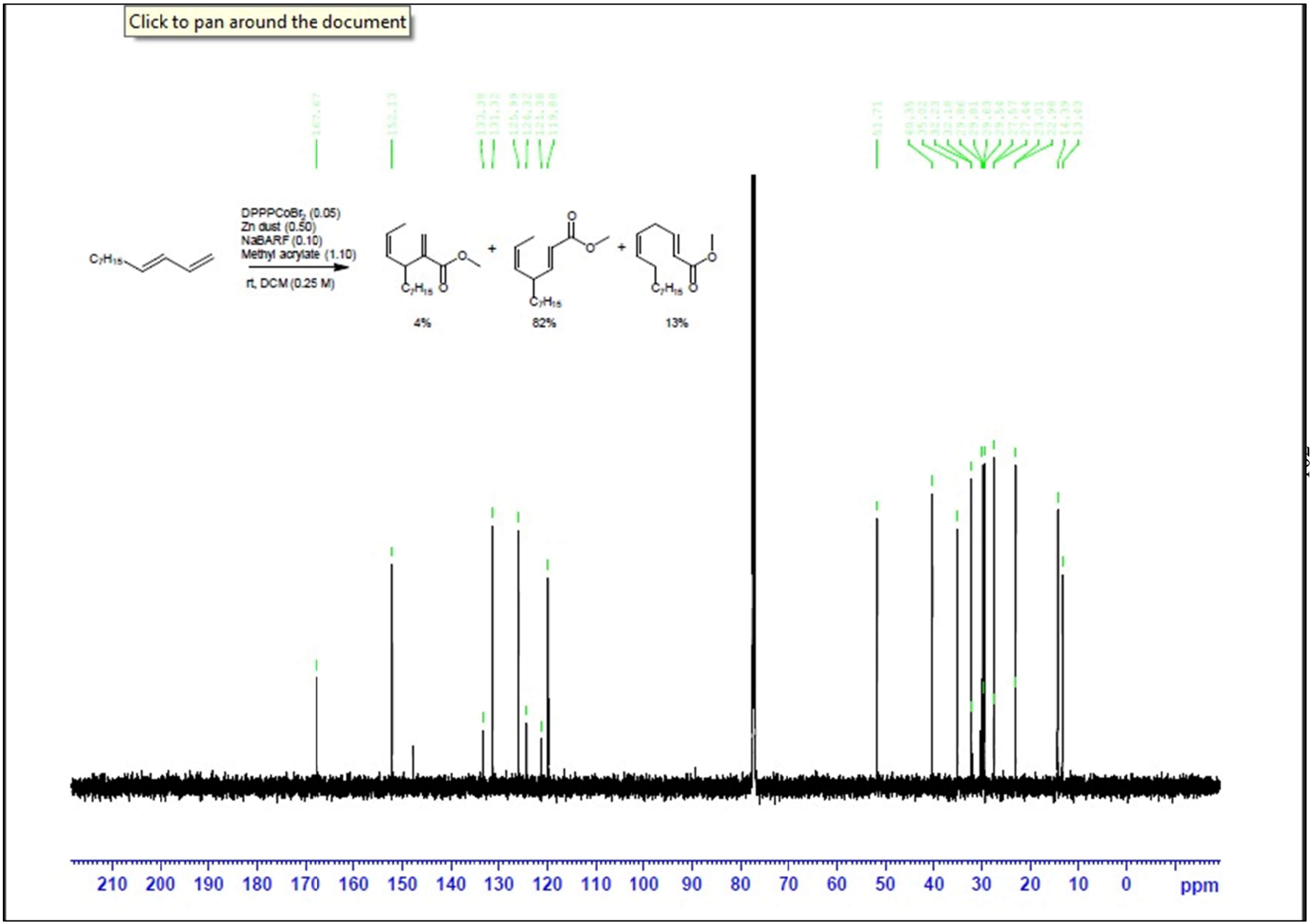
Click to pan around the document
DPPPCoBr2 (0.05)
Zn dust (0.50)
NaBARF (0.10)
Methyl acrylate (1.10)
rt, DCM (0.25 M)
4%
82%
13%
210 200 190 180 170 160 150 140 130 120 110 100 90 80 70 60 50 40 30 20 10 0 ppm

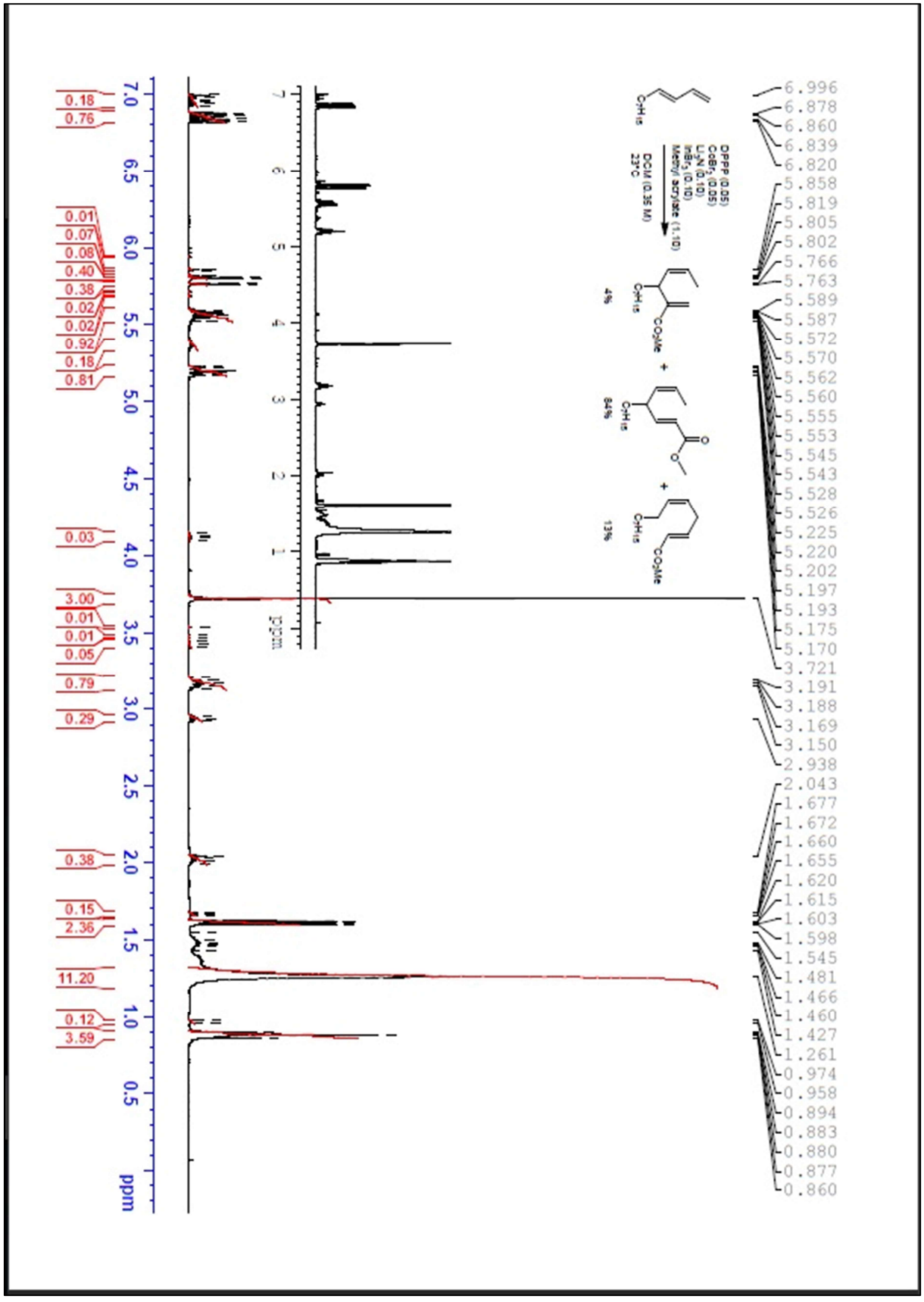
6.996
6.878
6.860
6.839
6.820
5.858
5.819
5.805
5.802
5.766
5.763
5.589
5.587
5.572
5.570
5.562
5.560
5.555
5.553
5.545
5.543
5.528
5.526
5.225
5.220
5.202
5.197
5.193
5.175
5.170
3.721
3.191
3.188
3.169
3.150
2.938
2.043
1.677
1.672
1.660
1.655
1.620
1.615
1.603
1.598
1.545
1.481
1.466
1.460
1.427
1.261
0.974
0.958
0.894
0.883
0.880
0.877
0.860
DPPP (0.05)
CoBr2 (0.05)
Li3N (0.10)
InBr3 (0.10)
Methyl acrylate (1.10)
DCM (0.35 M)
23°C
C6H13
CO2Me
4%
84%
13%
ppm
0.18
0.76
0.01
0.07
0.08
0.40
0.38
0.02
0.02
0.92
0.18
0.81
0.03
3.00
0.01
0.01
0.05
0.79
0.29
0.38
0.15
2.36
11.20
0.12
3.59

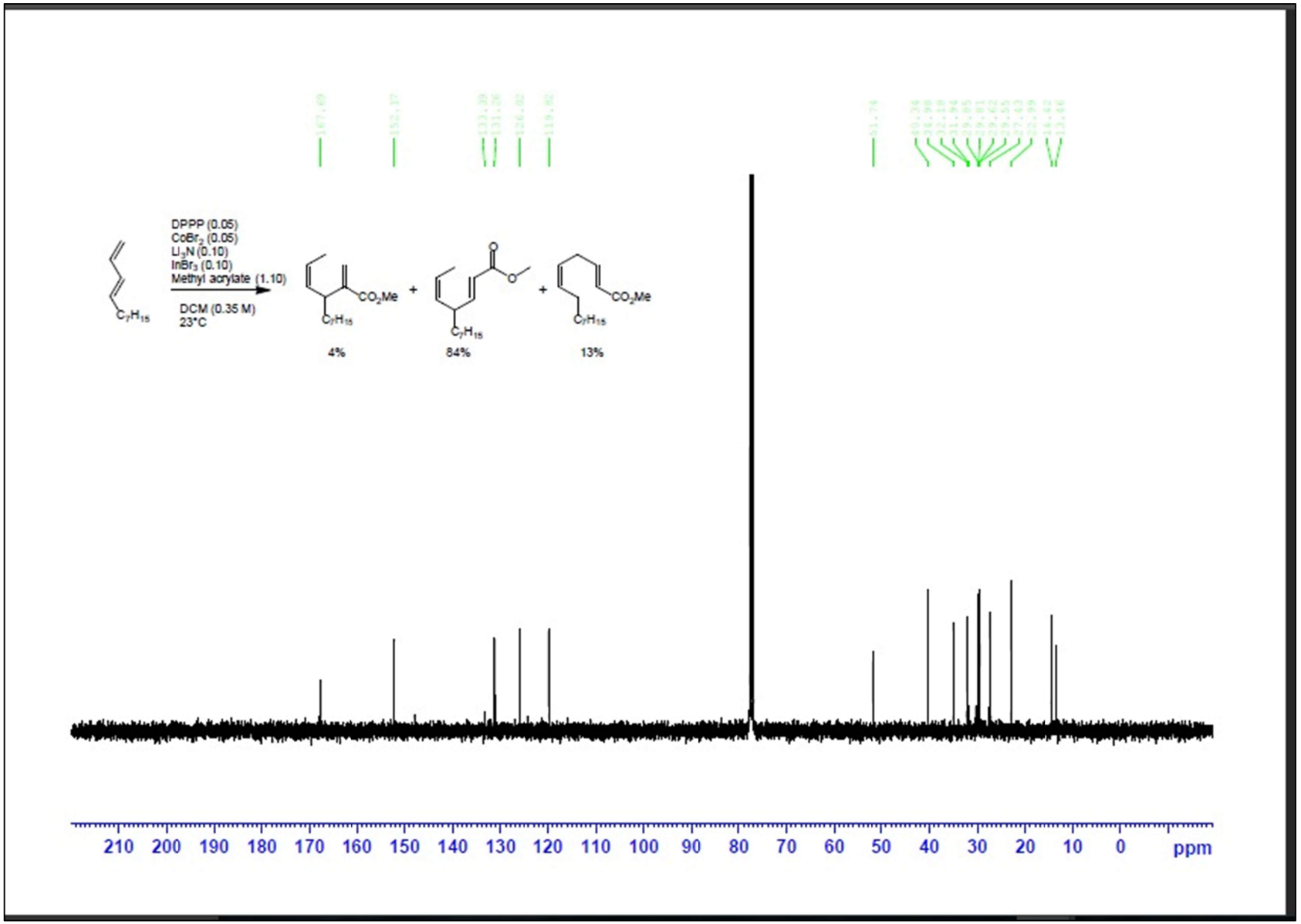
DPPP (0.05)
CoBr2 (0.05)
Li3N (0.10)
InBr3 (0.10)
Methyl acrylate (1.10)
DCM (0.35 M)
23°C
C7H15
CO2Me
4%
84%
13%
210 200 190 180 170 160 150 140 130 120 110 100 90 80 70 60 50 40 30 20 10 0 ppm

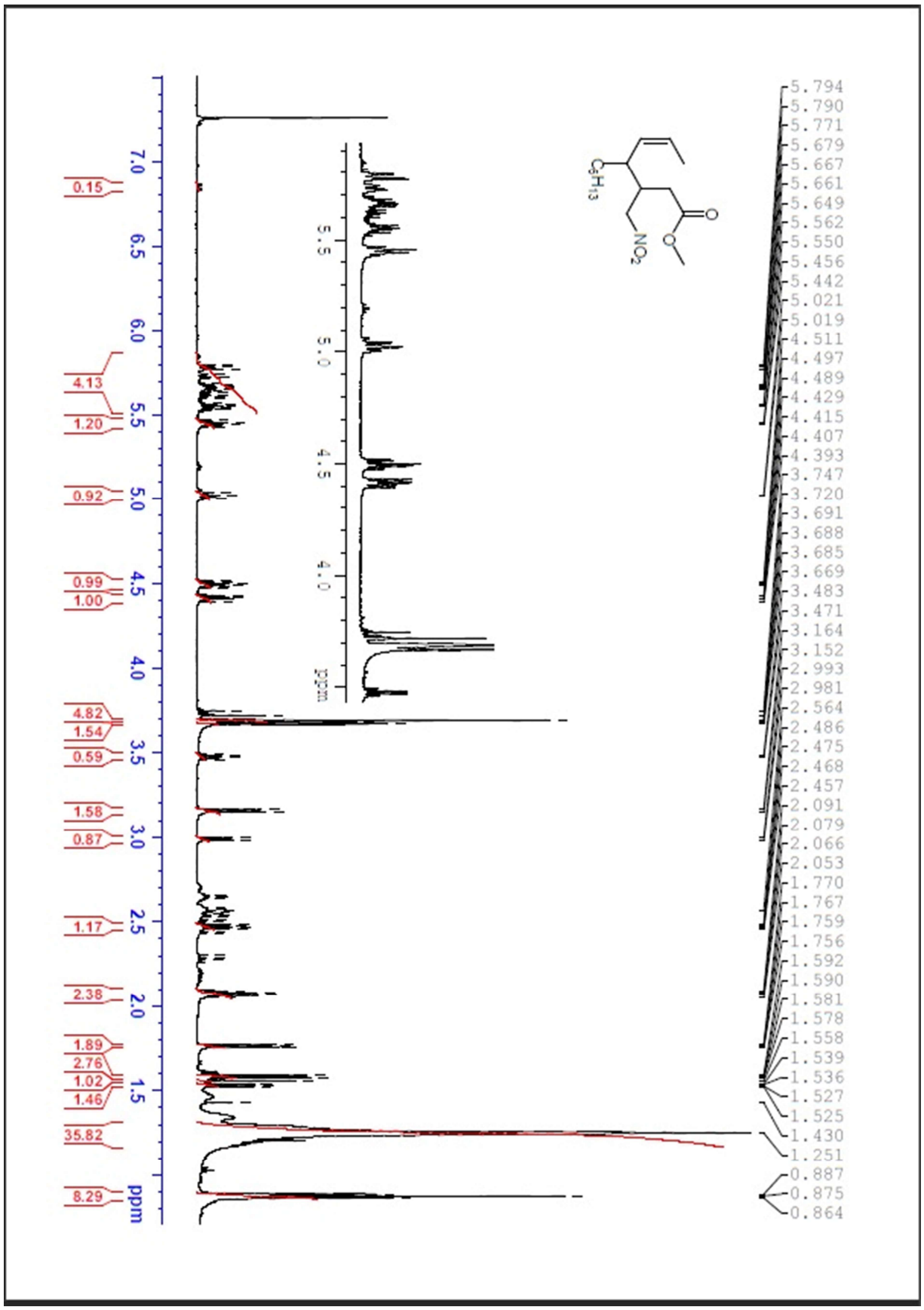
5.794
5.790
5.771
5.679
5.667
5.661
5.649
5.562
5.550
5.456
5.442
5.021
5.019
4.511
4.497
4.489
4.429
4.415
4.407
4.393
3.747
3.720
3.691
3.688
3.685
3.669
3.483
3.471
3.164
3.152
2.993
2.981
2.564
2.486
2.475
2.468
2.457
2.091
2.079
2.066
2.053
1.770
1.767
1.759
1.756
1.592
1.590
1.581
1.578
1.558
1.539
1.536
1.527
1.525
1.430
1.251
0.887
0.875
0.864
C5H13
NO2
O
O
ppm
0.15
4.13
1.20
0.92
0.99
1.00
4.82
1.54
0.59
1.58
0.87
1.17
2.38
1.89
2.76
1.02
1.46
35.82
8.29

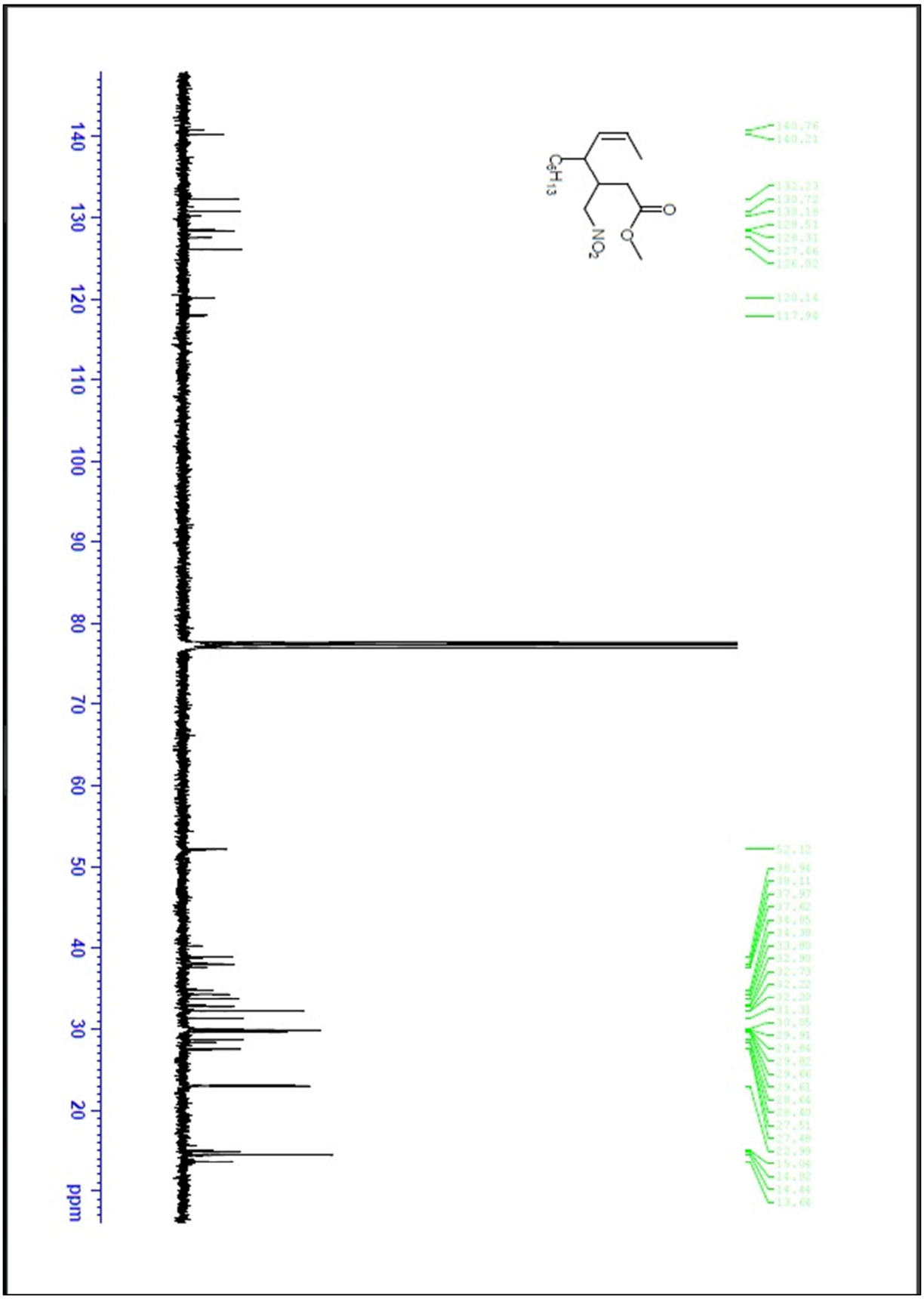
C6H13
NO2
O
O
ppm
140
130
120
110
100
90
80
70
60
50
40
30
20

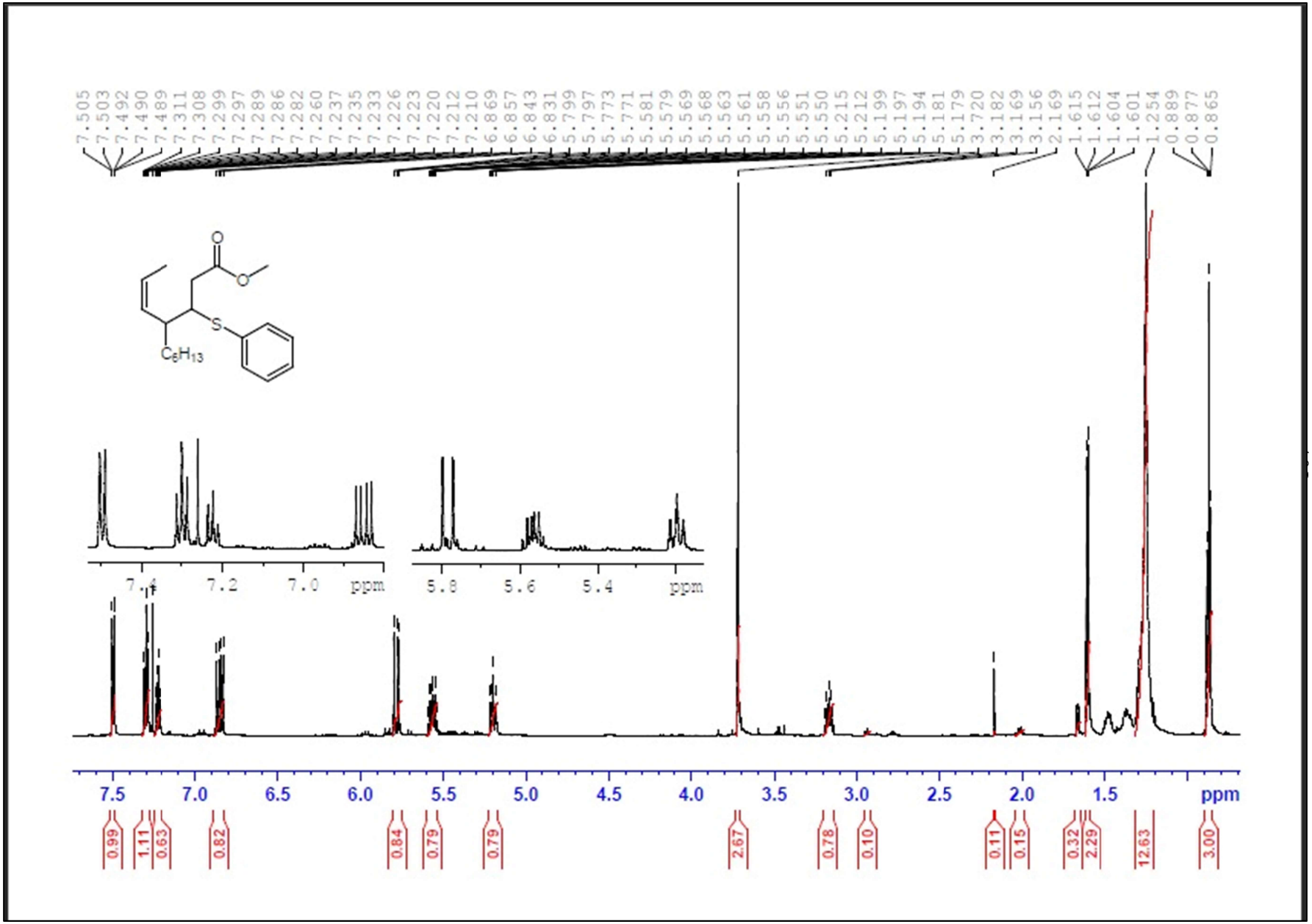
7.505
7.503
7.492
7.490
7.489
7.311
7.308
7.299
7.297
7.289
7.286
7.282
7.260
7.237
7.235
7.233
7.226
7.223
7.220
7.212
7.210
6.869
6.857
6.843
6.831
5.799
5.797
5.773
5.771
5.581
5.579
5.569
5.568
5.563
5.561
5.558
5.556
5.551
5.550
5.215
5.212
5.199
5.197
5.194
5.181
5.179
3.720
3.182
3.169
3.156
2.169
1.615
1.612
1.604
1.601
1.254
0.889
0.877
0.865
O
O
S
C6H13
7.4
7.2
7.0
ppm
5.8
5.6
5.4
ppm
7.5
7.0
6.5
6.0
5.5
5.0
4.5
4.0
3.5
3.0
2.5
2.0
1.5
ppm
0.99
1.11
0.63
0.82
0.84
0.79
0.79
2.67
0.78
0.10
0.11
0.15
0.32
2.29
12.63
3.00

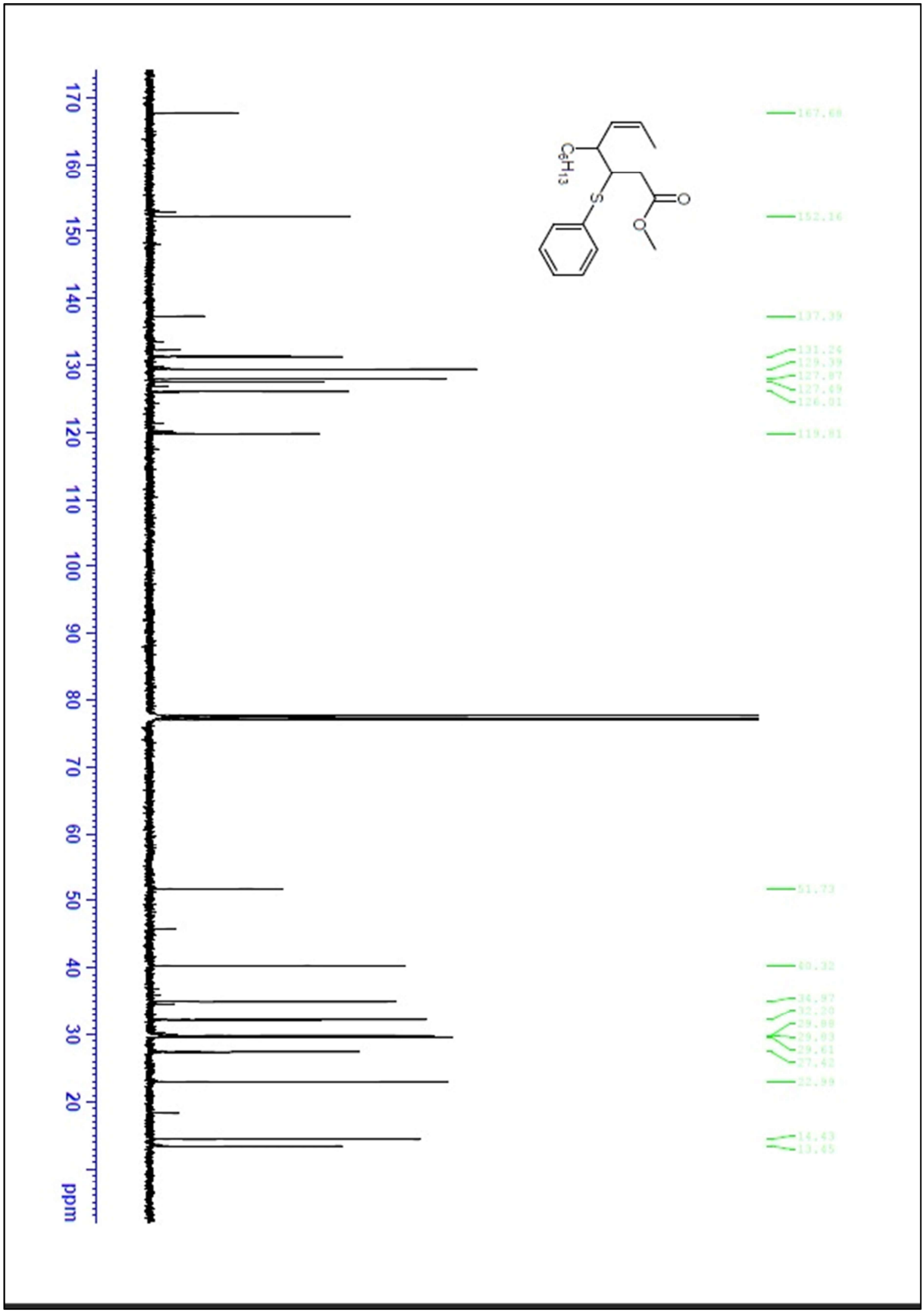
C6H13
S
O
O
167.68
152.16
137.39
131.26
129.39
127.87
127.49
126.01
119.81
51.73
40.32
34.97
32.20
29.88
29.03
29.61
27.42
22.99
14.43
13.45
170
160
150
140
130
120
110
100
90
80
70
60
50
40
30
20
ppm

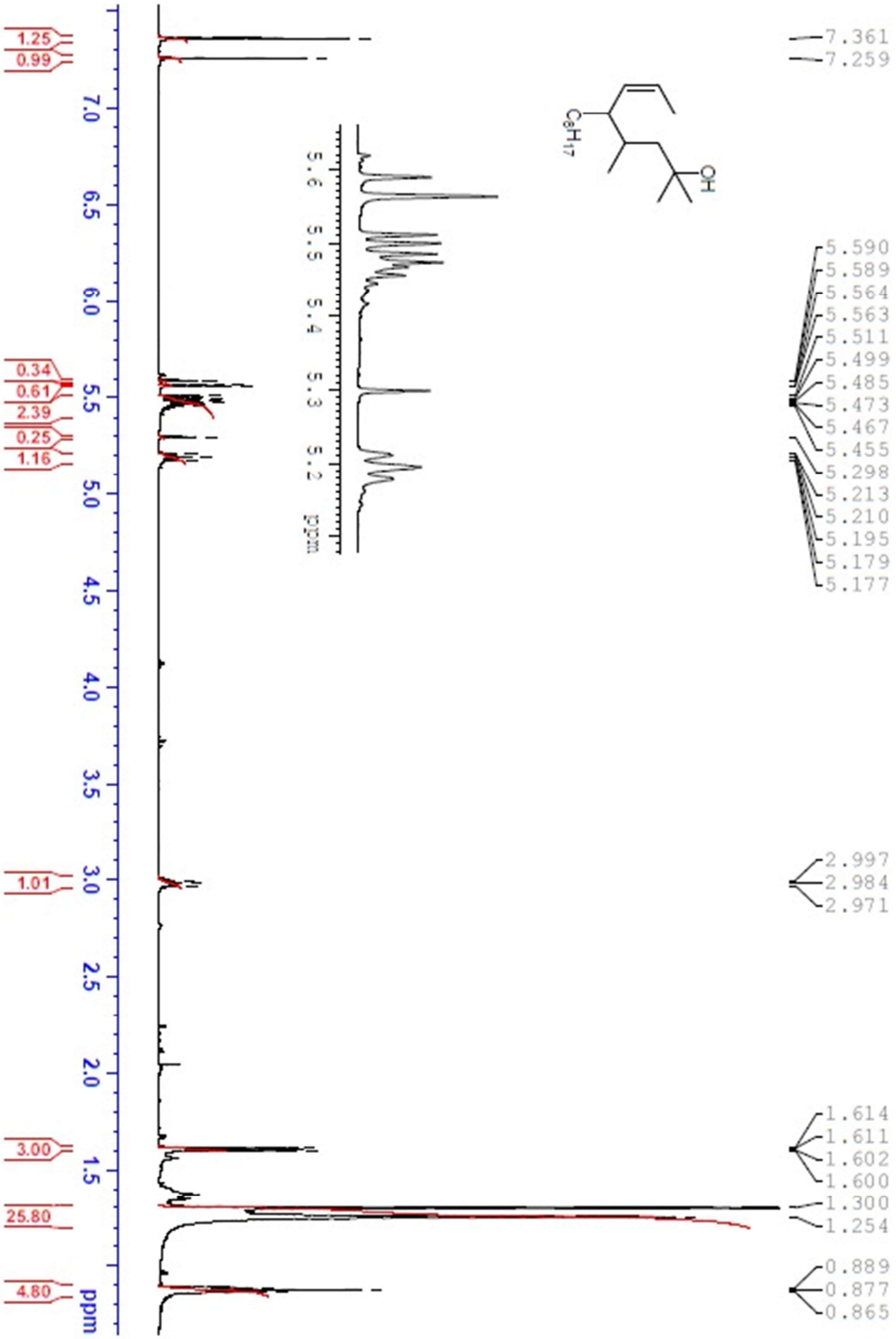
7.361
7.259
5.590
5.589
5.564
5.563
5.511
5.499
5.485
5.473
5.467
5.455
5.298
5.213
5.210
5.195
5.179
5.177
2.997
2.984
2.971
1.614
1.611
1.602
1.600
1.300
1.254
0.889
0.877
0.865
1.25
0.99
0.34
0.61
2.39
0.25
1.16
1.01
3.00
25.80
4.80
ppm
OH
C8H17

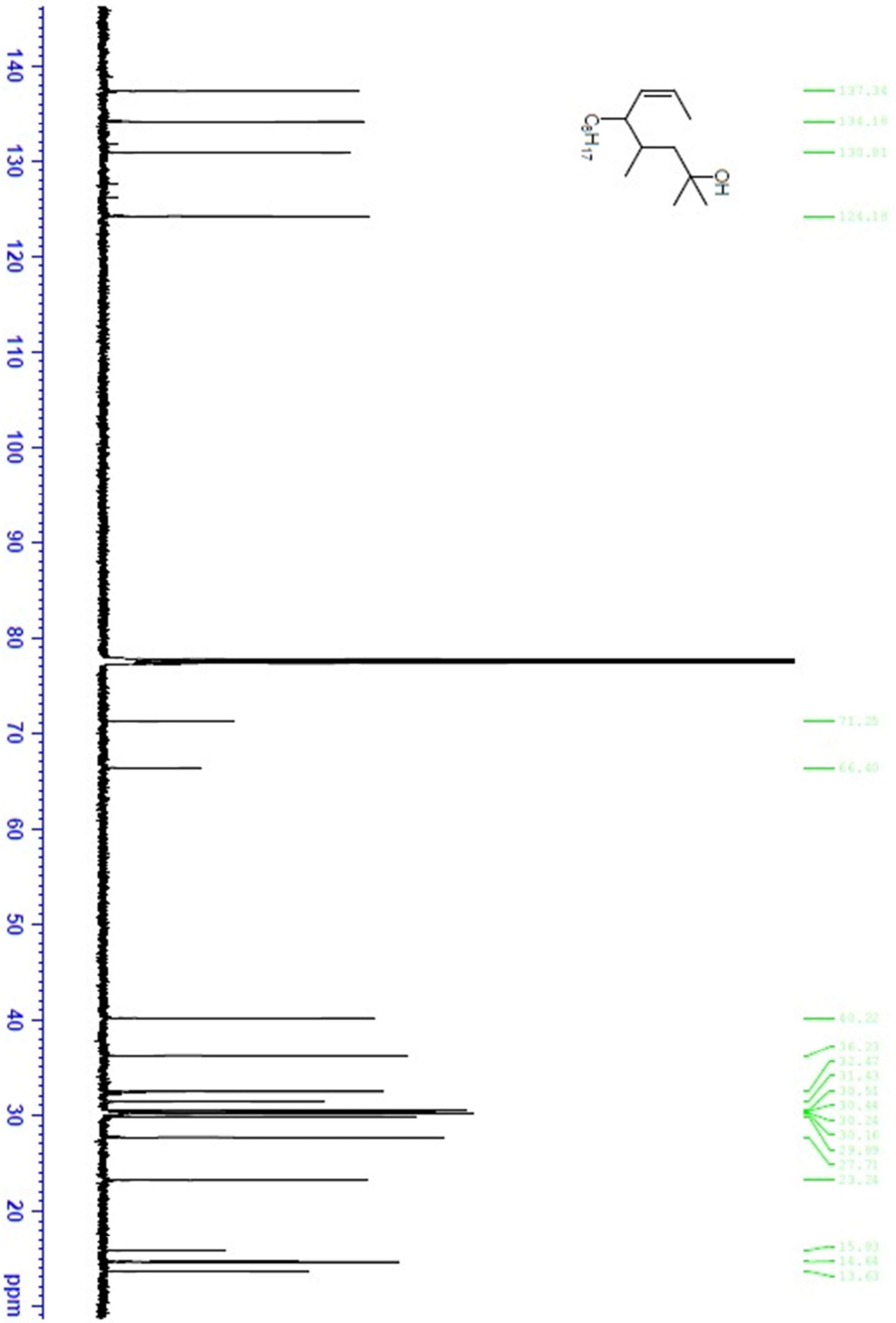
140
130
120
110
100
90
80
70
60
50
40
30
20
ppm
C8H17
OH
137.34
134.18
130.81
124.18
71.25
66.40
40.22
36.23
32.47
31.43
30.51
30.44
30.24
30.16
29.89
27.71
23.26
15.93
14.64
13.63